

UNIVERSIDADE FEDERAL DO RIO GRANDE DO SUL
ESCOLA DE ENGENHARIA
PROGRAMA DE PÓS-GRADUAÇÃO EM ENGENHARIA DE MINAS
METALÚRGICA E DE MATERIAIS - PPGE3M
LABORATÓRIO DE TECNOLOGIA MINERAL E AMBIENTAL - LTM

**ESTUDOS DE GERAÇÃO, CARACTERIZAÇÃO E USO DE
NANOBOLHAS NA FLOTAÇÃO DE ÁGUAS OLEOSAS**

DISSERTAÇÃO DE MESTRADO

Henrique Alberton de Oliveira

**Porto Alegre
2018**

UNIVERSIDADE FEDERAL DO RIO GRANDE DO SUL
ESCOLA DE ENGENHARIA
PROGRAMA DE PÓS-GRADUAÇÃO EM ENGENHARIA DE MINAS
METALÚRGICA E DE MATERIAIS - PPGE3M
LABORATÓRIO DE TECNOLOGIA MINERAL E AMBIENTAL - LTM

**ESTUDOS DE GERAÇÃO, CARACTERIZAÇÃO E USO DE
NANOBOLHAS NA FLOTAÇÃO DE ÁGUAS OLEOSAS**

Henrique Alberton de Oliveira

Dissertação apresentada ao programa de pós-graduação em engenharia de Minas, Metalúrgica e de Materiais da Universidade Federal do Rio Grande do Sul, como requisito parcial à obtenção do título de mestre em engenharia.

Área de concentração: Tecnologia Mineral, Ambiental e Metalurgia Extrativa.

Orientador:

Prof. Dr. Jorge Rubio

**Porto Alegre
2018**

“Não somos feitos sábios pela lembrança do passado, mas pela responsabilidade por nosso futuro”

George Bernard Shaw

Esta Dissertação será julgada para a obtenção do título de Mestre em Engenharia, área de concentração em Tecnologia Mineral, Ambiental e Metalurgia Extrativa pela seguinte Banca Examinadora do Curso de Pós-Graduação.

ORIENTADOR: PROF. DR. JORGE RUBIO

BANCA EXAMINADORA:

PROF. DR. ANDREA MOURA BERNARDES (PPGE3M – UFRGS)
PROF. DR. IVO ANDRÉ HOMRICH SCHNEIDER (PPGE3M – UFRGS)
DR. RAFAEL NEWTON ZANETI (DMAE)

Prof. Dr. Carlos Pérez Bergmann
Coordenador do PPGE3M/UFRGS

AGRADECIMENTOS

Às instituições MCTI/CNPq, FAPERGS e MEC/UFRGS/PPGE3M, pela bolsa de auxílio, pela verba para pesquisa, pelo suporte nas publicações e pela estrutura de excelência.

À minha mãe, Maria Lúcia, pelo apoio incondicional ao longo de toda minha formação. À minha família, pelo suporte e alento. À Marina, pelo amor, amizade e parceria. Aos meus amigos que estão comigo há tanto tempo.

Ao Laboratório de Tecnologia Mineral e Ambiental - LTM, na pessoa do seu coordenador – Jorge Rubio, pelo *Know-how* e *know-why* que me foram transmitidos.

À empresa Hidrocicle, pela parceria na execução de projetos que possibilitaram a aquisição de equipamentos e infraestrutura do LTM, permitindo a realização desse trabalho.

Aos colegas e amigos do LTM, Prof. Ivo André Schneider, André Azevedo, Ramiro Etchepare, Ana Flávia Rosa, Cassiano Rossi, Márcio Nicknig, Beatriz Firpo, Jéssica Weiler, e todos os outros que direta ou indiretamente colaboraram na realização do trabalho.

A todos os alunos bolsistas de Iniciação Científica do LTM, especialmente para Luciana Kaori, Luísa Neves, Marcelle Gressler, Caroline Alonso, Meiri Michita, que foram peças fundamentais na execução da metodologia experimental.

Aos amigos e colaboradores, Marcelo Fermann, Rafael Zaneti e Alex Rodrigues, por todo apoio técnico na montagem dos sistemas experimentais e discussões técnicas.

LISTA DE FIGURAS

- Figure 1.** Schematic illustration of the NBs generation system: (1) Feed water tank; (2) Ball valve; (3) Vacuum meter; (4) Centrifugal multiphase pump; (5) Pressure tank; (6) Pressure gauge; (7) Flowmeter; (8) Pressure gauge; (9) Needle valve; (10) Column; (11) Pressure sensors; (12) Sampler; (13) Temperature sensor; (14) pH meter; (15) LTM B-Sizer; (16) Recycling hose; (17) Atmospheric air; (18) Cooler; (19) Heat exchanger ... 25
- Figure 2.** NBs mean Sauter diameter as a function of the number of generation cycles for various saturation pressures. Liquid flow rate = 1000 L h⁻¹; air/liquid ratio = 7.5%; deionized water; pH 6 ± 0.4; surface tension = 72.2 mN m⁻¹ ± 0.2 28
- Figure 3.** NBs mean Sauter diameter as a function of the number of generation cycles at various saturation pressures. Liquid flow rate = 1000 L h⁻¹; air/liquid ratio = 7.5%; α-[Terpineol] = 100 mg L⁻¹; pH 6 ± 0.4; Surface tension = 50 mN m⁻¹ ± 1..... 29
- Figure 4.** Effect of the number of generation cycles on NBs concentration. Liquid flow rate = 1000 L h⁻¹; air/liquid ratio = 7.5%; deionized water; pH 6 ± 0.4. Surface tension = 72.2 mN m⁻¹ ± 0.2. 30
- Figure 5.** Effect of the number of generation cycles on NBs concentration. Liquid flow rate = 1000 L h⁻¹; air/liquid ratio = 7.5%; [α-terpineol] = 100 mg L⁻¹; pH 6 ± 0.4. Surface tension = 50 mN m⁻¹ ± 1..... 31
- Figure 6.** Effect of the number of generation cycles on NBs concentration (NBs ml⁻¹) without air injection. Liquid flow rate = 1000 L h⁻¹; DI water; pH 6 ± 0.4; surface tension = 72.2 mN m⁻¹ ± 0.2. 33
- Figure 7.** Effect of the number of generation cycles on NBs concentration (NBs ml⁻¹) without air injection. Liquid flow rate = 1000 L h⁻¹; [α-Terpineol] = 100 mg L⁻¹; pH 6 ± 0.4; surface tension = 50 mN m⁻¹ ± 1..... 34
- Figure 8.** Effect of operating pressure of the multiphase centrifugal pump on bubble generation. Conditions: pH 6 ± 0.3; Air/liquid ratio = 7.5%; Liquid flow rate = 1000 L h⁻¹, surface tension = 72.5 mN m⁻¹ (except condition "F"): A) Pressure = 1.5 bar; B) Pressure = 2.5 ar; C) Pressure = 3 bar; D) Pressure = 4 bar; E) Pressure = 5 bar; F) Pressure = 2.5 bar (surface tension = 50 mN m⁻¹); Temperature = 21 ° C ± 1..... 34
- Figure 9.** Effect of operating pressure on air holdup and concentration of NBs. Liquid flow rate = 1000 L h⁻¹; Air / liquid ratio = 8%; [α-Terpineol] = 100 mg.L⁻¹; pH 6 ± 0.4; surface tension = 50 ± 1 mN.m⁻¹. 36

- Figure 10.** Concentration of NBs as a function of storage time. The 0.0 point in the abscissa refers to the measurement performed (size obtained) 10 min after the generation of the NBs dispersion sample. Conditions: pH 6; $P_{\text{sat}} = 4$ bar; $[\alpha\text{-Terpineol}] = 100 \text{ mg L}^{-1}$ (surface tension = 50 mN m^{-1}); DI water (surface tension = 72.5 mN m^{-1}).
..... 37
- Figure 11.** Mean Sauter diameter of NBs as a function of storage time. The 0.0 point in the abscissa refers to the measurement performed (size obtained) 10 min after generation of the NBs dispersion sample. Conditions: pH 6; $P_{\text{sat}} = 4$ bar; $[\alpha\text{-terpineol}] = 100 \text{ mg L}^{-1}$ (surface tension = 50 mN m^{-1}); DI water (surface tension = 72.5 mN m^{-1}). 38
- Figure 12.** Flowchart of a mineral flotation unit with injection of MBs and NBs..... 39
- Figura 13.** Flowchart of a flocculation-flotation process for wastewater treatment with multiple bubble injection..... 40
- Figure 14.** Oily emulsion generation and treatment systems by flocculation-flotation with air MBs and NBs. (1) Saturator vessel; (2) Glass column for MBs separation and NBs isolation; (3) Glass column for flocculation and flotation stages and mechanical stirrer (Fisatom® 713D); (4) Ultra Turrax emulsifier for oil in water mixture..... 46
- Figure 15.** Flocculation-flotation for oil removal with MBs and NBs as a function of Dismulgan concentration. Conditions: initial [oil] = $337\text{-}484 \text{ mg L}^{-1}$; $[\text{NaCl}] = 30 \text{ g L}^{-1}$; pH 7; Saturation pressure = 5 bar; Saturation time = 30 min; Flotation time = 5 min. The error bars correspond to the standard deviation of triplicate tests. 50
- Figure 16.** Microphotographs of the different stages of the treatment of oily emulsion by flocculation-flotation: a) oily emulsion after free oil phase separation; b) oily flocs; c) treated water after 5 min of flotation. Conditions: initial [oil] = 390 mg L^{-1} ; $[\text{NaCl}] = 30 \text{ g L}^{-1}$, pH 7; $[\text{Dismulgan}] = 5 \text{ mg L}^{-1}$; $P_{\text{sat}} = 5$ bar; Saturation time = 30 min; Recycle rate = 25%; Flotation time = 5 min. 51
- Figure 17.** Oil removal efficiency by flocculation-flotation with MBs and NBs as a function of the saturation pressure and in the presence and absence of the flocculant (Dismulgan). Conditions: initial [oil] = $334 - 450 \text{ mg L}^{-1}$; $[\text{NaCl}] = 30 \text{ g L}^{-1}$; $[\text{Dismulgan}]$ concentration = 5 mg L^{-1} ; pH 7; Saturation time = 30 min; Recycle rate = 25%; Flotation time = 5 min. The error bars correspond to the standard deviation of the triplicate tests..... 52
- Figure 18.** Residual oil concentration after flocculation-flotation with MBs and NBs as a function of saturation pressure. Conditions: initial [oil] = $334 - 450 \text{ mg L}^{-1}$; $[\text{NaCl}] =$

30 g L ⁻¹ ; [Dismulgan] = 5 mg L ⁻¹ ; pH 7; Saturation time = 30 min; Recycle rate = 25%; Flotation time = 5 min; Emission limit = 29 mg L ⁻¹ . The error bars correspond to the standard deviation of the triplicate tests.....	53
Figure 19. Flocculation-flotation kinetics of oily flocs. Conditions: initial [oil] = 335 - 480 mg L ⁻¹ ; [NaCl] = 30 g L ⁻¹ ; [Dismulgan] = 5 mg L ⁻¹ ; pH 7; Saturation time = 30 min; Recycle rate = 25%.....	54
Figure 20. Efficiency of oil removal by flocculation-flotation assisted by NBs. Conditions: initial [oil] = 375 - 410 mg L ⁻¹ ; [NaCl] = 30 g L ⁻¹ ; pH 7; Saturation pressure = 2.5 bar; Saturation time = 30 min; Recycle rate of flotation = 25%; Flotation time = 5 min. The error bars correspond to the standard deviation of the triplicate tests.	55
Figure 21. Flotation kinetics of oily flocs with injection of isolated NBs, using oily emulsions with and without NaCl (30 g L ⁻¹). Conditions: [NaCl] = 30 g L ⁻¹ ; [Dismulgan] = 5 mg L ⁻¹ ; pH 7; Saturation pressure = 2.5 bar; Saturation time = 30 min; Recycle rate = 25%. The initial oil corresponds to the oil concentration after the phase separation step. The error bars correspond to the standard deviation of the triplicate tests.....	57
Figure 22. Oily emulsion generation unit 1) Water feed tank; 2) Helical high-pressure pump; 3) Manometers ; 4) Crude oil feed tank; 5) Oil dosing piston pump; 6) Flow constrictor (needle valve); 7) Oily emulsion storage tank; 8) Recirculation mixing pump.....	65
Figure 23. Oily emulsion treatment system by flocculation-column flotation. 1) Oily emulsion storage tank; 2) Air injection; 3) CMP; 4) Flow-meter; 5) Manometer; 6) Pressure vessel; 7) Needle valve; 8) Manometer; 9) Chemicals (flocculant polymer and NaOH) tanks; 10) Dosing pumps; 11) Rapid mixing FGR®; 12) Slow mixing FGR®; 13) Sampling point; 14) Flotation column; 15) Treated water outlet; 16) Sludge outlet.	67
Figure 24. Flocculation-column flotation unit for oily water treatment (3D perspective).	68
Figure 25. Emulsified oil separation by flocculation-column flotation. Effect of Dismulgan concentration on the residual oil and turbidity. Conditions: pH 7; liquid flow = 1 m ³ h ⁻¹ ; air/liquid ratio = 7.5% v/v; flotation column height = 1.5 m; HL = 10 m h ⁻¹ ; pump pressure = 4 bar; [oil feed] = 400 – 570 mg L ⁻¹	69

- Figure 26.** Emulsified oil separation by flocculation-column flotation. Effect of flotation column height. Conditions: pH 7; [Dismulgan] = 20 mg L⁻¹; air/liquid ratio = 7.5%; HL = 10 m h⁻¹; pump pressure = 4 bar. 70
- Figure 27.** Separation of emulsified oil by flocculation-column flotation with MBs and NBs. Effect of HL on oil removal efficiency. Conditions: pH 7; [Dismulgan] = 20 mg L⁻¹; air/liquid ratio = 7.5%; flotation column height = 2.5 m; pump pressure = 4 bar. [Oil feed] = 64 – 545 mg L⁻¹ 72
- Figura 28.** Fluxograma de processo de floculação-flotação para tratamento de efluentes líquidos com múltipla injeção de bolhas. ¹NBs geradas por vaso saturador ou bomba centrífuga multifásica – injeção de dispersão de NBs isoladas; ²Geração conjunta de MBs e NBs por bomba centrífuga multifásica. 81

LISTA DE TABELAS

Table 1. Concentration of NBs formed under various operating pressures at bench scale, using a saturation vessel, compared with a centrifugal multiphase pump (CMP). [α -Terpineol] = 100 mg L ⁻¹ (surface tension = 50 mN m ⁻¹); DI water (surface tension = 72.4 mN m ⁻¹).....	31
Table 2. Crude oil physicochemical and interfacial properties.....	45
Table 3. Oil removal by flocculation-flotation with MBs and NBs as a function of saturation pressure. Conditions: initial [oil] = 334-450 mg L ⁻¹ ; [NaCl] = 30 g L ⁻¹ ; [Dismulgan] concentration = 5 mg L ⁻¹ ; pH 7; Saturation time = 30 min; Recycle rate = 25%; Flotation time = 5 min. Mean values (standard deviation) of quadruplicate tests.	52
Table 4. Flocculation-flotation kinetics of oil with MBs and NBs. Experimental data on oil removal and correlation coefficients were calculated using the first order flotation kinetic model. Conditions: k = 1.3 min ⁻¹ (P _{sat} = 3.5 bar) and k = 1.8 min ⁻¹ (P _{sat} = 5 bar); pH 7; Dismulgan = 5 mg L ⁻¹ ; Saturation time = 30 min; Recycle rate = 25%.....	54
Table 5. Oil removal by flocculation-flotation assisted by NBs. Conditions: [NaCl] = 30 g L ⁻¹ ; pH 7; Saturation pressure = 2.5 bar; Saturation time = 30 min; Recycle rate = 25%; Flotation time = 5 min. Mean values (standard deviation) of triplicate experiments.....	56
Table 6. Crude oil physicochemical and interfacial properties.....	63
Table 7. Design and operation parameters of the flocculation-flotation units for oily water treatment. The residence times and G were calculated for the flows of 1 and 3 m ³ hour ⁻¹ , respectively.....	66
Table 8. Emulsified oil separation by flocculation-column flotation with MBs and NBs. Oil removal and turbidity reduction results of 8 replicates. Conditions: pH 7; HL = 10 m h ⁻¹ ; liquid flow = 1 m ³ h ⁻¹ ; air/liquid ratio = 7.5% v/v; column height = 2.5 m; [Dismulgan] = 20 mg L ⁻¹ , pump pressure = 4 bar, [NaCl] = 30 g L ⁻¹ and 100 g L ⁻¹	71

LISTA DE SÍMBOLOS

ΔF – Energia requerida na formação de bolhas de ar

γ - Tensão Superficial

μm – Micrômetro

ε_g – *Holdup* de gás

AFM – *Atomic Force Microscopy*

CONAMA – Conselho Nacional de Meio Ambiente

C_0 – Concentração inicial

C_f – Concentração final

d = Diâmetro

D_{32} – Diâmetro Médio de Sauter (volumétrico)

DAF – *Dissolved Air Flotation*

DI - Deionizada

DLS – *Dynamic Light Scattering*

EPA – *United States Environmental Protection Agency*

FAD – Flotação por Ar Dissolvido

F-NBs – Flotação com nanobolhas isoladas

G – Gradiente de velocidade

J_g – Velocidade superficial de gás

h = Altura

HL – *Hydraulic Loading*

k = Constante cinética

L = litro

LTM – Laboratório de Tecnologia Mineral e Ambiental

MBs – Microbolhas

NBs – Nanobolhas

nm - Nanômetro

NTA – *Nanoparticle Tracking Analysis*

NTU – Unidades Nefelométricas de Turbidez

P_o – Pressão Atmosférica

P+L – Produção mais limpa

P&D&I – Pesquisa, desenvolvimento e inovação

Psat – Pressão de Saturação

PZ – Potencial Zeta

Q_{ar} – Vazão de gás (ar)

Q_l – Vazão de líquido

r – Raio da bolha

R – Remoção calculada (experimental)

R_∞ - Remoção em condições estacionárias (teórica)

RGF[®] – Reator Gerador de Flocos

Rpm – Rotações por minuto

S_b – Fluxo superficial de bolhas

TAS – Taxa de aplicação superficial

T_{sup} – Tensão Superficial

UFRGS – Universidade Federal do Rio Grande do Sul

RESUMO

A presente dissertação consiste na apresentação de 3 artigos, envolvendo estudos básicos de geração e caracterização de micro e nanobolhas, e aplicação na flotação de óleo emulsificado em solução aquosa (salina). Nanobolhas ($D_{32} = 150 - 250$ nm) foram geradas por uma bomba centrífuga multifásica (Nikuni KTMD20N) e válvula agulha em uma coluna de reciclo, em pressões de operação variadas e diferentes tensões interfaciais ar/líquido. As nanobolhas foram resistentes ao cisalhamento causado no rotor da bomba e a altas pressões de operação, atingindo a maior concentração numérica ($4,1 \times 10^9$ nanobolhas mL^{-1}) na pressão de operação de 5 bar e tensão interfacial de 49 mN m^{-1} (holdup de ar = 6,8%). Em escala de bancada, emulsões oleosas (petróleo cru) em água salina foram floculadas utilizando uma poliacrilamida catiônica em pH 7. As melhores remoções de óleo foram obtidas na flotação com micro e nanobolhas utilizando uma pressão de saturação de 5 bar e 5 mg L^{-1} de Dismulgan. A flotação seguiu um modelo cinético de primeira ordem, com k de 1,3 e $1,8 \text{ min}^{-1}$ para P_{sat} de 3,5 e 5 bar, respectivamente. A injeção de nanobolhas em uma etapa de condicionamento após a floclação aumentou a eficiência geral da separação em até 11%. A separação com nanobolhas isoladas mostrou uma eficiência de remoção de óleo de 75 e 90%, com e sem NaCl (30 g L^{-1}). Foi estudado o processo de floclação em linha e flotação em coluna para o tratamento de emulsões oleosas contendo $70\text{-}400 \text{ mg L}^{-1}$ (turbidez = $70\text{-}226$ NTU) de óleo (petróleo cru) e salinidade (30 e 100 g L^{-1} NaCl). A floclação foi realizada com uma poliacrilamida catiônica, em dois Reatores Geradores de Flocos (RGF[®]), com estágios de mistura rápida e lenta (perda de carga = $0,9$ a $3,5$ bar). A flotação foi realizada em duas colunas ($1,5$ e $2,5$ m), com microbolhas ($5\text{-}80 \mu\text{m}$) e nanobolhas ($50\text{-}300$ nm de diâmetro, 10^8 nanobolhas mL^{-1}) geradas por uma bomba centrífuga multifásica e uma válvula agulha. A maior eficiência foi obtida com a coluna mais alta, em uma taxa de aplicação de 10 m h^{-1} , reduzindo o teor de óleo residual para 4 mg L^{-1} e turbidez para 7 NTU. Em alta taxa de aplicação superficial ($27,5 \text{ m h}^{-1}$), as concentrações de óleo residuais ficaram abaixo do padrão de emissão para plataformas marítimas (EPA - 29 mg L^{-1}), atingindo 18 mg L^{-1} .

ABSTRACT

The present dissertation consists in the presentation of 3 articles, involving basic studies on the generation and characterization of micro and nanobubbles, and application in flotation of emulsified oil in aqueous solution (saline). Nanobubbles ($D_{32} = 150-250$ nm) were generated by a centrifugal multiphase pump (Nikuni KTMD20N) and a needle valve in a recycle column, at various operating pressures and different air/liquid interfacial tensions. The nanobubbles were resistant to shear caused in the pump impellers and to high operating pressures, reaching the highest numerical concentration (4.1×10^9 nanobubbles mL^{-1}) at the operating pressure of 5 bar and interfacial tension of 49 mN m^{-1} (air holdup = 6.8%). On the bench scale, oily emulsions (crude oil) in saline water were flocculated using a cationic polyacrylamide at pH 7. The best oil removals were obtained in flotation with micro and nanobubbles using a saturation pressure of 5 bar and 5 mg L^{-1} of Dismulgan. The flotation followed a first-order kinetic model, with k of 1.3 and 1.8 min^{-1} for P_{sat} of 3.5 and 5 bar, respectively. Injection of nanobubbles in a conditioning stage after the flocculation increased the overall separation efficiency by up to 11%. Separation with isolated nanobubbles showed an oil removal efficiency of 75 and 90%, with and without NaCl (30 g L^{-1}). The in-line flocculation and column flotation process for the treatment of oily emulsions containing $70-400 \text{ mg L}^{-1}$ (turbidity = $70-226$ NTU) of oil (crude oil) and salinity (30 and 100 g L^{-1} NaCl) was studied. The flocculation was performed with a cationic polyacrylamide in two Flocc Generator Reactors (FGR[®]), with fast and slow mixing stages (load loss = 0.9 to 3.5 bar). The flotation was carried out in two columns (1.5 and 2.5 m), with microbubbles ($5-80 \mu\text{m}$) and nanobubbles (50-300 nm in diameter, 10^8 nanobubbles mL^{-1}) generated by a centrifugal multiphase pump and a needle valve. The highest efficiency was obtained with the highest column, with a hydraulic loading of 10 m h^{-1} , reducing the residual oil content to 4 mg L^{-1} and turbidity to 7 NTU. At high hydraulic loading (27.5 m h^{-1}), the residual oil concentrations were below the emission standard for offshore platforms (EPA - 29 mg L^{-1}), reaching 18 mg L^{-1} .

Sumário

1	INTRODUÇÃO	13
1.1	OBJETIVOS.....	15
1.1.1	Objetivo Geral	15
1.1.2	Objetivos Específicos.....	15
1.2	PLANO DE DISSERTAÇÃO.....	15
2	Integração dos artigos científicos.....	16
2.1	Artigo I – Nanobolhas: geração utilizando uma bomba multifásica, propriedades e características na flotação	17
2.2	Artigo II – Separação de petróleo emulsificado em água salina por flotação por ar dissolvido com micro e nanobolhas	17
2.3	Artigo III – Separação de petróleo emulsificado em água salina por flotação por ar dissolvido com micro e nanobolhas geradas por bomba centrífuga	18
3	Nanobubbles: generation using a multiphase pump, properties and features in flotation	21
3.1	INTRODUCTION	22
3.2	EXPERIMENTAL.....	23
3.2.1	Nanobubbles generation system	24
3.2.2	Nanobubbles characterization	25
3.2.3	Effect of operating pressure and water surface tension on NBs size and concentration.....	27
3.2.4	Effect of NBs generation cycles on NBs size and concentration	27
3.2.5	Microbubbles and air holdup measurements.....	27
3.3	RESULTS AND DISCUSSION.....	28
3.4	FINAL REMARKS	38
3.5	CONCLUSIONS	40
3.6	ACKNOWLEDGEMENTS	41

4	Separation of emulsified crude oil in saline water by dissolved air flotation with micro and nanobubbles	43
4.1	Introduction	44
4.2	Materials and methods	45
4.2.1	Synthetic produced water.....	45
4.2.2	Flocculation-flotation studies for oil/water separation	46
4.2.3	Flotation with MBs and NBs.....	47
4.2.4	Flotation assisted by NBs.....	48
4.2.5	Flotation with isolated NBs (F-NBs).....	48
4.2.6	Microscopy imaging	49
4.2.7	Oil concentration analysis	49
4.3	Results and discussion	49
4.3.1	Flotation with MBs and NBs.....	49
4.3.2	Flotation assisted by NBs.....	55
4.3.3	Flotation with isolated NBs (F-NBs)	56
4.4	Conclusion.....	57
4.5	ACKNOWLEDGEMENTS	58
5	Separation of emulsified crude oil in saline water by flotation with micro and nanobubbles generated by a multiphase pump	60
5.1	INTRODUCTION	61
5.2	EXPERIMENTAL.....	63
5.2.1	Materials.....	63
5.2.2	Oil-in-water emulsion generation system	64
5.2.3	Bubble generation.....	65
5.2.4	Flocculation.....	65
5.2.5	Flotation	66
5.3	RESULTS AND DISCUSSION.....	68

5.3.1	Effect of the flocculant concentration.....	68
5.3.2	Effect of flotation column height.....	69
5.3.3	Effect of Hydraulic Loading	71
5.4	FINAL REMARKS	73
5.5	CONCLUSIONS	74
5.6	ACKNOWLEDGEMENTS	74
6	OUTRAS Produções científico-tecnológicas	76
7	Considerações finais.....	77
8	Conclusões	79
9	Sugestões de trabalhos futuros.....	80
10	REFERÊNCIAS BIBLIOGRÁFICAS	83

1 INTRODUÇÃO

Nanobolhas (NBs) são cavidades gasosas com tamanho de diâmetro na escala nanométrica (1–1000 nm). Ocorrem como unidades altamente estáveis, dispersas em meio líquido (*bulk NBs*), ou adsorvidas em superfícies sólidas (NBs interfaciais ou superficiais), e não apresentam movimento de ascensão típico de microbolhas (MBs; 1–100 μm) e bolhas macrométricas ($\sim 100 \mu\text{m}$ –2 mm). Devido a peculiaridades nas suas propriedades físicas, químicas e físico-químicas, o potencial de aplicação das NBs em diversos processos vem sendo intensamente pesquisado por diversos autores nos últimos anos, incluindo a flotação mineral e a flotação avançada de poluentes aquosos.

As principais propriedades das NBs são a alta estabilidade, longevidade e rápida adesão em superfícies e partículas coloidais hidrofóbicas. Estas características têm ampliado o número de aplicações na medicina, na limpeza de superfícies, na indústria da mineração, em sistemas de geração de energia, na agricultura, na aceleração do metabolismo em espécies animais e vegetais, na composição de concretos pozolânicos, na remoção de poluentes e outras áreas diversas (Agarwal et al., 2011; Azevedo et al., 2016; Cavalli et al., 2015; Ebina et al., 2013; Khoshroo et al., 2018; Liu et al., 2008; Liu et al., 2012; Lukianova-Hleb et al., 2014; Lukianova-Hleb et al., 2012; Oshita & Liu, 2013).

As principais aplicações das NBs na área ambiental (flotação de poluentes aquosos e tratamento de efluentes) incluem a remoção de precipitados coloidais e nanopartículas (orgânicas e inorgânicas) por flotação assistida por NBs ou por NBs isoladas (processo de “flutuação” – separação de partículas coloidais pela diminuição da densidade dos agregados) (Amaral Filho et al., 2016; Etchepare et al., 2017; Calgaroto et al., 2016), limpeza de superfícies sólidas (Liu e Craig, 2009; Zhu et al., 2016), defouling e/ou prevenção de fouling de membranas de tratamento de águas e efluentes ou da indústria química e alimentícia (Wu et al., 2008; Ghadimkhani et al., 2016), aeração de sistemas aeróbios e no crescimento de micro-organismos específicos utilizados no tratamento de efluentes e/ou remediação de áreas degradadas (Temesgen et al., 2017), e a remediação de ambientes aquáticos degradados (Hu e Xia, 2018).

Embora o potencial tecnológico da utilização de NBs seja enorme, ainda são muito poucas as aplicações dessas tecnologias em escala real, principalmente nas áreas de

engenharia, estando ainda limitadas ao setor acadêmico, em fase de pesquisa e desenvolvimento de tecnologias para transferência ao setor produtivo e de serviços. Maiores investigações na geração e aplicações sustentáveis dessas bolhas nanométricas são necessárias para viabilização de produtos tecnológicos na área de tratamento e reúso de águas e efluentes líquidos.

Diversos processos geram efluentes contaminados com óleos, como na extração de petróleo (água produzida) e indústrias que utilizam derivados de combustíveis fósseis (gasolina, diesel, óleo BPF etc.). Há ainda águas oleosas oriundas da lavagem de pisos, tanques e peças, processos de usinagem, entre outros. Na forma emulsificada, o diâmetro de gotas de óleo está, frequentemente, abaixo de 50 μm . Sua separação por processos gravitacionais é difícil devido à estabilidade do sistema, sendo geralmente utilizados os processos físico-químicos auxiliados por agentes desestabilizantes (Da Rosa, 2002). O tratamento de efluentes oleosos em plataformas marítimas apresenta dificuldades técnicas devido às limitações de área física, peso dos equipamentos e o tempo de residência da água produzida a bordo, que geralmente não ultrapassa 15 min (Gabardo, 2007). Neste contexto, existe a necessidade de desenvolver e aprimorar processos de tratamento com alta taxa de processamento para este efluente, especialmente em unidades compactas, que ocupem áreas reduzidas nas plataformas.

A flotação por ar dissolvido (FAD) (Rodrigues e Rubio, 2007) é um método físico-químico de separação extensamente empregado no tratamento de águas e de efluentes oleosos emulsificados (Santander et al., 2011; Santo et al., 2012). A distribuição de tamanho de bolhas e gotas de óleo desempenha um papel fundamental na eficiência de flotação. As bolhas pequenas (micro e nanobolhas) apresentam grandes áreas superficiais, que são bastante úteis na agregação e separação das gotículas (Santander, Rodrigues, & Rubio, 2011; Saththasivam, Loganathan, & Sarp, 2016). Em células de flotação, o aumento da relação altura/diâmetro (H/D) proporciona uma maior probabilidade de colisão, adesão e arraste dos agregados (Yanatos et al., 1988). Desta maneira, a utilização de colunas como células de separação constitui uma alternativa tecnológica bastante promissora no tratamento de efluentes em alta taxa de aplicação superficial (m h^{-1}) (Rubio e Zaneti, 2009; Zaneti et al., 2012; 2011).

1.1 OBJETIVOS

1.1.1 Objetivo Geral

O objetivo geral desta dissertação é desenvolver estudos básicos de geração e caracterização de micro e nanobolhas, e aplicação na flotação de óleo emulsificado em solução aquosa (salina).

1.1.2 Objetivos Específicos

Os objetivos específicos são os seguintes:

- Projeto e montagem para a geração e caracterização de micro e nanobolhas de ar por cavitação hidrodinâmica utilizando uma bomba centrífuga multifásica e válvula agulha. Avaliação de parâmetros operacionais e comparação com a geração por depressurização de água saturada em ar;
- Estudo, em nível de bancada de flotação, para a separação de emulsões óleo/água, com: i. MBs e NBs conjuntas, ii. NBs isoladas, iii. condicionamento prévio com NBs.
- Estudo em nível piloto (regime contínuo), de remoção de óleo emulsificado em água salina, por floculação-flotação (floculação em linha e flotação em coluna), com geração conjunta de MBs e NBs por bomba centrífuga multifásica

1.2 PLANO DE DISSERTAÇÃO

Esta dissertação é apresentada na forma de artigos científicos, publicados em periódicos internacionais e está organizada em três partes, cada uma sendo constituída pelos seguintes itens:

Parte I: Introdução, Objetivos gerais e específicos e Integração de artigos;

Parte II: Artigos Científicos - Cada artigo científico representa um Capítulo, sendo dividido em, no mínimo: Introdução, Materiais e Métodos, Resultados, Conclusões e Referências Bibliográficas;

Parte III: Considerações finais, Produção Científico-Tecnológica Associada à Dissertação, Conclusões, Sugestões para trabalhos futuros e Bibliografias;

Os trabalhos elaborados e realizados durante esta dissertação foram desenvolvidos no Departamento de Engenharia de Minas da UFRGS, no Laboratório de Tecnologia Mineral e Ambiental – LTM.

2 INTEGRAÇÃO DOS ARTIGOS CIENTÍFICOS

A presente dissertação envolveu trabalhos de pesquisa em geração, caracterização e aplicação de dispersões aquosas de nanobolhas. Os estudos avaliaram os mecanismos envolvidos na geração e os efeitos das nanobolhas em processos de remoção de óleo emulsificado. O trabalho contribuiu para validar o potencial tecnológico das nanobolhas em sistemas de flotação na área ambiental.

Os principais avanços e metas técnicas do trabalho foram:

- i. O desenvolvimento de uma técnica otimizada de geração de NBs dispersas em água por cavitação hidrodinâmica utilizando uma bomba centrífuga multifásica e constritor de fluxo tipo válvula agulha, resultando em uma elevada concentração de bolhas por volume de dispersão;
- ii. Melhor entendimento dos efeitos da pressão de saturação e tensão interfacial do líquido na geração de NBs, e da confirmação da estabilidade destas dispersões de NBs em tempos longos;
- iii. Melhor entendimento das interações (aprisionamento e agregação) de NBs com gotículas de óleo emulsificado e dispersas;
- iv. Desenvolvimento e avaliação em escala de bancada de técnicas de flotação por ar dissolvido, flotação assistida por NBs e de "flutuação" com NBs isoladas na separação de óleo emulsificado;
- v. Desenvolvimento e aplicação em escala piloto de uma técnica de floculação em linha utilizando dispersões aquosas com grande concentração de NBs e MBs geradas por bomba centrífuga multifásica, para separação de óleo emulsificado por flotação em coluna;
- vi. Avaliação da influência dos parâmetros de processo concentração de reagente, altura de coluna e taxa de aplicação superficial na eficiência de separação de óleo emulsificado;
- vi. Transferência do conhecimento adquirido aos setores científico e produtivo, a partir de publicações em periódicos internacionais.

Estas metas técnicas foram os objetos das publicações internacionais realizadas e a integração destes artigos científicos alcança o objetivo geral proposto para esta dissertação.

Este trabalho foi objeto do Projeto Tecnova (2015-2017) - FAPERGS, intitulado "Desenvolvimento de projeto e qualificação de unidade de flotação a ar dissolvido para tratamento de água produzida", desenvolvido e executado no LTM em parceria com a empresa Hidrocicle.

2.1 ARTIGO I – NANOBOLHAS: GERAÇÃO UTILIZANDO UMA BOMBA MULTIFÁSICA, PROPRIEDADES E CARACTERÍSTICAS NA FLOTAÇÃO

A partir de referências de literatura que reportam as vantagens das NBs geradas por cavitação hidrodinâmica, por sistemas consistidos de bombas centrífugas e constritores de fluxo do tipo tubos de venturi adaptados (cavitation tube), na recuperação de partículas minerais em processos de flotação em coluna (Ahmadi et al., 2014; Fan et al., 2010a, 2010b, 2010c, 2010d; Sobhy, 2013; Sobhy & Tao, 2013), foi desenvolvido um estudo conceitual de geração de NBs em regime contínuo (recirculação de água), utilizando um sistema composto por bomba centrífuga e constritor de fluxo tipo válvula agulha, avaliando a concentração numérica de NBs por unidade de líquido e seu tamanho médio, buscando atingir uma condição ótima de geração de NBs em alta taxa.

Foi utilizado um equipamento com a técnica *Nanoparticle Tracking Analysis* (NTA, ZetaView[®], *Particle Metrix*, Alemanha), que permite a quantificação das NBs em sistemas líquidos (número de NBs mL⁻¹) e a sua caracterização físico-química com medidas de tamanho e potencial zeta. Foram avaliados parâmetros envolvidos na geração de NBs por cavitação hidrodinâmica (pressão de saturação e tensão interfacial do líquido).

2.2 ARTIGO II – SEPARAÇÃO DE PETRÓLEO EMULSIFICADO EM ÁGUA SALINA POR FLOTAÇÃO POR AR DISSOLVIDO COM MICRO E NANOBOLHAS

Neste artigo foi investigado o efeito das NBs na remoção de petróleo emulsificado em água salina, em escala de bancada. A descoberta da geração de NBs no processo de

FAD é um processo de separação das NBs e MBs (Calgaroto et al., 2014), e da remoção de precipitados coloidais de amina (Calgaroto et al., 2016) como antecedentes técnicos da pesquisa sobre nanobolhas no LTM motivaram a investigação dos seus efeitos nos processos de flotação para o tratamento de efluentes diversos, com poluentes-alvo orgânicos ou inorgânicos.

Este artigo avaliou os parâmetros concentração de reagente flocculante (poliacrilamida catiônica - Dismulgan) e pressão de saturação, na FAD aplicada na remoção de petróleo emulsificado. Foi obtida uma melhora na eficiência de separação quando os flocos oleosos foram condicionados com NBs previamente à injeção de bolhas maiores. Ainda, as NBs isoladas mostraram-se capazes de separar petróleo emulsificado. Os parâmetros de resposta foram o teor de óleo residual, eficiência de remoção e cinética de flotação.

Os resultados são explicados em termos de fenômenos interfaciais, que fazem com que as NBs auxiliem na agregação das gotículas de óleo (hidrofóbicas), diminuam sua densidade e aumentem a probabilidade de captura por outras bolhas.

2.3 ARTIGO III – SEPARAÇÃO DE PETRÓLEO EMULSIFICADO EM ÁGUA SALINA POR FLOTAÇÃO POR AR DISSOLVIDO COM MICRO E NANOBOLHAS GERADAS POR BOMBA CENTRÍFUGA

Este estudo abrange os conhecimentos desenvolvidos nos trabalhos anteriores, aplicando micro e nanobolhas geradas por uma bomba centrífuga multifásica na separação de óleo (petróleo) emulsificado por flocculação em linha e flotação em coluna

Foi desenvolvido um sistema de flocculação em linha e flotação em coluna, com alta taxa de aplicação superficial ($TAS > 10 \text{ m h}^{-1}$), para o tratamento de emulsões oleosas sintéticas contendo petróleo bruto (água produzida simulada). A flocculação em linha foi realizada em um flocculador hidráulico serpentinado do tipo Reator Gerador de Flocos (RGF[®]), produto de uma patente desenvolvida no LTM, e foi constituído de etapas de mistura rápida e lenta. Esta tecnologia permite a formação de flocos aerados, consistidos de gotículas de óleo com bolhas (NBs e MBs) aderidas/aprisionadas. Bolhas foram geradas por cavitação hidrodinâmica, utilizando uma bomba centrífuga multifásica e um constritor de fluxo tipo válvula agulha, no modelo do Artigo I. A coluna de flotação teve altura variável entre 1,5 e 2,5 m.

PARTE II

Artigo I

NANOBUBBLES: GENERATION USING A MULTIPHASE PUMP, PROPERTIES AND FEATURES IN FLOTATION

Artigo publicado no periódico Minerals Engineering, volume 112, 2017,
páginas 18-26.

3 NANOBUBBLES: GENERATION USING A MULTIPHASE PUMP, PROPERTIES AND FEATURES IN FLOTATION

Ramiro Etchepare, Henrique Oliveira, Marcio Nicknig, André Azevedo, Jorge Rubio*

Laboratório de Tecnologia Mineral e Ambiental, Departamento de Engenharia de Minas- PPGE3M, Universidade Federal do Rio Grande do Sul, Av. Bento Gonçalves, 9500, Prédio 43819 - Setor 6, CEP: 91501-970, Porto Alegre, RS, Brazil,

www.ufrgs.br/lm, *Corresponding author: jrubio@ufrgs.br

ABSTRACT

The importance of nanobubbles is now widely known, particularly their applications and potential in mineral processing. The actual challenge is to generate a high concentration of bubbles (number per water volume) in a sustainable manner at high flow rates. The main objective of this work was to develop a new method for generating highly-loaded nanobubbles aqueous solutions by hydrodynamic cavitation using a centrifugal multiphase pump (CMP) and a needle valve. Nanobubbles (150-200 nm) were formed, at 22°C, with the pump and a recycle column, at various operating pressures and air/liquid surface tension. Nanobubbles were resistant to shearing caused by pump impellers and to high operating pressures (up to 5 bar) throughout several bubble generation cycles. The size of the nanobubbles remained constant, and their numeric concentration increased as a function of these cycles, reaching equilibrium after 29 cycles; this was dependent on pump pressure and the surface tension of the solution. The highest concentration (4×10^9 nanobubbles mL^{-1}) was obtained at 5 bar and 49 mN m^{-1} surface tension (air holdup = 6.8% and D32 of microbubbles in the range between 62 – 70 μm). These phenomena can be explained by Henry's Law and the lower energy required for bubble formation when the interfacial tension (air / water) decreases and when the differential pressure in the cavitation zone increases. The mean diameter and concentration of these nanobubbles did not vary significantly over a period of two months, demonstrating the high stability of these concentrated nanobubbles. It is concluded that the procedure has great potential in future applications in ore flotation and wastewater treatment and reuse.

KEYWORDS: nanobubbles generation, multiphase pump, flotation

3.1 INTRODUCTION

The generation, characterization and application of nanobubbles (NBs) are fast-growing research areas. This interest is mainly attributed to important peculiarities of their physical, chemical and physicochemical properties. Their technological potential in several areas is now recognized, including advanced flotation to remove aqueous pollutants and enhance mineral fines values (Ahmadi et al., 2014; Fan et al., 2010a; Fan, Zhao, & Tao, 2012; FAN et al., 2010; Sobhy & Tao, 2013).

The main properties of NBs are their high stability, longevity and rapid adhesion onto hydrophobic surfaces. These features have expanded their applications in medicine, surface cleaning, mining, energy systems, agriculture, acceleration of metabolism in animal and plant species, removal of pollutants and other areas (Agarwal et al., 2011; Cavalli et al., 2015; Ebina et al., 2013, US20070286795, 2007, 8945353, 2015; G. Liu et al., 2008; S. Liu et al., 2012; Lukianova-Hleb et al., 2014, 2012; Oh, Han, & Kim, 2015; Polman, 2013).

Recent studies have demonstrated the potential of these NBs in the separation of amine and sulfate precipitates by dissolved air flotation (DAF) (Amaral Filho et al., 2016; Calgaroto et al., 2016). However, more research studies of the procedures for quantification and effective generation (higher concentration) are needed, as well as a better understanding of their interfacial (air/liquid, solid/liquid, air/air₂) and structural properties (mainly stability mechanisms).

The DAF process is a conventional method for treating liquid effluents bearing low solids content utilizing microbubbles (MBs – 30-70 μm diameters) and bubbles nucleation after passing a flow constrictor (Rafael Teixeira Rodrigues & Rubio, 2007; J. Rubio, Carissimi, & Rosa, 2007). The bubbles generation is based on a production of an air-saturated water (so called dead-end saturation) whereby the compressed air is injected into a pressurized vessel and water flows in counter-current through the vessel, dissolving away part of the air (Edzwald & Haarhoff, 2011). An upcoming alternative is called open-end saturation, where a centrifugal multiphase pump (CMP) is used for air saturation and bubbles generation by hydrodynamic cavitation (André Azevedo, Etchepare, & Rubio, 2017; C. H. Lee, An, Kim, Ahn, & Cho, 2007; Pioltine & Reali, 2011; R. N. Zaneti, Etchepare, & Rubio, 2013). Herein, the atmospheric air is continuously injected into the low-pressure suction side of a special CMP, where the

shearing effect caused by the pump impellers breaks the air into small bubbles and, as the water flows through the system, the high operating pressure and large interfacial area of the bubbles enhance the dissolution of air into the water.

It was recently reported that in the DAF process using saturator vessels, MBs and NBs are generated together (Calgaroto et al., 2014a) and a bubble separation technique was developed (Calgaroto et al., 2015b). Azevedo et al. (2016) studied the generation of NBs in a bench system which consisted of a saturator vessel and a needle valve and quantified the concentration of NBs as a function of saturation pressure and liquid surface tension.

This study is a continuation of a series focusing on the generation as highly loaded NBs aqueous dispersions, characterization, interfacial properties and stability/lifetime. This study was addressed to develop a method of generation and dispersion of air NBs in aqueous medium via hydrodynamic cavitation. A CMP was employed to generate air NBs and MBs in a semi-continuous system. Air NBs were characterized in terms of size, size distribution, concentration and stability, and the effects of generation cycles, air/liquid superficial tension, pump operational pressure and air injection were evaluated. Gas dispersion parameters as MBs size and air holdup were measured and calculated, respectively, at various operational conditions.

3.2 EXPERIMENTAL

Materials

Deionized (DI) water at room temperature ($22^{\circ}\text{C} \pm 1$) with a conductivity of $3 \mu\text{S}\cdot\text{cm}^{-1}$, a surface tension of $72.5 \pm 0.1 \text{ mN m}^{-1}$ and pH 5.5 was used to prepare NBs aqueous dispersions. DI water was obtained by ultrapurification of tap water with a reverse-osmosis cartridge and modules of ion-exchange resins and activated carbon.

A sulfochromic solution was used to remove any organic compounds from all glass materials, then rinsing with abundant DI water. NaOH and HCl solutions from Vetec[®] (Rio de Janeiro - RJ, Brazil) were used for pH adjustments.

α -Terpineol (supplied by Química Maragão; Turvo – SC, Brazil) ($\text{CH}_3 - \text{C}_6\text{H}_9 - (\text{OH}) - \text{C}_3\text{H}_5$), a 154 g mol^{-1} molecular weight commercial terpene alcohol, was used to reduce the water surface tension.

Methods

3.2.1 Nanobubbles generation system

Bubbles were generated in a semi-continuous system with a recycle column associated with a CMP as illustrated in Figure 1. The column, made of acrylic resin, had an internal diameter of 10 cm and 240 cm height. The main components of the bubble generation system were the stainless steel CMP (Nikuni, KTM20ND) and a needle valve with fine adjustment (Parker, N800, 1/2"). Atmospheric air was injected into the pump by vacuum pressure at a controlled flow with the aid of an air rotameter and sheared by pump impellers, resulting in an air/liquid mixture. The multiphasic flow was subjected to various operating pressures to dissolve air in water in a pressure tank (stainless steel); the saturated water was forced through the needle valve and injected into the base of the column for bubble generation.

The NBs generation system was operated by recirculation of a fixed volume of 40 L of DI water (or α -Terpineol solution) at a flow rate of 1,000 L h⁻¹. The superficial liquid velocity in the column was 0.035 m s⁻¹, and the residence time in the system was approximately 2.1 min. A PVC feed-water tank was equipped with a heat exchanger (cooling coil in stainless steel), and the water temperature in the system was controlled and adjusted to 22°C by circulation of refrigerated fluid (Maqtermo[®], LS 03 AR CF/220/GE).

Before the tests, the equipment was cleaned by circulating the sulfochromic acid solution for 5 min, followed by DI water rinsing for 10 min (three times). In the last cleaning procedure, the water conductivity and particle concentration were measured to ensure the absence of ions (maximum conductivity of 3 μ S.cm⁻¹) and nanoparticles (below the detection limit of the NTA analysis – see description in the next item, 10⁵ particles.mL⁻¹).

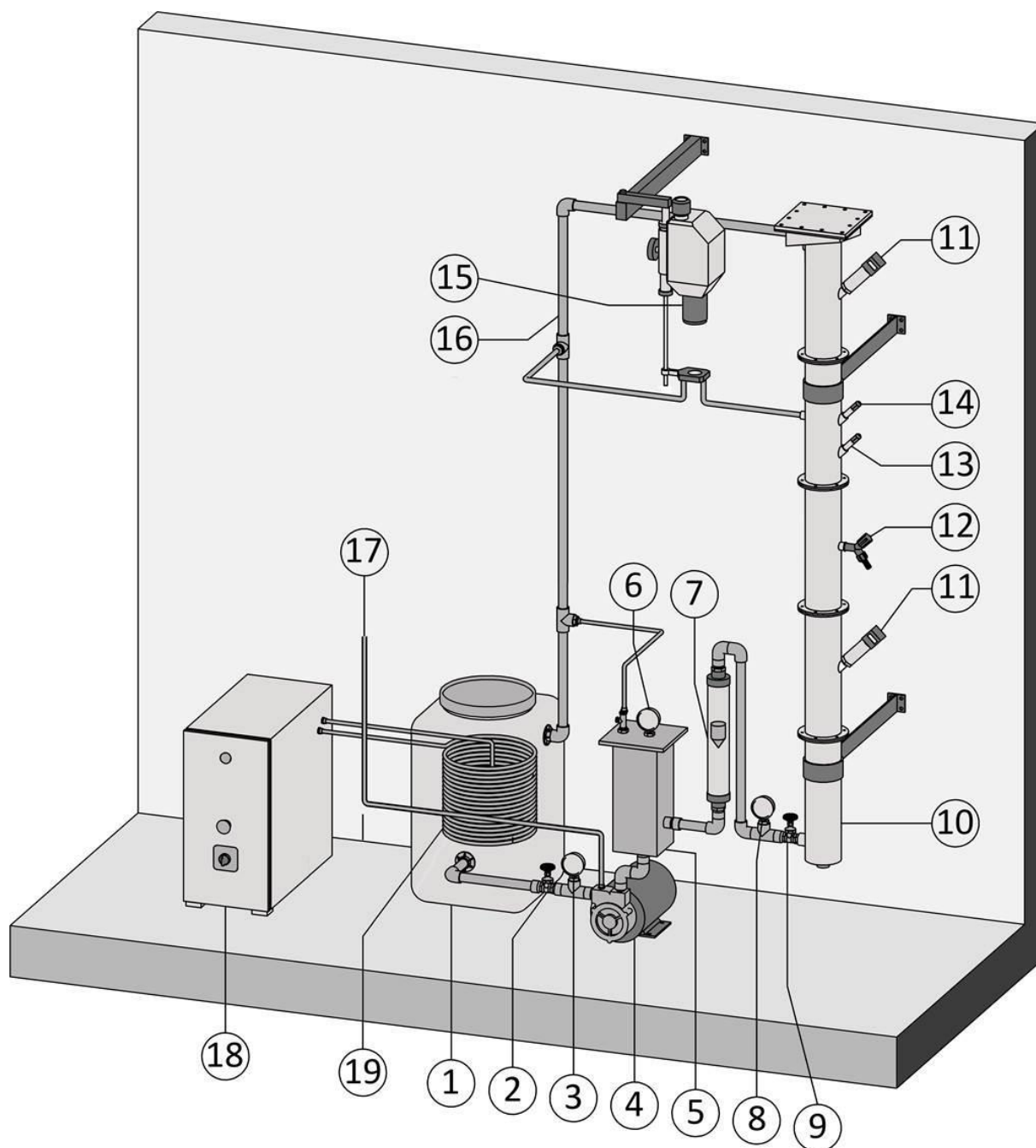


Figure 1. Schematic illustration of the NBs generation system: (1) Feed water tank; (2) Ball valve; (3) Vacuum meter; (4) Centrifugal multiphase pump; (5) Pressure tank; (6) Pressure gauge; (7) Flowmeter; (8) Pressure gauge; (9) Needle valve; (10) Column; (11) Pressure sensors; (12) Sampler; (13) Temperature sensor; (14) pH meter; (15) LTM B-Sizer; (16) Recycling hose; (17) Atmospheric air; (18) Cooler; (19) Heat exchanger

3.2.2 Nanobubbles characterization

Concentration, mean size and size distribution of NBs were measured in a nanoparticle tracking analysis (NTA) instrument (ZetaView[®], Particle Metrix, Germany) at room

temperature. ZetaView[®] is equipped with a built-in cell and a laser diffraction microscope with a video camera (CCD) to capture the motion of particles/bubbles.

The NTA technique explores light scattering and Brownian motion to obtain distribution size data for nanoparticles. A laser beam (525 nm) passes through the nanoparticles and is scattered, resulting in a compressed beam with a reduced profile and high power density. The suspended particles in the path of this beam scatter light are, visualized with the objective lens of the microscope. Then, a video camera captures particles within the field of the cell view.

ZetaView (version 8.02.30.02) records a video file of individual particles and simultaneously identifies and tracks the center of each particle frame by frame. The software determines the average distance moved by each particle in the x and y directions to determine the particle diffusion coefficient (Dt). The sample temperature (T) and solvent viscosity are measured and calculated, respectively, and the sphere-equivalent hydrodynamic diameter (d) of the bubbles can be measured using the Stokes-Einstein equation (Eq. 1).

$$Dt = \frac{TK_b}{3\pi\eta d} \quad (1)$$

Because the optical field of view is fixed and the depth of the illuminating beam is approximately 10 μm , the scattering volume can be estimated. By counting the bubbles within the field of view, it is possible to extrapolate this figure to an equivalent estimated value for concentration in terms of bubbles per mL.

For sample conditioning, a bubble separation procedure was conducted exploiting the fact that MBs rise and collapse at the liquid surface, while NBs remain in suspension for long periods (Calgaroto et al., 2015b). The samples containing NBs dispersions were carefully injected into the NTA cell using a sterile glass syringe (5 mL capacity) until the liquid reached the tip of the nozzle.

The obtained values of mean size, size distribution and number of NBs are the arithmetically calculated values for three measurements of each sample. The range of particle size measurement is from 10 nm to 3 μm , and the particle concentration vary from 10^5 to 10^{10} particles per mL.

3.2.3 Effect of operating pressure and water surface tension on NBs size and concentration

The NBs concentration and size were investigated in triplicate tests at different operating pressures (2.5 – 5 bar) and surface tension values. The air/water surface tension was modified with a 100 mgL⁻¹ α -Terpineol solution. The surface tension was determined at room temperature on a Kruss[®] tensiometer (Model 8451) using the *DuNouy* static method with a platinum ring.

3.2.4 Effect of NBs generation cycles on NBs size and concentration

Trials were conducted by recirculating water in the system up to 3 h to assess the effect of the continuous generation cycles of NBs. Each cycle corresponds to one residence time, equivalent to the total water volume pumped through the column overcoming the storage capacity of the system (40 L). Thus, samples were collected at various time intervals to determine size and concentration of NBs. Two different experiments were performed for each CMP operating with and without air injection) and surface tension.

3.2.5 Microbubbles and air holdup measurements

The MBs size distribution was measured using the LTM B-Sizer technique (R. T. Rodrigues & Rubio, 2003). This technique basically consists of MBs sampling within the flotation column (central spine) using a steel sampler tube. These samples were displayed in the glass horizontal display of a "cuvette cell", and digital images were obtained with the aid of a digital camera coupled to a microscope.

Captured images were processed using MATLAB[®] image analysis software. To analyze images generated from the LTM-BSizer and data generation (D32 calculation technique), a MATLAB[®] version 5.3.0.10183 (R11) script was used. For each result obtained, 30 images were analyzed.

At low surface tensions, when the concentration of MBs is high the bubbles overlap each other in the "cuvette cell", making difficult the sampling somewhat by the software; this increased the standard deviation of the D32 readings. To avoid this issue, a large number of images were considered and after qualitative analysis, the best ones were worked out with the software.

The air holdup (volume fraction of air bubbles in the water column) was calculated by measuring the pressure difference (Δp) between two points of the column filled with

water and bubbles using two hydrostatic pressure sensors (Pressure Transmitter SP98, Sitron®) calibrated to a pressure range from 0 to 0.15 bar and positioned in the column with 80 cm between them (Figure 1). A ΔP_0 (blank) was first measured using DI water without generating bubbles, so the decrease in the hydrostatic pressure after bubbles generation corresponds to the fraction of air bubbles injected in the system and the following equation 2 (Matiolo, Testa, Yianatos, & Rubio, 2011) was used to calculate the air holdup.

$$\text{Air Holdup} = \frac{\Delta P_0 - \Delta P}{\Delta P_0} \quad (2)$$

where

ΔP_0 = pressure difference in the blank sample;

ΔP = pressure difference after bubbles generation.

3.3 RESULTS AND DISCUSSION

Figures 2 and 3 show the effect of generation cycles on the average diameter of NBs which remained almost constant along the cycles, between 200 and 250 nm with a size distribution of 50-400 nm, indicating a low degree of NBs coalescence in this pump.

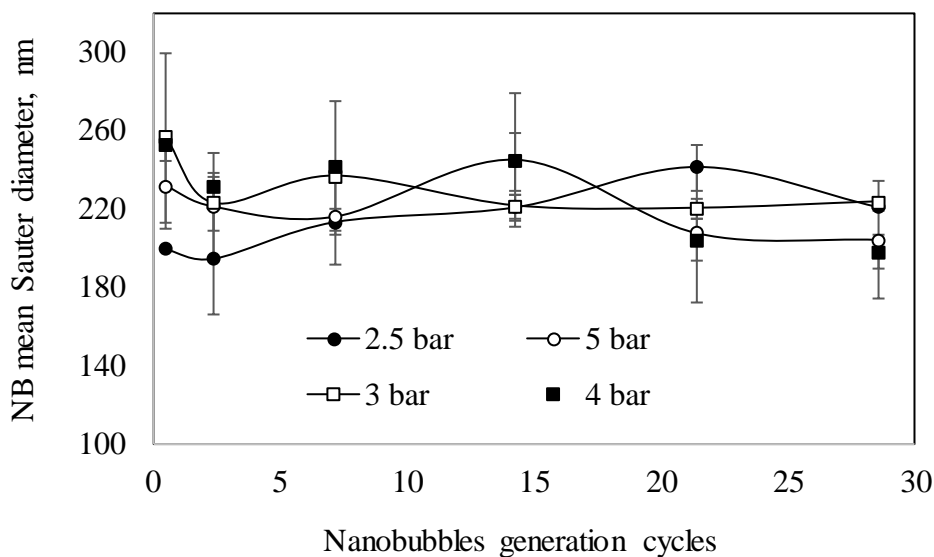


Figure 2. NBs mean Sauter diameter as a function of the number of generation cycles for various saturation pressures. Liquid flow rate = 1000 L h⁻¹; air/liquid ratio = 7.5%; deionized water; pH 6 ± 0.4; surface tension = 72.2 mN m⁻¹ ± 0.2

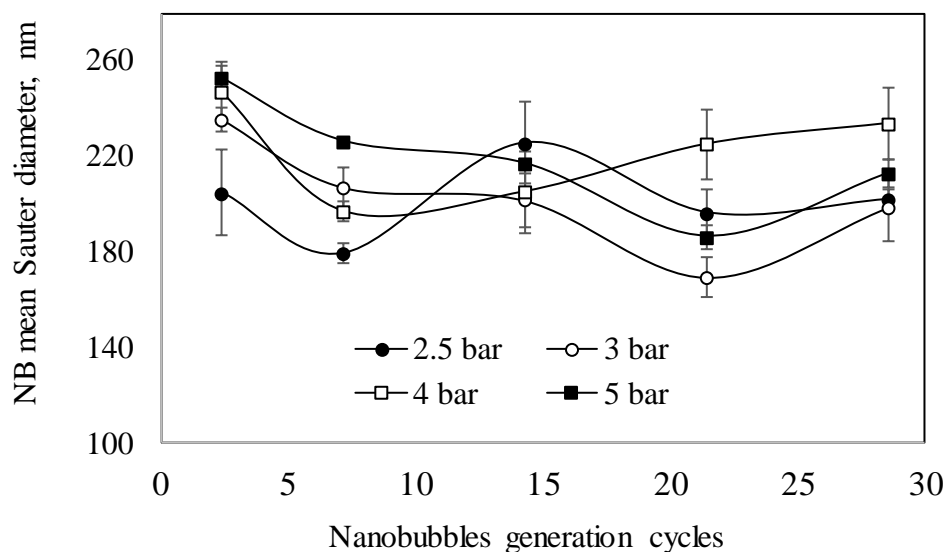


Figure 3. NBs mean Sauter diameter as a function of the number of generation cycles at various saturation pressures. Liquid flow rate = 1000 L h⁻¹; air/liquid ratio = 7.5%; α -[Terpineol] = 100 mg L⁻¹; pH 6 \pm 0.4; Surface tension = 50 mN m⁻¹ \pm 1.

The effect of operating pressure and the number of generation cycles on the concentration of NBs is shown in Figures 4 and 5. Herein, the NBs showed to be resistant to the shearing effect of the pump impellers and to high pressure during the several generation cycles (and air-saturation in water), increasing the concentration with the operating pressure and cycles. These results are close to those reported by Rodrigues and Rubio (2003) during MBs generation, explained by the Henry's Law. Thus, with increasing pressure, more air is dissolved; consequently, more cavities are formed, and more bubbles are generated when flow is depressurized through the needle valve. The increase in pressure upstream of the constriction device (needle valve) results in a higher-energy dissipation rate and a higher collapse pressure (Gogate and Pandit, 2000). Thus, an optimum inlet pressure should be ensured at a constant flow rate.

The highest NBs concentration in DI water (72.5 mN m⁻¹ surface tension) was obtained after 29 cycles (61 min), with values reaching 1.5 x 10⁸ NBs mL⁻¹ at a P_{sat} of 4-5 bar. Then, the concentration of NBs remained constant. This is due to an equilibrium condition, between the air dissolved in water (at a supersaturated condition) and the NBs formed and stabilized in solution. Under this condition, the air available for NBs

generation is completely diffused into the cavities and gas nuclei available; after this critical period, the generation of NBs ceased.

Figures 12 and 13 also show that the concentration of NBs in α -terpineol (50 mN m⁻¹ the air/liquid interfacial tension) was approximately 25 times higher than that obtained using DI water, reaching a maximum value of 4 x 10⁹ NBs mL⁻¹ after 29 cycles with a P_{sat} of 5 bar. This phenomenon is similar to that observed in the generation of MBs (Rodrigues and Rubio, 2003) and is explained in terms of the minimum energy required for bubble formation (T. Takahashi, Miyahara, & Mochizuki, 1979), which is lower when reducing the surface tension (Equation 3).

$$\Delta F = \frac{16\pi\gamma^3}{3(P_{sat}-P_o)^2} \quad 3$$

where γ is the surface tension of the liquid, and P_o is the atmospheric pressure.

The enhancement of the number of NBs in the presence of surfactant may also be attributed to interfacial phenomena. According to Klassen and Mokrousov, (1963), Wu, (1969) and Zhou, (1996), the stabilization of cavities and gas nuclei after the adsorption of surfactant at the air/liquid interface provides mechanical strength to resist pressure fluctuations. The presence of surfactants also reduces the intensity of bubble bursts as reported by Gogate and Pandit (2001).

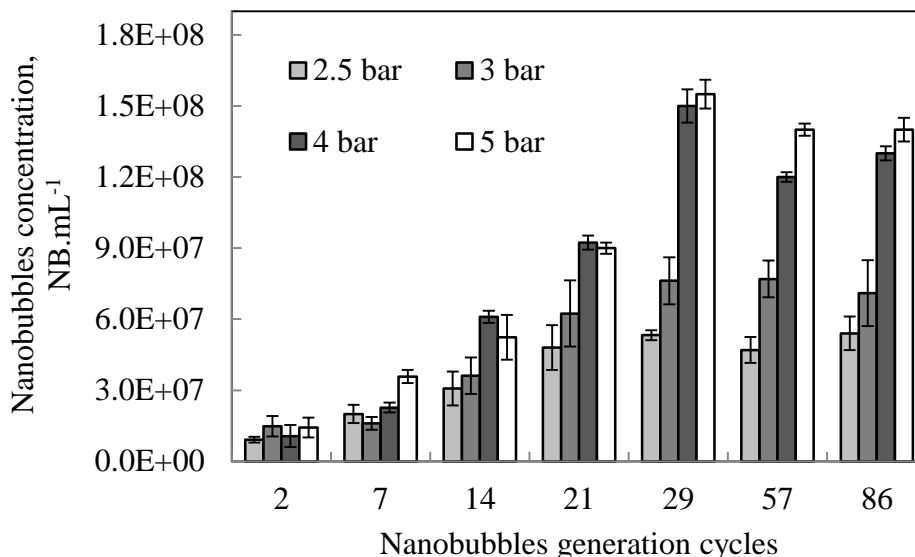


Figure 4. Effect of the number of generation cycles on NBs concentration. Liquid flow rate = 1000 L h⁻¹; air/liquid ratio = 7.5%; deionized water; pH 6 ± 0.4. Surface tension = 72.2 mN m⁻¹ ± 0.2.

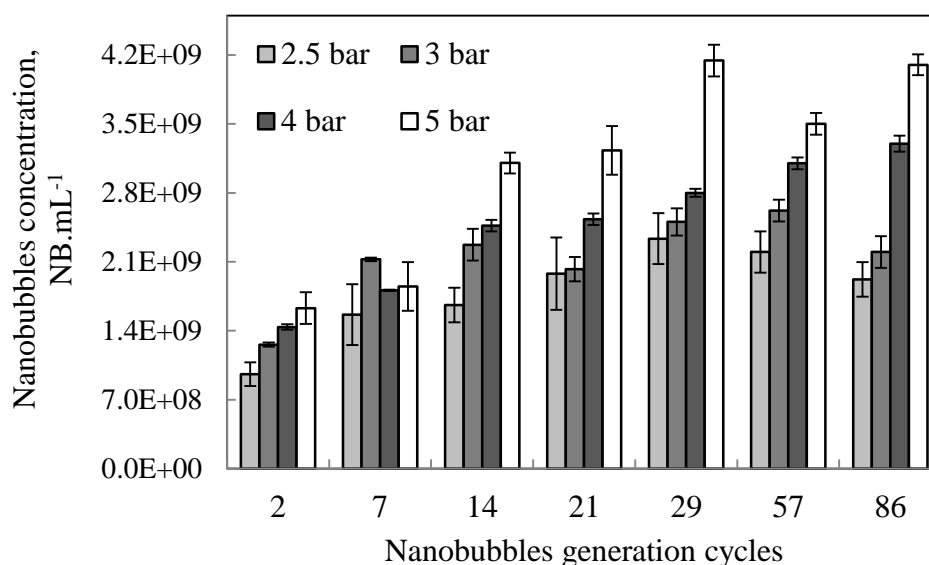


Figure 5. Effect of the number of generation cycles on NBs concentration. Liquid flow rate = 1000 L h⁻¹; air/liquid ratio = 7.5%; [α -terpineol] = 100 mg L⁻¹; pH 6 \pm 0.4. Surface tension = 50 mN m⁻¹ \pm 1.

Table 1 summarizes data on the effect of the operating pressure on NBs formation with a multiphase pump. Results show that contrary to the NBs generation by depressurization of air-saturated water from saturator vessel in a needle valve (A. Azevedo et al., 2016), the concentration of NBs is directly proportional to saturation pressure (P_{sat}).

In air-in water-saturators-flow constrictors, interactions occurred between MBs and NBs leading to coalescence and/or entrapment highly reducing the concentration of NBs.

Table 1. Concentration of NBs formed under various operating pressures at bench scale, using a saturation vessel, compared with a centrifugal multiphase pump (CMP). [α -Terpineol] = 100 mg L⁻¹ (surface tension = 50 mN m⁻¹); DI water (surface tension = 72.4 mN m⁻¹).

Pressure (bar)	Concentration of NBs obtained with DI water (NBs mL ⁻¹)		Concentration of NBs obtained with 100 mg L ⁻¹ α -Terpineol solution (NBs mL ⁻¹)	
	Saturator Vessel*	CMP	Saturator Vessel*	CMP
2.5	3.3 x 10 ⁸	5.3 x 10 ⁷	1.5 x 10 ⁹	2.39 x 10 ⁹
3	2.06 x 10 ⁸	7.6 x 10 ⁷	0.91 x 10 ⁹	2.51 x 10 ⁹
4	1.89 x 10 ⁸	1.5 x 10 ⁸	0.61 x 10 ⁹	2.8 x 10 ⁹
5	1.22 x 10 ⁸	1.55 x 10 ⁸	0.32 x 10 ⁹	4.1 x 10 ⁹

These bubble interactions do not appear to occur while the continuous generation of NBs by CMP. Here, the use of operating pressures > 3 bar resulted in a higher population of NBs and MBs, the latter evidenced in photographs of bubbles in Figure 16 and by the air holdup values (Figure 17).

Additional mechanisms to enhance the ratio of NBs / MBs by hydrodynamic cavitation in CMP's appear to be the following:

- i. Hydrodynamic cavitation by mechanical agitation. The movement of the pump impellers and the pressure distribution in the vane region create high and low pressure areas in the periphery and inner impellers. This results in pressure gradients and formation of cavities in the low pressure zones (Brennen, 1995; Grainer-Allen, 1970; Zhou, Xu, Finch, Masliyah, & Chow, 2009);
- ii. Hydrodynamic cavitation by axial flow shearing. The liquid flow (or gas-liquid mixture) is split (divided) into several spiral rotating vortexes, moving along a special chamber and the discharge piping from the pump. This rotational movement is maintained until the kinetic energy is depleted, producing an intense shear through respective centrifugal forces, triggering nucleation and gas bubble formation by pressure fluctuation (Brennen, 1994, 1995; Hua, Falcone, Teodoriu, & Morrison, 2012);
- iii. Hydrodynamic cavitation through depressurized flow constriction. When the supersaturated liquid is forced through the needle valve, the pressure is reduced below the vapor pressure of the liquid, and cavities consequently form and partially collapse when the pressure values reset at the device

output and column entry (Calgaroto et al., 2014a; Zhou, 1996; Zhou, Xu, Finch, Hu, & Rao, 1997; Zhou et al., 2009).

These mechanisms explain some results found here, showing that the concentration of NBs increases when the pump is operated without injection of air (Figures 6 and 7) Under these conditions, the number of formed NBs was obviously lower than the values observed with air injection inside the pump. The main reason for this behavior is the difference in the quantity of air dissolved under these conditions (supersaturation \times ambient pressure). The number of NBs is higher when the generated cavities are stabilized by diffusion of more dissolved air into these cavities (Zhou et al., 2009).

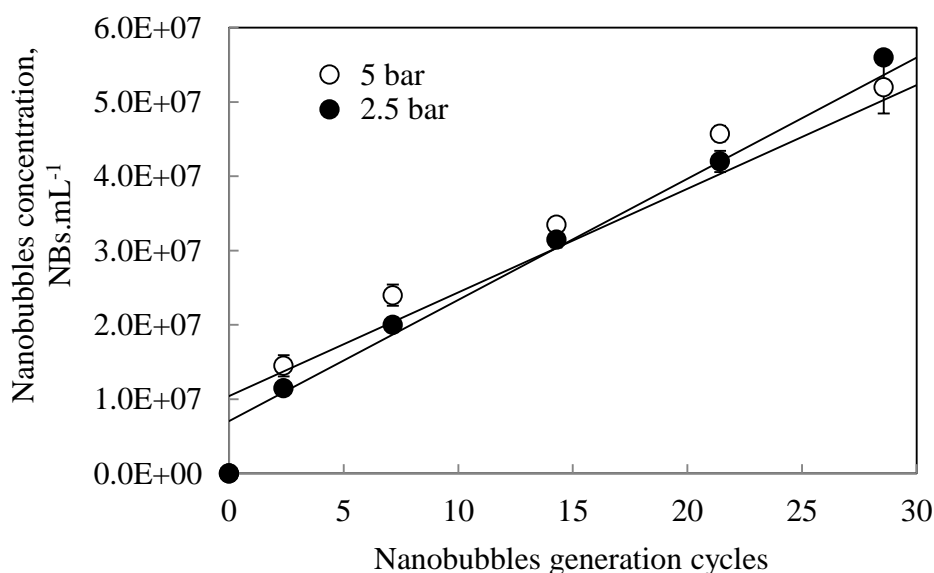


Figure 6. Effect of the number of generation cycles on NBs concentration (NBs ml⁻¹) without air injection. Liquid flow rate = 1000 L h⁻¹; DI water; pH 6 \pm 0.4; surface tension = 72.2 mN m⁻¹ \pm 0.2.

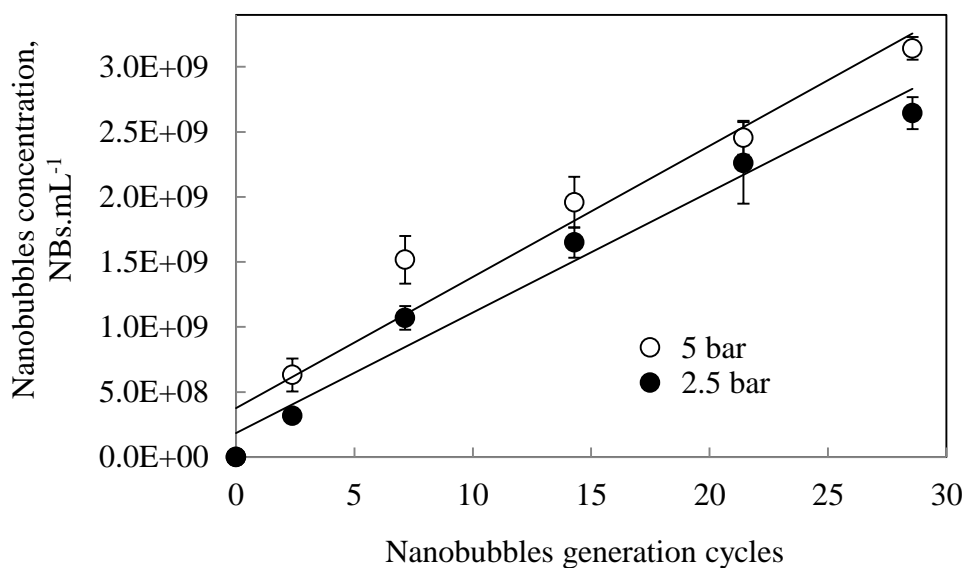


Figure 7. Effect of the number of generation cycles on NBs concentration (NBs ml⁻¹) without air injection. Liquid flow rate = 1000 L h⁻¹; [α -Terpineol] = 100 mg L⁻¹; pH 6 \pm 0.4; surface tension = 50 mN m⁻¹ \pm 1.

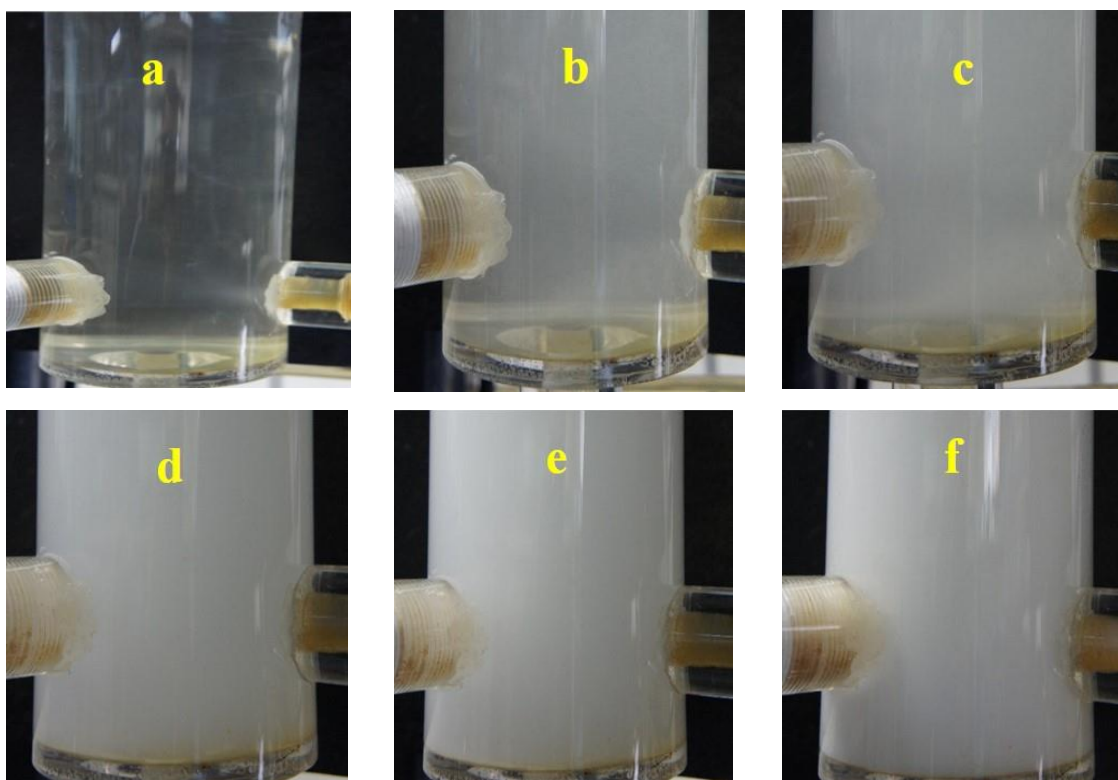


Figure 8. Effect of operating pressure of the multiphase centrifugal pump on bubble generation. Conditions: pH 6 \pm 0.3; Air/liquid ratio = 7.5%; Liquid flow rate = 1000 L h⁻¹, surface tension = 72.5 mN m⁻¹ (except condition "F"): A) Pressure = 1.5 bar; B) Pressure = 2.5 ar; C) Pressure = 3

bar; D) Pressure = 4 bar; E) Pressure = 5 bar; F) Pressure = 2.5 bar (surface tension = 50 mN m⁻¹); Temperature = 21 ° C ± 1.

In summary, by utilizing these three phase pumps, all generation phenomena occurred simultaneously, resulting in the formation of highly loaded NBs aqueous dispersions. This information is important because the concentration of NBs formed by different techniques are scarce in the literature, especially at high flow rates (if published!).

Liu et al. (2013) reported a value of 1.97×10^8 NBs mL⁻¹, Oh et al. (2015) 2.8×10^8 NBs mL⁻¹; and Ohgaki et al. (2010) 1.9×10^{13} NBs mL⁻¹. Yet, in the work of Liu et al. (2013), the method of generation of NBs was not described; in the work of Oh et al. (2015) the gas phase was hydrogen in gasoline in a gas-liquid dispersion and the bubbles formed after passing a membrane module. Ohgaki et al. (2010) used scanning electron microscopy (SEM) to measure the concentration of NBs, but the size distribution of NBs was not published. This technique is considered an indirect and imprecise, which may lead to measurements with little consistency. The reported values are about 100 thousand-fold higher than those reported in the present work!

Figure 9 shows the concentration of NBs and the air holdup values as a function of the operating pressure for the same number of generation cycles. The results showed that the air holdup values, and number of MBs follow the same tendency of increase observed for the concentration of NBs. The highest holdup value observed (6.8%) was obtained at 4-5 bar, where the concentration of NBs was close to 4×10^9 NBs mL⁻¹ (see also the photographs of the MBs in Figure 8). The D32 of the air MBs formed were constant in the range between 62-70 μm, similarly to those values obtained by Rodrigues (2004), who employed a multiphase pump (Edur[®]) for the MBs generation.

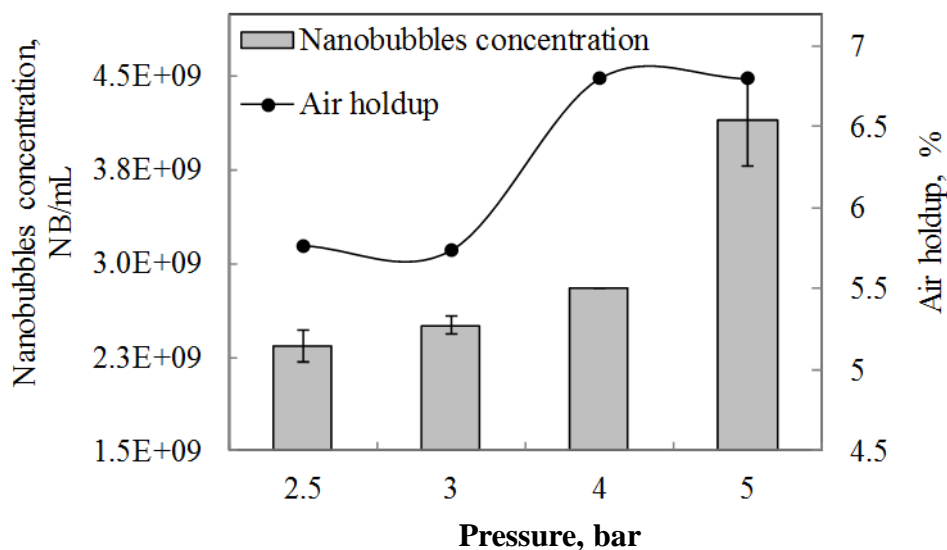


Figure 9. Effect of operating pressure on air holdup and concentration of NBs. Liquid flow rate = 1000 L h⁻¹; Air / liquid ratio = 8%; [α -Terpineol] = 100 mg.L⁻¹; pH 6 \pm 0.4; surface tension = 50 \pm 1 mN.m⁻¹.

The existence of Bulk NBs and their stability when dispersed in aqueous solutions are being fully studied, constitutes an exciting research theme, with many authors discussing the theories and mechanisms to explain their peculiar properties (A. Azevedo et al., 2016; S. Liu et al., 2013; Seddon, Lohse, Ducker, & Craig, 2012; Ushikubo et al., 2010; Weijs, Seddon, & Lohse, 2012; Zhang & Seddon, 2016). Figures 10 and 11 show data on the evolution of D32 and concentration of NBs over 60 days. The results validated the high stability and longevity observed by many authors, for these bubbles when dispersed in water. Hence, not only the size but also the number of NBs showed small variations during the full storage period. These results are consistent with results obtained by other authors, showing that NBs are stable for days or even months (Oh et al., 2015; Ohgaki et al., 2010; Ushikubo et al., 2010). The D32 values of the NBs generated in an α -terpineol solution were slightly lower than those for NBs generated in DI water, probably by repulsion interfacial forces which might lead to some coalescence during storage.

Moreover, in air-saturated /microsolid-free liquids, as in the present work, these NBs are remarkably stable probably due to (among others) the following phenomena: i. Absence or minimum rising rate of ascent of NBs; ii. Balance of double layer repulsive

and hydrophobic attractive forces; iii. The degree of metastability achieved as a function of the high concentration of NBs, which prevents the diffusive flow of gas molecules from inside the NBs to the liquid (Creux, Lachaise, Graciaa, & Beattie, 2007; Henry, Parkinson, Ralston, & Craig, 2008; Seddon et al., 2012; Weijs et al., 2012).

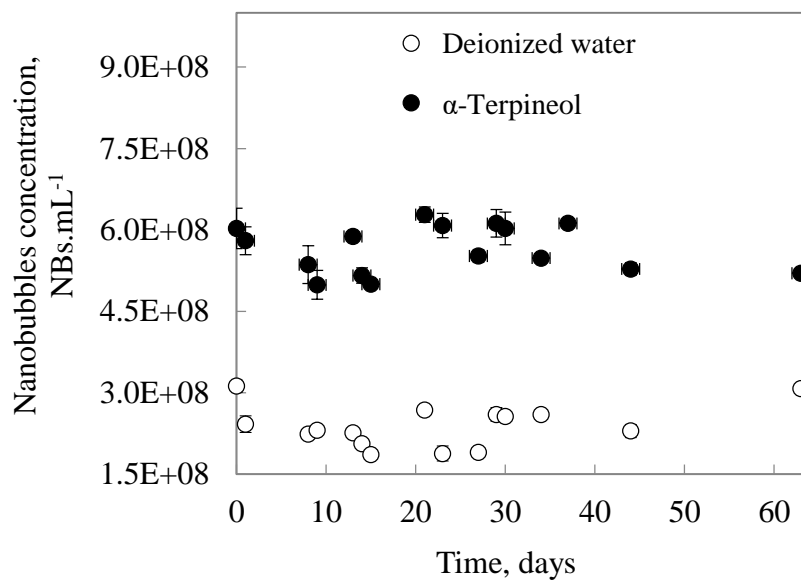


Figure 10. Concentration of NBs as a function of storage time. The 0.0 point in the abscissa refers to the measurement performed (size obtained) 10 min after the generation of the NBs dispersion sample. Conditions: pH 6; $P_{sat} = 4$ bar; $[\alpha\text{-Terpineol}] = 100 \text{ mg L}^{-1}$ (surface tension = 50 mN m^{-1}); DI water (surface tension = 72.5 mN m^{-1}).

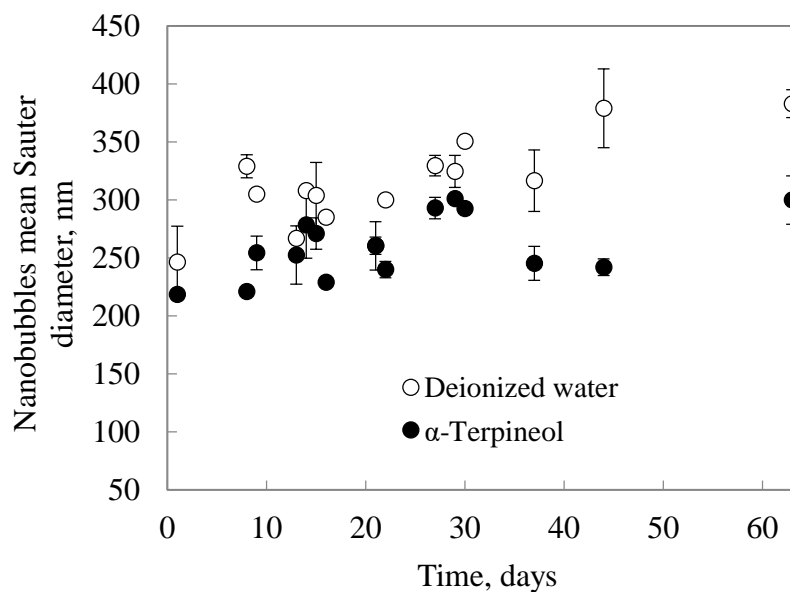


Figure 11. Mean Sauter diameter of NBs as a function of storage time. The 0.0 point in the abscissa refers to the measurement performed (size obtained) 10 min after generation of the NBs dispersion sample. Conditions: pH 6; $P_{sat} = 4$ bar; $[\alpha\text{-terpineol}] = 100 \text{ mg L}^{-1}$ (surface tension = 50 mN m^{-1}); DI water (surface tension = 72.5 mN m^{-1}).

3.4 FINAL REMARKS

Although residence times in multiphase pumps generally are lower than that using saturation vessels, the mechanism of hydrodynamic cavitation operating in the various zones of the pump allowed to form higher NBs concentrations compared with the results obtained with saturator vessel (A. Azevedo et al., 2016).

Advantages for sustainable bubbles generation with CMP include:

- i. Higher volumetric efficiency, providing a large mass of air per unit volume of recirculation;
- ii. Elimination of saturation chambers and;
- iii. Air may be supplied from the atmosphere rather than by an air compression unit (Ross, Smith, & Valentine, 2000).

It is believed that these kinds of pumps (Edur, 2017; Hellbender, 2017, Nikuni, 2017), with special suction chambers for air injection and cavitation, have a high potential for generating MBs and NBs and for future applications, at high flow-rates. Main areas are:

mineral or pollutants flotation and ozonation systems for water and wastewater treatment.

In mineral flotation the NBs are believed to improve the aggregation and hydrophobization of solids and enhance the recovery of organic and inorganic particles. More, a new generation of DAF units may be possible maximising the formation and/or injection of the NBs. Figures 12 and 13 depict some alternatives for “multi-bubble” flotation for mineral flotation recovery and for pollutants separation.

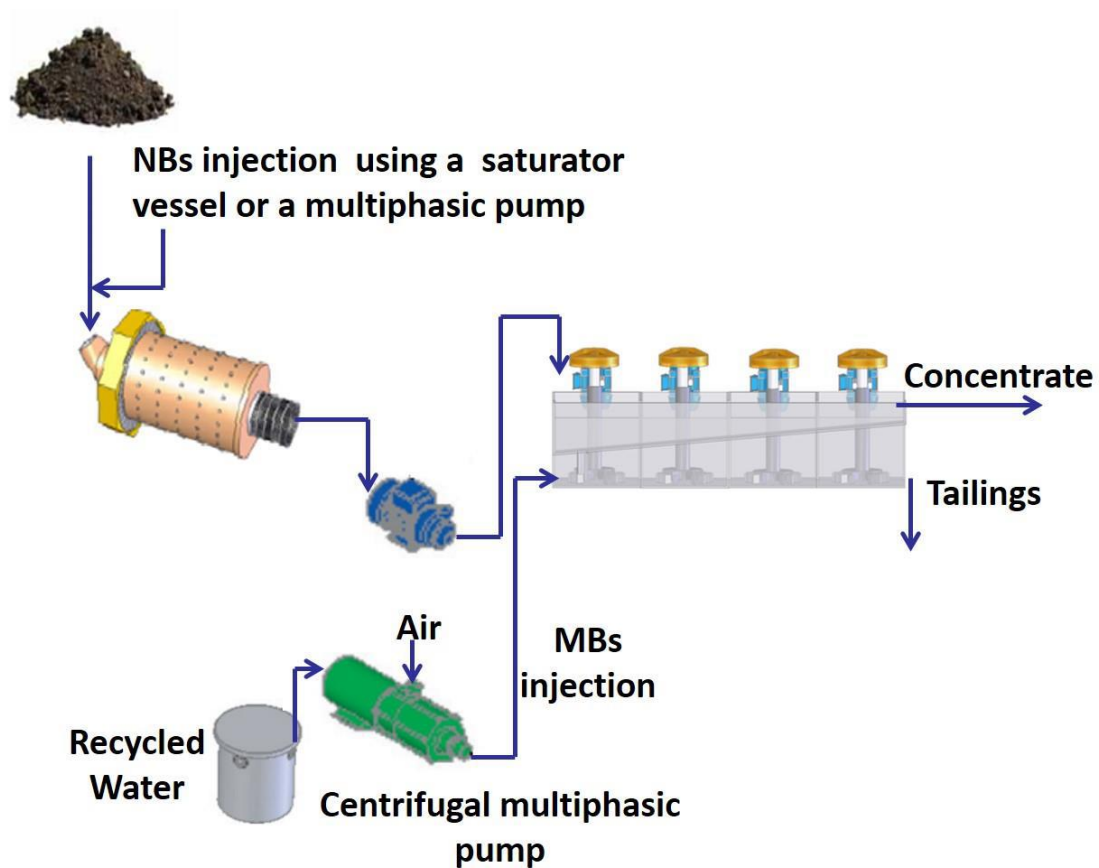


Figure 12. Flowchart of a mineral flotation unit with injection of MBs and NBs.

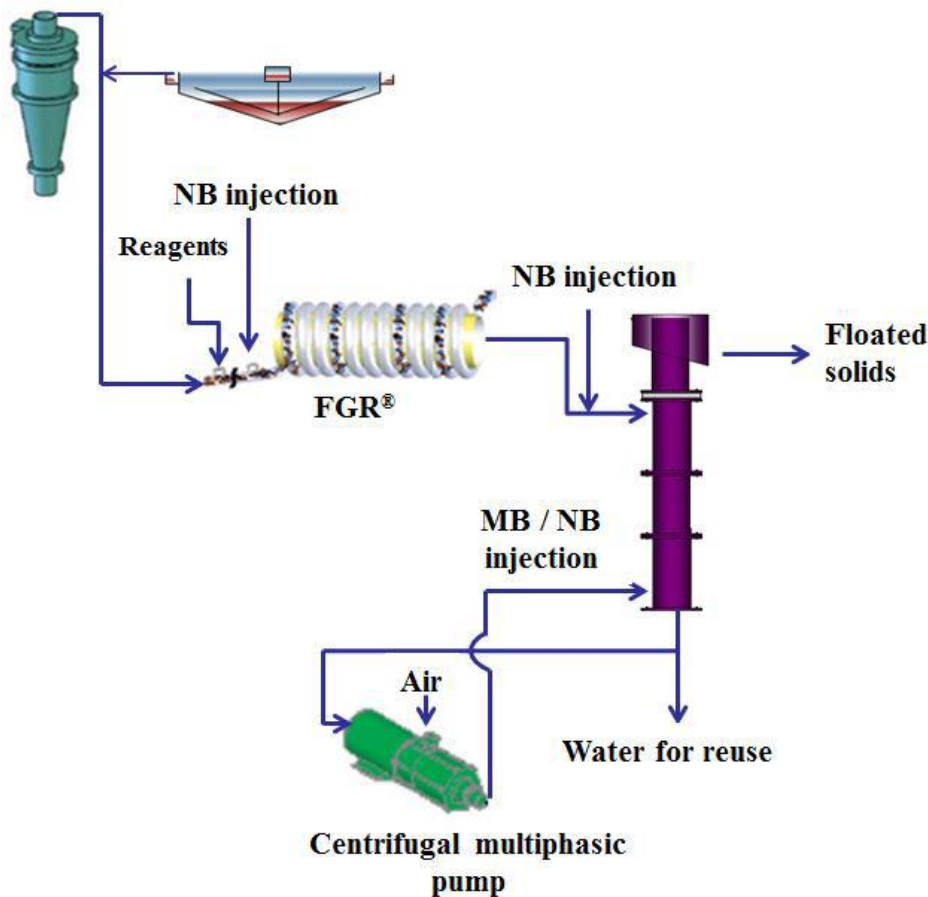


Figure 13. Flowchart of a flocculation-flotation process for wastewater treatment with multiple bubble injection.

3.5 CONCLUSIONS

The results suggest that centrifugal multiphase pumps (CMP) have a great potential for bulk nanobubbles generation at high rate, reaching a maximum nanobubbles concentration (4.1×10^9 nanobubbles mL^{-1}) after approximately 29 operation cycles (residence time = 2.1 min). This optimum condition was obtained at 4-5 bar and low liquid/air surface tension (49 mN m^{-1}). The bulk nanobubbles dispersions were stable for over 60 days, with no decrease in nanobubbles concentration and mean size, proving the high stability and longevity of these bubbles aqueous dispersions. Nanobubbles were resistant to the shearing effect of the pump impellers and to the high pressure during the several generation cycles. Yet, the air holdup reached 6.8% operating at 5 bar in a α -terpineol solution (surface tension = 49 mN m^{-1}). It is believed that the results will broaden the applications of the CMP for bubble generation in flotation either in

mineral processing or in the environmental area, and/or in many other technological areas exploring the physicochemical properties and features of nanobubbles.

3.6 ACKNOWLEDGEMENTS

The authors would like to thank the Brazilian Institutes that supported this study, namely, CNPq, CAPES, FAPERGS and UFRGS. We would like to especially thank to Katia Wilberg, Marcelo Fermann and Alex Rodrigues for their assistance in the setting up, literature review and experimental together with all LTM students.

Artigo II

SEPARATION OF EMULSIFIED CRUDE OIL IN SALINE WATER BY DISSOLVED AIR FLOTATION WITH MICRO AND NANOBUBBLES

Artigo publicado no periódico Separation and Purification Technology,
volume 187, 2017, páginas 326–332.

4 SEPARATION OF EMULSIFIED CRUDE OIL IN SALINE WATER BY DISSOLVED AIR FLOTATION WITH MICRO AND NANOBUBBLES

Etchepare^{1,2}, R.; Oliveira¹, H.; Azevedo, A; Rubio, J.

*Laboratório de Tecnologia Mineral e Ambiental, Departamento de Engenharia de Minas, PPGE3M, Universidade Federal do Rio Grande do Sul, Av. Bento Gonçalves, 9500, Prédio 43427 - Setor 4, CEP: 91501-970, Porto Alegre, RS, Brazil, www.ufrgs.br/lm, Corresponding author: jrubio@ufrgs.br

Abstract

This work investigates the separation of emulsified crude oil in saline water (30 g L⁻¹ NaCl) with microbubbles (MBs, D₃₂ = 30-40 μm) and nanobubbles (NBs, D₃₂ = 150-350 nm). Bubbles were generated simultaneously by the depressurization of air-saturated water through a flow constrictor (needle valve). The emulsified oil, after gravity separation of the "free" oil, was flocculated with a cationic polyacrylamide (Dismulgan) at pH 7 and removed by: i. Flotation with MBs and NBs; ii. "Floatation" by NBs; and iii. Flotation with MBs and NBs following floc conditioning by NBs. The best oil removal (> 99% efficiency) was obtained at 5 bar and 5 mg L⁻¹ of Dismulgan, reducing the oil content (feed concentration = 334-484 mg L⁻¹) in the treated water to < 1 mg L⁻¹. Furthermore, the use of low saturation pressure (P_{sat} = 3.5 bar), resulted in a treated water with oil concentrations lower than 29 mg L⁻¹ (EPA standards for offshore discharge). Best results were obtained at a low energy for bubble formation, followed by efficient precipitation and nucleation, at a fairly low air/feed emulsified oil interfacial tension (55 mN m⁻¹). The flotation was very fast and followed a first-order model, with a flotation kinetic constant of 1.3 and 1.8 min⁻¹ for P_{sat} of 3.5 and 5 bar, respectively. The injection of isolated NBs (3x10⁸ NBs mL⁻¹), in a conditioning stage after flocculation (with 1 and 3 mg L⁻¹ Dismulgan) increased the hydrophobicity of the aggregates, improved the adhesion between bubbles and oily flocs and the overall efficiency of the flotation process from 73 to 84%, and from 92 to 95%, respectively. "Floatation" (simply flocs rising with isolated NBs) resulted in oil removal efficiencies of 75 and 90% with and without NaCl (30 g L⁻¹). It is believed that the NBs entrap and adhere inside the flocculated oil droplets, forming aerated oily flocs, which subsequently assist the MBs in the flotation process. This finding appears to have potential in improving oil separation by flotation.

Keywords: nanobubbles; flotation; separation of oil in water emulsions; produced water treatment.

4.1 INTRODUCTION

Flotation is extensively employed in the removal of emulsified oils from aqueous dispersions, after destabilization by flocculation. The size distribution of bubbles and oil droplets plays a key role in flotation efficiency. Small bubbles are preferred because of their large surface areas, which are shown to be very useful in the aggregation of droplets (Santander et al., 2011; Saththasivam et al., 2016). Conversely, larger bubbles tend to rise rapidly, which results in lower collision efficiency. The adhesion between bubble and oil droplet is another key factor for flotation efficiency. The formation of stable bubble-droplets aggregates depends on a number of factors, such as the ratio of bubble / droplet size, their numeric concentration, salinity, oil viscosity, fluid velocity and turbulence. Among these factors, the gas dispersion parameters are considered the most important in oil-water separation (Rawlins, 2009).

Produced water is wastewater generated in petroleum prospecting that is composed of a mixture of water from wells and process water (Gabardo, Platte, Araujo, & Pulgatti, 2011; NSC, 2002; Veil, Puder, Elcock, & Redweik, 2004). Flotation is usually applied in its treatment at offshore platforms (Fakhru'l-Razi et al., 2009), and the effluent should meet the emission limit (EPA Oil and Gas Effluent Guidelines (EPA, 1979)) of 29 mg L⁻¹ total oil concentration average for monthly and 42 mg L⁻¹ for daily maximum for offshore disposal.

Recent studies have found that in dissolved air flotation (DAF) microbubbles (MBs) and nanobubbles (NBs) are formed (A. Azevedo et al., 2016; Calgaroto et al., 2014a). The generation and applications of NBs are an emerging and fast-growing research area because of their physical, chemical and physicochemical properties.

Reports and news about flotation with NBs to remove pollutants from waters and wastewaters are scarce. Recent studies have demonstrated the potential of these fine bubbles in solid-liquid separation and mineral treatment (Calgaroto et al., 2016; Fan et al., 2010a, 2010b, 2010c; FAN et al., 2010). Recently, the removal of amine and sulfate precipitates from aqueous solutions using isolated NBs (F-NBs) and DAF assisted by NBs were studied (Amaral Filho, Azevedo, Etchepare, & Rubio, 2016; Calgaroto et al., 2016). The DAF assisted by NBs consists in the injection of an aqueous dispersion of

NBs in a conditioning stage (with or without flocculants) promoting aggregation and hydrophobization of the particles to be removed.

It is believed that NBs may play an important role in the aggregation and stabilization of these aggregates (flocs) by adhering to and/or entraining inside (entrapment) the flocs, generating capillary bridges between oil droplets, and improving their hydrophobicity and the probability of adhesion with MBs (Calgaroto, Azevedo, & Rubio, 2015b; Calgaroto et al., 2016). The aim of this study was to evaluate the role of NBs on various multi-bubble flotation configurations: MBs and NBs, DAF assisted by NBs, and “floatation” (flotation without lifting power) with isolated NBs (F-NBs), on the removal of emulsified oil after destabilization / flocculation at the bench level.

4.2 MATERIALS AND METHODS

4.2.1 Synthetic produced water

Ultrapure (DI) water at room temperature ($22^{\circ}\text{C} \pm 1$) with a conductivity of $3 \mu\text{S cm}^{-1}$, a surface tension of $72.5 \pm 0.1 \text{ mN m}^{-1}$ and pH 5.5 was used to prepare the synthetic produced water. DI water was obtained by ultrapurification of tap water with a reverse osmosis cartridge and modules of ion-exchange resins and activated carbon.

The petroleum (crude oil) used in this study was supplied by a local oil refinery (REFAP, Petrobras, southern Brazil). This oil was characterized in terms of its physicochemical and interfacial properties (Table 2).

Table 2. Crude oil physicochemical and interfacial properties

Parameters	Value
Density, 25°C (g mL^{-1})	0.88
API Grade ($^{\circ}\text{API}$)	23
Viscosity, 25°C (cP)	42
Superficial tension (oil/water), 25°C (mN m^{-1})	28

The brine solution for synthetic produced water was made by dissolving 30 g L^{-1} of NaCl (99.5%, Vetec[®], Brazil) into 1 L of DI water. Then, 1.6 g of crude oil was slowly dripped into the brine solution for emulsification with an Ultra Turrax mixer (IKA, 24,000 rpm, 10 min). The emulsion was left to stand in an acrylic column for 1h for the separation of the free oil phase to obtain a well stabilized oil-in-water emulsion.

Solutions of 0.1 M NaOH (Vetec[®], Brazil) were prepared for pH adjustment in the destabilization/flocculation stage.

The destabilization and flocculation of the emulsion was conducted using Dismulgan V3377 (Clariant[®], Rio Grande do Sul, Brazil) (1 to 10 mg L⁻¹), a flocculation polymer (polyacrylamide) widely used on offshore petroleum platforms.

4.2.2 Flocculation-flotation studies for oil/water separation

The experiments were performed using the system shown in Figure 1, which consisted of: i. saturator vessel made of acrylic (1) for bubble generation (2.5 L, h = 400 mm, diameter = 110 mm, equipped with a manometer and a needle valve); ii. a glass column (2) for the separation of MBs (2 L, h = 250 mm, diameter = 100 mm) using the technique described by Calgaroto et al. (Calgaroto et al., 2015b, 2014b); and iii. a glass column (3) for the flocculation and flotation stages (2.5 L, h = 330 mm, diameter = 100 mm) and a mechanical stirrer Fisatom[®] brand (model 713D).

The glass column (2) had one input receiving the depressurized flow (MBs and NBs) from the saturator vessel and one output connected to the glass column (3), to inject the isolated NBs. With flotation by MBs and NBs together, the glass column (2) was not employed.

Figure 14 shows a schematic representation of the bench system for generation and treatment of oily emulsion by flocculation-flotation with MBs and NBs.

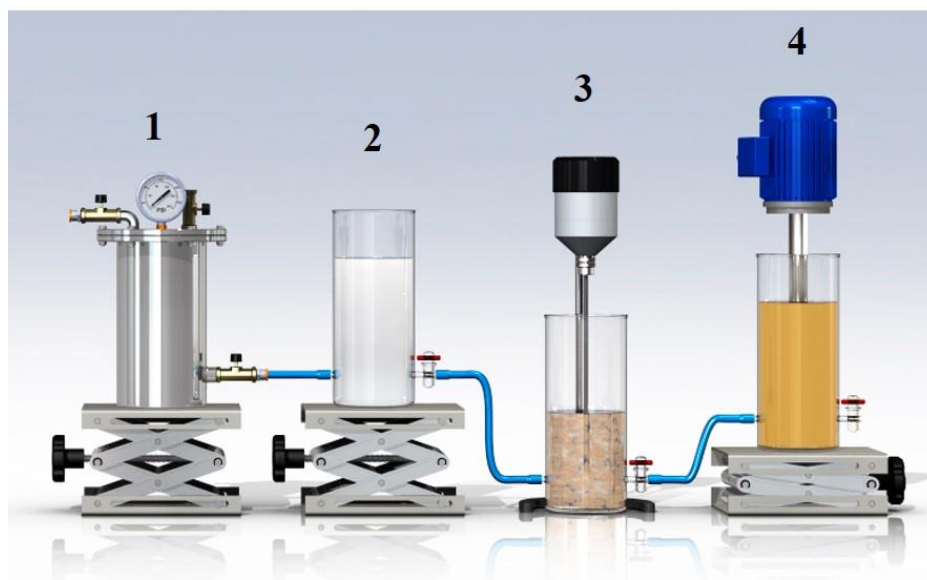


Figure 14. Oily emulsion generation and treatment systems by flocculation-flotation with air MBs and NBs. (1) Saturator vessel; (2) Glass column for MBs separation and NBs isolation; (3) Glass

column for flocculation and flotation stages and mechanical stirrer (Fisatom® 713D); (4) Ultra Turrax emulsifier for oil in water mixture.

4.2.3 Flotation with MBs and NBs

The bubbles formed by depressurization and hydrodynamic cavitation of the flow of air saturated water through the needle valve were injected directly into the glass column (3) (without separation of MBs and NBs). To perform the tests, a volume of 800 mL of the oily emulsion was transferred to the glass column (3). Flocculation was performed using rapid mixing stages (1 min, $G = 2,400 \text{ s}^{-1}$), followed by slow mixing (5 min, $G = 30 \text{ s}^{-1}$) by the use of the mechanical agitator.

The effect of the saturation pressure (P_{sat}) on the oil removal was observed between 2.5 and 6 bar by injecting compressed air and adjusting the relief valve in the saturator vessel over 30 min. Flotation was performed with 200 mL of bubble suspension into the flotation cell, corresponding to a recycle ratio of 25%.

Aliquots of 100 mL were collected for oil concentration analysis after 1 h of separation of the free oil phase, and from the clarified liquid (treated water) after 5 min of flotation. All experimental assays were performed in triplicate and the results were analyzed in terms of oil removal efficiency (%), according to Equation 1.

$$\text{Efficiency (\%)} = 100 - \frac{[(C_f \times F) \times 100]}{C_0}$$

(1)

where, C_f is the final oil concentration; F is the dilution factor (1.2) corresponding to the volume (200 mL) of saturated water injected; C_0 is the initial oil concentration.

The air/oil ratio (Equation 2) was calculated using the theoretical calculation of air saturation in water (Henry's Law) and the volume of precipitated air per liter of water for different values of P_{sat} calculated by Rodrigues and Rubio (R. T. Rodrigues & Rubio, 2003) using a saturation efficiency of 95% in the saturator vessel.

$$\text{Ratio}_{\text{oil}}^{\text{air}} = \frac{(v_{\text{air}} \times F2) \times 0.95}{(C_{\text{oil}} \times F1)}$$

(2)

where C_{oil} is the initial oil concentration (mg L^{-1}); $F1$ is the correction factor corresponding to the volume of liquid (oily emulsion) used (800 mL); v_{air} is the volume of precipitated air (mL L^{-1}); $F2$ is the correction factor corresponding to the volume of saturated water used (200 mL).

The effect of P_{sat} on flotation kinetics was evaluated at a P_{sat} of 3.5 and 5 bar. Treated water samples were collected at different flotation times (0 – 300 s) for measuring residual oil concentration. The results were expressed in terms of the percentage of oil removal (Equation 1) and flotation kinetic parameter data was adjusted to the first-order flotation model (Zuñiga, 1935). The flotation kinetic constant k was obtained using Equation 3.

$$\ln\left(\frac{R_{\infty}}{R_{\infty}-R}\right) = kt$$

(3)

The García-Zuñiga kinetic model of flotation is given by Equation 4.

$$R = R_{\infty}(1 - e^{-kt})$$

(4)

Where, R is the calculated oil removal (experimental) (%); R_{∞} is the removal of oil under stationary conditions (theoretical, at $t = 300$ s) (%); k is the kinetic constant (s^{-1}); t is the flotation time (s).

4.2.4 Flotation assisted by NBs

The conditioning of the oily flocs with a NBs suspension ahead of flotation was evaluated. Two different concentrations of Dismulgan (1 and 3 mg L^{-1}) were employed. After flocculation, 800 mL of NBs suspension were added to 800 mL of oily flocs suspension for the conditioning of the flocs for 5 min at slow mixing ($G = 30 \text{ s}^{-1}$). Finally, flotation was done by depressurizing 400 mL of air saturated water in $P_{\text{sat}} = 5$ bar. Blank experiments were conducted by adding pure deionized water instead of NBs suspension in the conditioning stage. All experimental arrays were performed in triplicate and the results of oil removal efficiency were obtained using Equation 1.

4.2.5 Flotation with isolated NBs (F-NBs)

For the F-NBs, the MBs separation procedure (A. Azevedo et al., 2016; Calgaroto et al., 2014a) was done in the glass column (2) and 200 mL of NBs suspension was placed into the flotation column. The F-NBs was evaluated with and without the addition of NaCl (30 g L^{-1}) in the oily emulsion. Blank experiments were conducted with pure deionized water instead of NBs suspension for flotation. All results corresponded to triplicate tests and the oil removal efficiencies were obtained using Equation 1.

4.2.6 Microscopy imaging

Optical microphotographs were taken of the different stages of oily emulsion separation by flocculation-flotation. An optical microscope Olympus[®], model BX41 was employed with an objective magnification of 1000X coupled to a high-performance digital microscope camera, Olympus DP73 (17.28 megapixel resolution).

Samples of 100 mL were collected for analysis as follows: i. Oily emulsion, after free phase separation; ii. Oily flocs after 5 min of flocculation with Dismulgan; iii. Treated water after 5 min of flotation. One drop of each sample was used for visualization under the microscope.

4.2.7 Oil concentration analysis

The oil concentration in the emulsions and in the treated effluent was determined with an oil analyzer (Horiba[®], model OCMA-350, Japan). Measurements were based on the energy absorption in the infrared spectrum at the wavelength range of 3.5 - 3.6 μm . Thus, the amount of energy absorbed in this range is assumed to be directly proportional to the oil concentration of the sample. For the extraction of the oil contained in the sample, the solvent poly-trichloroethylene (S-316, Horiba[®]) was used.

4.3 RESULTS AND DISCUSSION

4.3.1 Flotation with MBs and NBs

Figure 15 shows the effect of the Dismulgan concentration on emulsified oil removal efficiency by flotation with MBs and NBs. The results showed that oil removal increases as a function of the concentration of Dismulgan, and the best treatment conditions was obtained with 5 mg L⁻¹. At this reagent concentration, the removal efficiency was almost complete (>99%), yielding a residual oil concentration of 1 mg L⁻¹.

The role of coagulant-flocculating agents in the destabilization of oil-in-water emulsions to promote the coalescence of oil droplets is well discussed in the literature and the mechanisms involved are based on van der Waals and hydrophobic forces (Bensadok, Belkacem, & Nezzal, 2007; El-Gohary, Tawfik, & Mahmoud, 2010; Karhu, Kuokkanen, Kuokkanen, & Rämö, 2012; Tansel & Pascual, 2011; Zouboulis & Avranas, 2000). Figure 16 shows microphotographs obtained from the oily emulsion

(after separation of the free oil phase), the flocs formed with Dismulgan and the treated water after flotation.

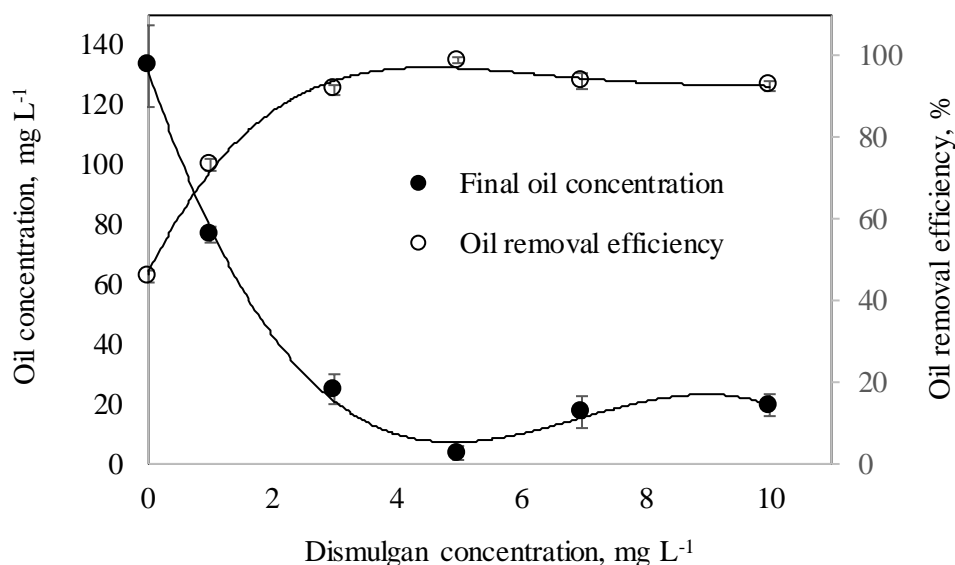


Figure 15. Flocculation-flotation for oil removal with MBs and NBs as a function of Dismulgan concentration. Conditions: initial [oil] = 337-484 mg L⁻¹; [NaCl] = 30 g L⁻¹; pH 7; Saturation pressure = 5 bar; Saturation time = 30 min; Flotation time = 5 min. The error bars correspond to the standard deviation of triplicate tests.

Oil droplets with a diameter greater than 20 μm are considered available for flotation (Moosai & Dawe, 2003), however those of finer sizes (<10 μm) may not become coalesced on the flocs due to Brownian motion (Atarah, 2011). Consequently, this process is less efficient if the residence time is low. Therefore, a similar emulsion generation technique employed by Santander et al. (Santander et al., 2011) was applied, reporting an oil droplet size with a mean Sauter diameter (D_{32}) of 15 μm , and oil droplets with diameter smaller than 10 μm (Figure 3). Thus, the destabilization of the emulsified oil droplets with 5 mg L⁻¹ of Dismulgan and the application of MBs and NBs allowed good collision and adhesion of these bubbles to the flocs, reducing the oil content to a final concentration of 1 mg L⁻¹ in the treated water.

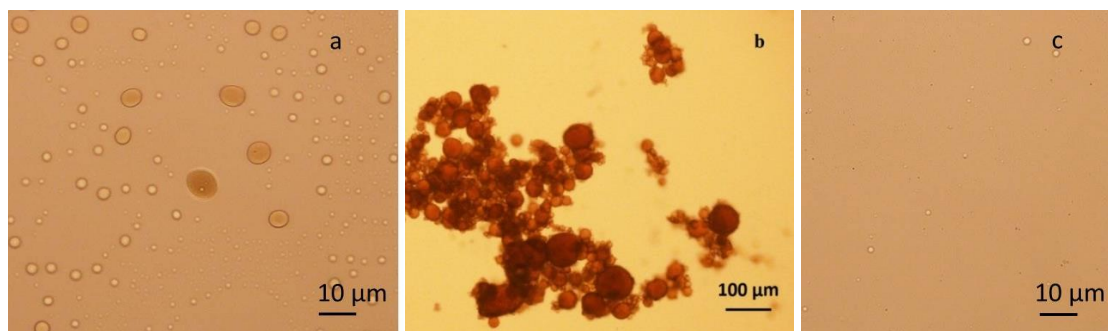


Figure 16. Microphotographs of the different stages of the treatment of oily emulsion by flocculation-flotation: a) oily emulsion after free oil phase separation; b) oily flocs; c) treated water after 5 min of flotation. Conditions: initial [oil] = 390 mg L⁻¹; [NaCl] = 30 g L⁻¹, pH 7; [Dismulgan] = 5 mg L⁻¹; Psat = 5 bar; Saturation time = 30 min; Recycle rate = 25%; Flotation time = 5 min.

The effect of Psat on oil removal efficiency is shown in Figure 17. The best results were obtained with saturation pressures of 5 and 6 bar, with removal efficiencies > 99% and a mean residual oil concentration of less than 2 mg L⁻¹. It was also observed that the non-flocculated oil droplets did not float properly, leading to an unsatisfactory oil removal efficiency (<70% and a residual concentration >100 mg L⁻¹).

More, in terms of residual oil concentration and practical aspects, the results showed that with a Psat of 3.5 bar the removal efficiency was about 93%. As shown in Table 3 and Figure 18, the residual oil concentration obtained was below the EPA Oil and Gas Effluent Guidelines (EPA, 1979) for monthly average emission limit for offshore waters (29 mg L⁻¹), proving the potential of the flotation process with MBs and NBs with low saturation pressures (meaning less energy consumption).

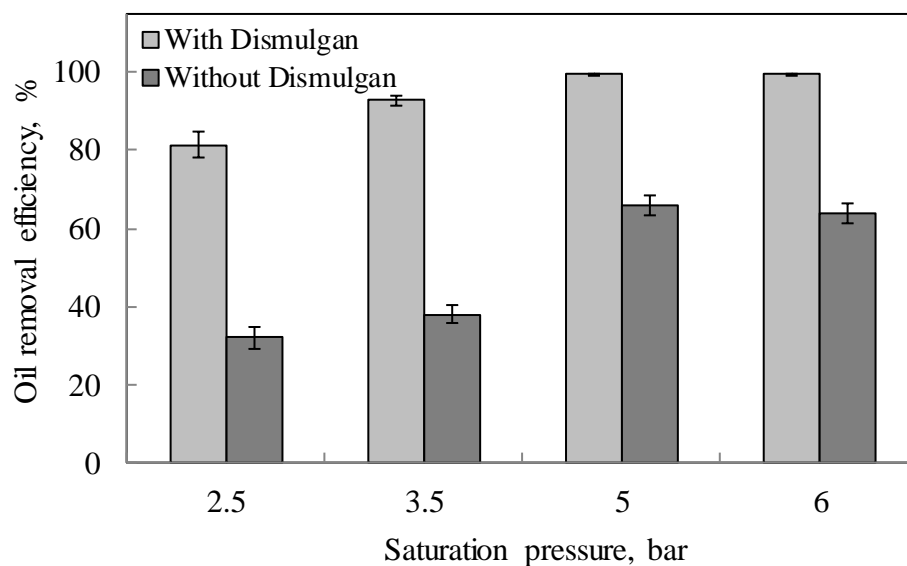


Figure 17. Oil removal efficiency by flocculation-flotation with MBs and NBs as a function of the saturation pressure and in the presence and absence of the flocculant (Dismulgan). Conditions: initial [oil] = 334 - 450 mg L⁻¹; [NaCl] = 30 g L⁻¹; [Dismulgan] concentration = 5 mg L⁻¹; pH 7; Saturation time = 30 min; Recycle rate = 25%; Flotation time = 5 min. The error bars correspond to the standard deviation of the triplicate tests.

Table 3. Oil removal by flocculation-flotation with MBs and NBs as a function of saturation pressure. Conditions: initial [oil] = 334-450 mg L⁻¹; [NaCl] = 30 g L⁻¹; [Dismulgan] concentration = 5 mg L⁻¹; pH 7; Saturation time = 30 min; Recycle rate = 25%; Flotation time = 5 min. Mean values (standard deviation) of quadruplicate tests.

P_{sat}, bar	Feed oil concentration, mg L⁻¹	Residual oil concentration, mg L⁻¹	Oil removal efficiency, %
2.5	378 (25)	70 (10)	82 (3)
3.5	391 (25)	28 (4)	93 (1)
5	395 (29)	2 (1.2)	99.6 (0.3)
6	402 (39)	1.4 (0.5)	99.7 (0.1)

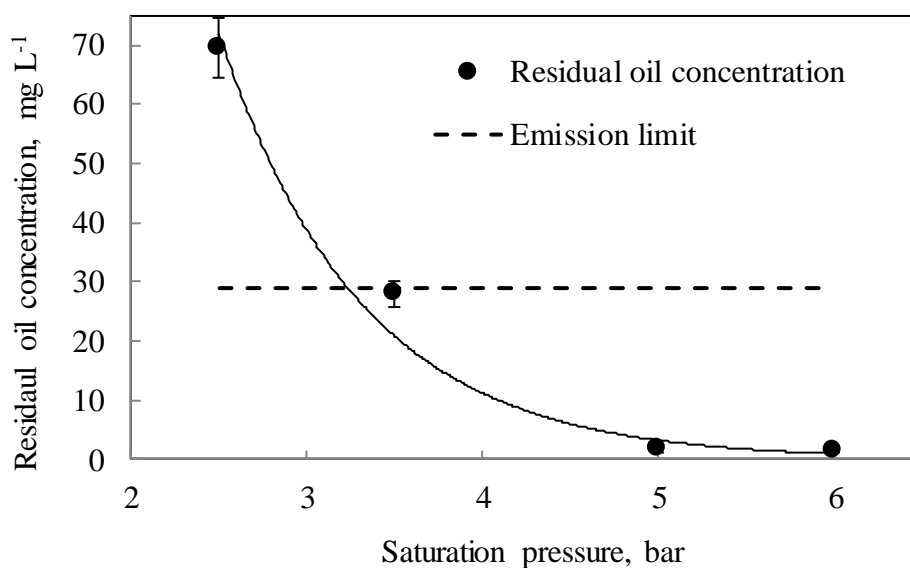


Figure 18. Residual oil concentration after flocculation-flotation with MBs and NBs as a function of saturation pressure. Conditions: initial [oil] = 334 - 450 mg L⁻¹; [NaCl] = 30 g L⁻¹; [Dismulgan] = 5 mg L⁻¹; pH 7; Saturation time = 30 min; Recycle rate = 25%; Flotation time = 5 min; Emission limit = 29 mg L⁻¹. The error bars correspond to the standard deviation of the triplicate tests.

Figure 19 shows the flotation kinetics at saturation pressures of 3.5 and 5 bar. The best results were obtained at higher saturation pressures. This fact may be explained in terms of the higher air / oil ratio (higher collision efficiency) obtained with 5 bar (0.06 mL mg⁻¹) compared to 3.5 bar (0.04 mL mg⁻¹). The flotation with both saturation pressures was relatively fast, with stabilization of the oil removal efficiency after 3 min. This flotation followed a first-order model with a flotation kinetic constant of 1.3 and 1.8 min⁻¹ for P_{sat} of 3.5 and 5 bar, respectively. Table 4 summarizes the experimental and calculated oil removal data and corresponding correlation coefficients.

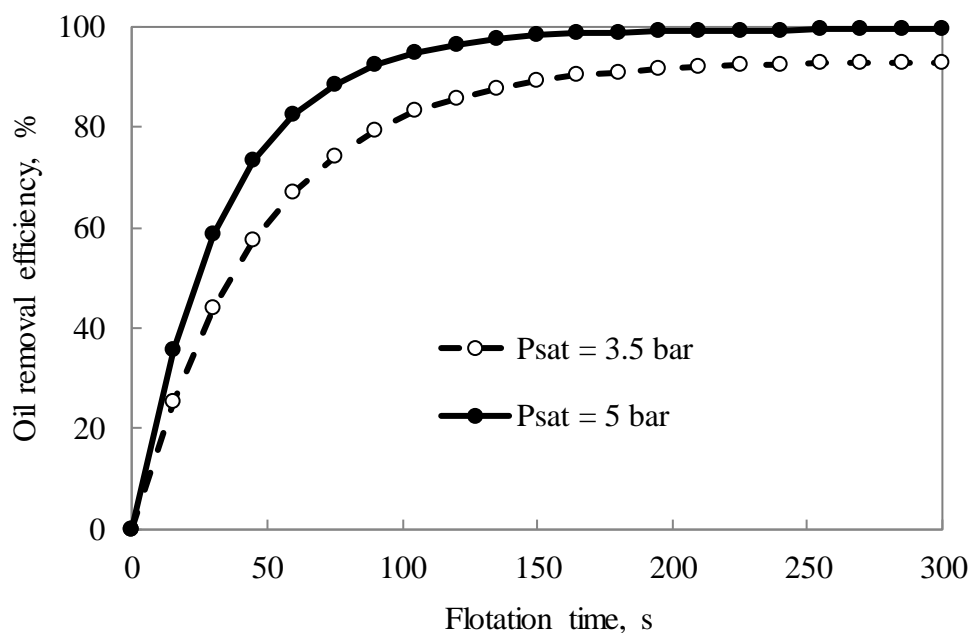


Figure 19. Flocculation-flotation kinetics of oily flocs. Conditions: initial [oil] = 335 - 480 mg L⁻¹; [NaCl] = 30 g L⁻¹; [Dismulgan] = 5 mg L⁻¹; pH 7; Saturation time = 30 min; Recycle rate = 25%.

Table 4. Flocculation-flotation kinetics of oil with MBs and NBs. Experimental data on oil removal and correlation coefficients were calculated using the first order flotation kinetic model. Conditions: $k = 1.3 \text{ min}^{-1}$ ($P_{\text{sat}} = 3.5 \text{ bar}$) and $k = 1.8 \text{ min}^{-1}$ ($P_{\text{sat}} = 5 \text{ bar}$); pH 7; Dismulgan = 5 mg L⁻¹; Saturation time = 30 min; Recycle rate = 25%.

Flotation time, s	$P_{\text{sat}} = 3.5 \text{ bar}$			$P_{\text{sat}} = 5 \text{ bar}$		
	Experimental R, %	R_{∞} , %	Correlation coefficient	Experimental R, %	R_{∞} , %	Correlation coefficient
0	0	0.0	1	0	0.0	1
10	53	18	2.97	53	25	2.08
20	69	32	2.14	70	44	1.57
40	71	53	1.33	76	69	1.10
80	91	76	1.19	93	90	1.03
300	96	93	1	99	99	1

4.3.2 Flotation assisted by NBs

Figure 20 and Table 5 show the results of flotation assisted by NBs. It was observed that, in comparison to the flotation process, the inclusion of the floc conditioning step with NBs promoted an improvement in the overall oil removal. The NBs appear to interact with the (hydrophobic) oil droplets, aggregating them and forming aerated precipitates, a phenomena already reported in literature (Attard, 2003; Calgaroto et al., 2015b, 2016; Hampton & Nguyen, 2009; Schubert, 2005).

Mishchuk (Mishchuk, 2005) carried out a theoretical analysis on the attractive forces in a particulate system in the presence of NBs and concluded that these ultra-fine bubbles adhered to the particles, reducing the local density of the solid-liquid interface. They also modify the absolute value of van der Waals forces, improving the degree of aggregation by increasing the attraction between these particles. Moreover, the study by Stöckelhuber et al. (Klaus Werner Stöckelhuber, Boryan Radoev, Andreas Wenger, & Schulze†, 2003) demonstrated that NBs cause the rupture of the liquid film between a bubble and a hydrophobic surface without the introduction of a hydrophobic force mechanism. These authors have found that the repulsive DLVO forces in this liquid film are overlaid by waves of capillary forces that deform the surface of this film. These mechanisms may explain the results where the NBs facilitated the adhesion between bubbles and oily flocs, increasing the overall efficiency of the flotation process.

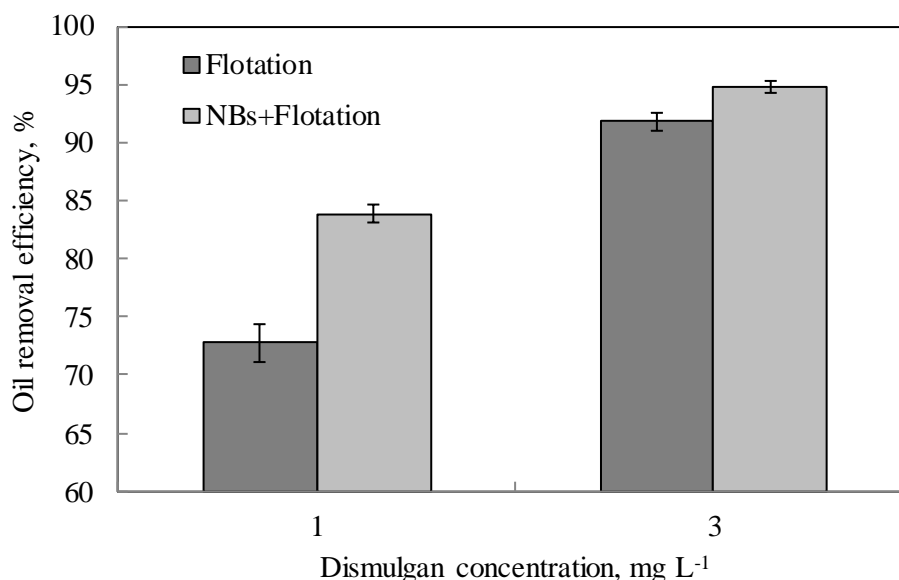


Figure 20. Efficiency of oil removal by flocculation-flotation assisted by NBs. Conditions: initial [oil] = 375 - 410 mg L⁻¹; [NaCl] = 30 g L⁻¹; pH 7; Saturation pressure = 2.5 bar; Saturation time =

30 min; Recycle rate of flotation = 25%; Flotation time = 5 min. The error bars correspond to the standard deviation of the triplicate tests.

Table 5. Oil removal by flocculation-flotation assisted by NBs. Conditions: [NaCl] = 30 g L⁻¹; pH 7; Saturation pressure = 2.5 bar; Saturation time = 30 min; Recycle rate = 25%; Flotation time = 5 min. Mean values (standard deviation) of triplicate experiments.

Parameters	Dismulgan = 1 mg L ⁻¹		Dismulgan = 3 mg L ⁻¹	
	Flotation assisted by NBs	Flotation	Flotation assisted by NBs	Flotation
[oil] Initial	398 (8)	380 (9)	413 (4)	389 (32)
[oil] Final	64 (5)	104 (7)	22 (2)	32 (7)

4.3.3 Flootation with isolated NBs (F-NBs)

Figure 21 shows the results of the floatation conducted with isolated NBs (F-NBs). The residual oil concentrations in the treated water were 34 mg L⁻¹ (without NaCl) and 80 mg L⁻¹ (with NaCl 30 g L⁻¹), and oil removal efficiency reached an equilibrium (90% and 75%, respectively), after 10 min of flotation. The results indicated that the NBs contribute to the rising of these aggregates. The NBs, once adhered, occluded and/or entrapped them at the solid/liquid interface, decreasing the relative density of these flocs and also increased their hydrophobicity.

Yet, these results indicate a slightly lower oil removal efficiency of floatation with isolated NBs with NaCl 30g L⁻¹ rather than a solution without salt. These results are probably due to the lower concentration of NBs obtained under these conditions (7.1×10^7 NBs mL⁻¹, $P_{\text{sat}} = 2.5$ bar) when compared to NBs formed in DI water (3.3×10^8 NBs mL⁻¹; $P_{\text{sat}} = 2.5$ bar), which validates and reinforces the role of NBs in the separation of these oily aggregates. The F-NBs has already been observed in previous studies of this research group, in the flotation of amine precipitate (Calgaroto et al., 2016) and ferric hydroxide (R. Etchepare, Azevedo, Calgaroto, & Rubio, 2017). However, this seems to be the first report in the literature of flocculation / NBs floatation for the treatment of emulsified oil.

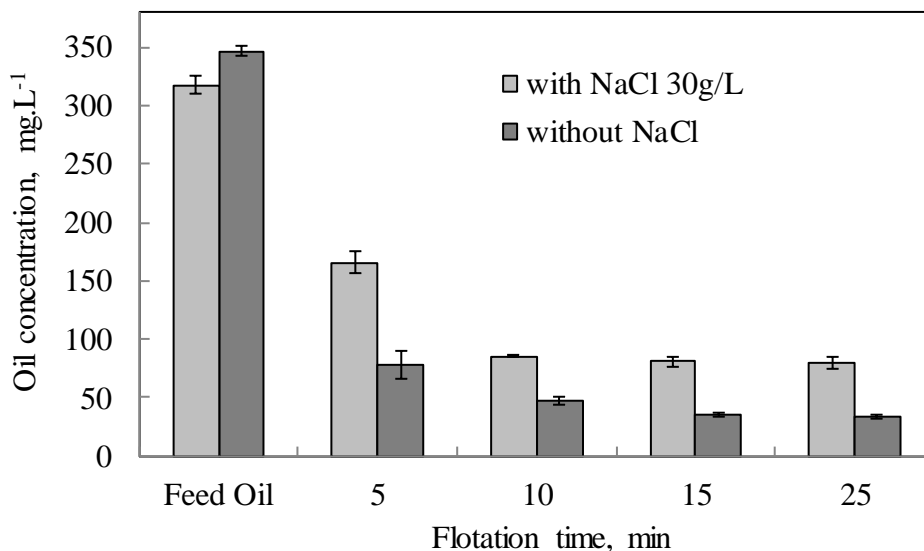


Figure 21. Flotation kinetics of oily flocs with injection of isolated NBs, using oily emulsions with and without NaCl (30 g L⁻¹). Conditions: [NaCl] = 30 g L⁻¹; [Dismulgan] = 5 mg L⁻¹; pH 7; Saturation pressure = 2.5 bar; Saturation time = 30 min; Recycle rate = 25%. The initial oil corresponds to the oil concentration after the phase separation step. The error bars correspond to the standard deviation of the triplicate tests.

4.4 CONCLUSION

Flocculation with 5 mg L⁻¹ of Dismulgan at pH 7, followed by flotation (P_{sat} of 5 bar) with MBs and NBs showed an oil removal efficiency higher than 99%, yielding a residual oil content of 1 mg L⁻¹. The use of a P_{sat} of 3.5 bar gave a treated water with a residual oil concentration lower than the emission limit (29 mg L⁻¹) of oily produced water on offshore oil platforms. The flotation followed a first-order model with a kinetic constant of 1.3 and 1.8 min⁻¹ at P_{sat} of 3.5 and 5 bar, respectively. A NBs conditioning stage after the flocculation with 1 mg L⁻¹ of Dismulgan resulted in an increase in flotation efficiency from 73 to 84%. Flotation of the oily flocs with isolated NBs resulted in oil removal efficiencies of up to 90%. The results clearly demonstrated the high potential and the role of NBs in the overall oil removal efficiency in the treatment of these wastewaters.

4.5 ACKNOWLEDGEMENTS

The authors would like to thank all the Brazilian Institutes that supported this study, namely, CNPq, CAPES, FAPERGS, and UFRGS. We would like to especial thank Alex Rodrigues, Prof Adriana Pohlmann and M.Sc. Selma Calgaroto from the Chemistry Department at our university and to all students of LTM for their assistance.

Artigo III

SEPARATION OF EMULSIFIED CRUDE OIL IN SALINE WATER BY FLOTATION WITH MICRO AND NANOBUBBLES GENERATED BY A MULTIPHASE PUMP

Artigo publicado no periódico *Water Science and Technology*, 76.10, pp. 2710, 2017.

5 SEPARATION OF EMULSIFIED CRUDE OIL IN SALINE WATER BY FLOTATION WITH MICRO AND NANOBUBBLES GENERATED BY A MULTIPHASE PUMP

Oliveira, H. A.; Azevedo, A. C.; Etchepare, R¹. and Rubio, J.

Laboratório de Tecnologia Mineral e Ambiental (LTM), Departamento de Engenharia de Minas, PPGE3M, Universidade Federal do Rio Grande do Sul; Avenida Bento Gonçalves, 9500, CEP: 91501-970 – Porto Alegre – RS.

jrubio@ufrgs.br ; www.ufrgs.br/ltn

Abstract

The flocculation-column flotation with hydraulic loading ($HL > 10 \text{ m h}^{-1}$) was studied for the treatment of oil-in-water emulsions containing $70 - 400 \text{ mg L}^{-1}$ (turbidity = $70 - 226 \text{ NTU}$) of oil and salinity (30 and 100 g L^{-1}). A polyacrylamide (Dismulgan - 20 mg L^{-1}) flocculated the oil droplets, using two flocc generator reactor (FGR[®]), with rapid and slow mixing stages (head loss = 0.9 to 3.5 bar). Flotation was conducted in two cells (1.5 and 2.5 m) with microbubbles (MBs, $5-80 \mu\text{m}$) and nanobubbles (NBs, $50 - 300 \text{ nm}$ diameter, concentration of 10^8 NBs mL^{-1}). Bubbles were formed using a centrifugal multiphase pump, with optimized parameters and a needle valve. The results showed higher efficiency with the taller column reducing the residual oil content to 4 mg L^{-1} and turbidity to 7 NTU . At high HL (27.5 m h^{-1}), the residual oil concentrations were below the standard emission (29 mg L^{-1}), reaching to 18 mg L^{-1} . The best results were obtained with high concentration of NBs (apart from the bigger bubbles). Mechanisms involved appear to be attachment and entrapment of the NBs onto and inside the flocs. Thus, the aggregates were readily captured, by bigger bubbles (mostly MBs) aiding shear withstanding. Advantages are the small footprint of the cells, low residence time and high processing rate.

Keywords: nanobubbles; oil removal; column flotation; centrifugal multiphase pump.

1. Current Address: Departamento de Hidráulica e Saneamento, Universidade Federal do Paraná, 81531-980 Curitiba, PR, Brazil

5.1 INTRODUCTION

Dissolved air flotation (DAF) is a solid-liquid separation method widely employed in emulsified oily wastewater treatment (Al-Shamrani, James, & Xiao, 2002a, 2002b; J Rubio, Souza, & Smith, 2002; Santander et al., 2011; Santo et al., 2012; Saththasivam et al., 2016; Zouboulis & Avranas, 2000). The process consists of the rapid depressurization of air-saturated water from pressurized tanks for the generation of bubbles and subsequent solid/liquid and/or liquid/liquid separation. Recently (A. Azevedo et al., 2016; Calgaroto et al., 2014a), the presence of the nanobubbles (NBs) in DAF operation was discovered, a fact unknown for years. The role of these NBs in flotation, together with microbubbles (MBs) is being studied extensively by our research group (Amaral Filho et al., 2016; Azevedo et al., 2017; Calgaroto et al., 2016, 2015, Etchepare et al., 2017a, 2017b).

An upcoming and promising alternative for the saturation of air in water in DAF applications is open-end saturation (A. Azevedo et al., 2017; Ramiro Etchepare, 2016; C. H. Lee et al., 2007; Pioltine & Reali, 2011), so-called flotation with a multiphase pump (F-MP), in which air is continuously injected into the low-pressure suction side of a special centrifugal multiphase pump (CMP). This unit provides efficient air dissolution into the liquid, and a high generation of MBs (30-100 μm) and NBs (100-850 nm) is attained due to the depressurization of the multiphase flow, the hydrodynamic cavitation caused by the flow constrictor and by the shearing effects inside the pump chamber impellers.

Etchepare et al. (2017c) investigated the generation of NBs by a CMP and its operating parameters to obtain a high concentration of these bubbles in the F-MP (approximately 4×10^9 NBs mL^{-1} at 5 bar). These authors reported that the mechanisms of hydrodynamic cavitation inside the pump chamber and downstream of the flow constrictors are responsible for a high concentration of NBs in these systems. This technique was compared to other methods of NBs generation (Azevedo et al., 2016; Liu et al., 2012; Ushikubo et al., 2010; Calgaroto et al., 2014; Azevedo et al., 2017; Calgaroto et al., 2016, 2015).

Recent studies of emulsified oil removal by flotation at bench scale (R. Etchepare, Oliveira, Azevedo, et al., 2017; Ramiro Etchepare, 2016) showed an increase in the oil removal by conditioning oily aggregates (flocs) with NBs, followed by flotation with

MBs. The authors discussed the role of NBs in the oil floatation phenomena, after the entrapment of NBs into flocs and a reduction of their relative density. Other studies have also demonstrated that NBs improve the aggregation of colloids and fine particles and increase the contact angle at the solid/liquid/air interface, which increases the probability of flotation due to an improvement in bubble-particle adhesion mechanism and stability of these aggregates (Fan et al., 2013).

Most of the technologies available for petroleum produced water (PW) treatment, such as membrane filtration, centrifugation, biological treatment, among others, present many limitations regarding operational costs, high footprint (low hydraulic loadings - HL) and low efficiency (Fakhru'l-Razi et al., 2009). The most conventional PW treatment in offshore platforms consists of a gravimetric separation stage (hydrocyclone) followed by flotation (Zheng et al., 2016). The treated effluent must meet the emission limit standards determined by many agencies, namely the EPA Effluent Guideline for Oil and Gas extraction (CFR 40.435). For offshore water disposal the limit is about 29 mg L⁻¹ of oil for a monthly average and 42 mg L⁻¹ for a daily maximum. The PW treatment on offshore platforms presents technical challenges due to the limitations of available area, equipment weight and low residence time, which usually does not exceed 15 min (Gabardo et al., 2011). Thus, there is a need to develop and improve treatment processes with high processing rates, especially in compact units that occupy reduced areas (low-footprint).

Carissimi and Rubio (2005a) developed a helical coiled hydraulic flocculator, a so-called Flocs Generator Reactor (FGR[®]). This type of flocculator has been used in aerated floc formation by the injection of air bubbles upstream of the reactor and presents high processing rates, requires low residence times and a small foot-print area for installation (Carissimi & Rubio, 2005b). Aerated flocs are structures composed of flocs and bubbles which are farly light and rapidly rise in flotation systems (Carissimi & Rubio, 2005b; Da Rosa & Rubio, 2005; Oliveira & Rubio, 2012; Rafael Teixeira Rodrigues & Rubio, 2007). Another important feature of these structures is the high shear resistance during turbulent conditions. It is believed that NBs generated at a high rate by the CMP may play an important role in aerated floc resistance due to capillary forces inside these structures.

Column flotation technologies appear as alternatives for high rate DAF utilities in offshore platforms. Zaneti et al. (2012, 2011) studied flocculation-column flotation with a multiphase pump for the treatment and reuse of vehicle wash wastewater (high suspended solids concentrations) and reported the use of HL higher than 20 m h^{-1} . The main advantages of column flotation for wastewater treatment are its high throughput and flux pattern (plug flow), which allows better contact between bubbles and particles and requires lower residence times leading to higher HL (Jorge Rubio & Zaneti, 2009).

Filippov et al. (2000) reported that by increasing the relation of height/diameter of the column in precipitate flotation, the turbulence caused by liquid flow and bubble rising movement may be reduced, thereby improving flotation efficiency.

In this work, MBs and NBs were generated by a CMP feed column with bubbles for oil removal in a semi-continuous pilot rig. This process utilized flocculation in a FGR[®] and column flotation for the separation of the oily flocs. The objectives of the study were to evaluate the generation of bubbles in a multiphase pump and the influence of operating parameters (reagent concentration, column height and hydraulic loading) on oil removal efficiency.

5.2 EXPERIMENTAL

5.2.1 Materials

The petroleum (crude oil) was supplied by a local oil refinery (REFAP, Petrobras, southern Brazil) and characterized in terms of its physicochemical and interfacial properties (Table 6).

For the generation of the oil-in-water emulsion, tap water and industrial salt (iodine free NaCl, Mossoró[®], Brazil) were employed.

Table 6. Crude oil physicochemical and interfacial properties

Parameters	Value
Density, 25° C (g mL^{-1})	0.88
API Grade (°API)	23
Viscosity, 25° C (cP)	42
Superficial tension (oil/water), 25° C (mN m^{-1})	28

A commercial cationic polyacrylamide (Dismulgan V3377, Clariant[®]) was employed for oil emulsion destabilization and flocculation after adjusting medium pH at 7 with a solution of NaOH 1 % w/w (Vetec[®], Brazil).

Oil concentration analyses were performed by spectrometry using a Horiba OCMA-350 device. Tetrachloroethylene (C₂Cl₄, Sigma Aldrich[®]) was used for the extraction of the oil from the samples and hydrochloric acid (HCl 5% v/v, Dinâmica Química[®]) was used for pH adjustment. Anhydrous sodium sulfate (Na₂(SO)₄; Sigma Aldrich[®]) was employed to remove residual humidity from the organic phase.

Methods

5.2.2 Oil-in-water emulsion generation system

The oily emulsion generation system (Figure 22) was composed of: i. A tap water feed tank. ii. A helical high-pressure pump (Netzsch, NEMO[®]); iii. A dosing piston pump (OMEL[®] DMP-02) for inline oil injection; iv. A flow constrictor (needle valve) with manometers upstream and downstream of the pipe, and v. An oily emulsion storage tank (1 m³) with a centrifugal pump for mixing the salt (Schneider[®] BCR 2000).

The process consisted of the injection of crude oil at high pressure through the depressurizing needle valve, followed by a pressure drop (12 bar) and high shear caused by the passage of the oily-water mixture through the flux constrictor. This procedure allowed the formation of a stable oily emulsion with oil contents ranging from 60 to 450 mg L⁻¹. According to Santander et al. (2011) the oil droplet volumetric mean diameter (D₃₂) is inversely proportional to the pressure drop, and the application of 12 bar resulted in oil droplets with a D₃₂ of 10 - 15 μm. NaCl (30 to 100 g L⁻¹) was added into the oil wastewater storage tank and dissolved by recirculation with a centrifugal pump.

Feed oil concentrations (< 200 mg.L⁻¹) were obtained by diluting the oily emulsion with tap water (1:1).

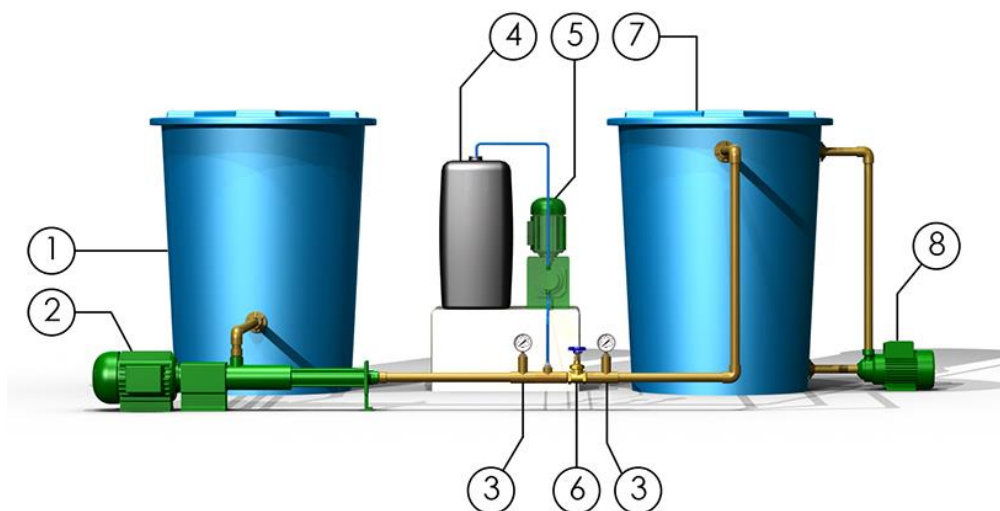


Figure 22. Oily emulsion generation unit 1) Water feed tank; 2) Helical high-pressure pump; 3) Manometers ; 4) Crude oil feed tank; 5) Oil dosing piston pump; 6) Flow constrictor (needle valve); 7) Oily emulsion storage tank; 8) Recirculation mixing pump.

5.2.3 Bubble generation

The bubble generation unit consisted of a CMP (Schneider[®] ME-1315 or ME-1420), operating with a pressure of 4 bar and liquid flow varying between 1 and 3 m³ h⁻¹. The injection (air/liquid ratio 7.5%) was controlled by an air rotameter (ASA[®]) positioned in the suction line of the CMP, with a vacuum meter gauge (FabrePrimar[®]). A PVC pressure vessel (external diameter = 110 mm, height = 0.95 m), with a pressure gauge (NuovaFima[®]) was employed to relieve the excess air and increase the air in water saturation and dissolution time to about 27 s. A needle-type valve was used as a flow constrictor for hydrodynamic cavitation and the formation of MBs (5 – 80 μm) and NBs (50 – 300 nm). The liquid flow was measured by a liquid rotameter (AppliTech[®]) positioned downstream of the pressure vessel.

5.2.4 Flocculation

The flocculation unit was composed of two flocculation units-FGR[®] (details in Table 2) that use the kinetic energy of the liquid flow along the helical tubular reactors. The system was composed of a rapid mixing stage (low residence time and high velocity

gradient - G) for dispersion of the flocculant and NaOH, and a slow mixing stage (high residence time and reduced G) for the formation of stable flocs.

Bubbles generated upstream of the reactor, adhere to and entrap aggregates, forming large aerated flocs with low density. These flocs floated very rapidly (high flotation kinetics), similarl to the results published by Oliveira and Rubio (2012). The head loss in the system was measured by manometers which were positioned in the inlet and outlet of the reactor. Reactants (flocculation polymer and NaOH) were injected by two diaphragm-dosing pumps (EXATTA®) located downstream of bubble injection.

The effect of the flocculation reagent (Dismulgan V 3377) on oil removal by flotation was studied in the range of 5 – 30 mg L⁻¹ in duplicate tests.

5.2.5 Flotation

The flotation column had a variable height (1.5 and 2.5 m) and a square section with 33 cm edges (Table 7). The treated water outlet was positioned in the lower third part of the column and the sludge removed from the top of the column was disposed of in a drying bed that consisted of alternating layers of gravel, coarse and fine sands amounting 0.5 m³ the total volume.

Table 7. Design and operation parameters of the flocculation-flotation units for oily water treatment. The residence times and G were calculated for the flows of 1 and 3 m³ hour⁻¹, respectively.

Flocculation unit	Rapid mixing	Lenght (m)	6
		Inner diameter (m)	0.011
		Volume (m ³)	0.0006
		Residence time (min)	0.03 – 0.01
		G ¹ (s ⁻¹)	663 - 2300
Slow mixing		Lenght (m)	24
		Inner diameter (m)	0.035
		Volume (m ³)	0.023
		Residence time (min)	1.4 – 0.47
		G ¹ (s ⁻¹)	30 – 102
Flotation unit	Column	Height (m)	1.5 - 2.5
		Edges (m)	0.33
		Inner area (m ²)	0.11

	Volume (m ³)	0.16 - 0.27
	Residence time (min)	16 – 5.5
	Air/liquid ratio	7.5%
CMP	Operating pressure (bar)	4

¹ Mixture G was calculated by the following equation (Tchobanoglous, Burton, Stensel, & Metcalf & Eddy., 2003): $G = \sqrt{\gamma \frac{H_f}{\mu t}}$, where G = velocity gradient (s⁻¹); γ = specific weight of liquid mass (kgf m⁻³); H_f = head loss (m); μ = absolute viscosity of liquid mass (N s m⁻¹); t = residence time (s).

Schematic images of the oily emulsion treatment system by flocculation-column flotation with CMP are shown in Figures 23 and 24.

The results were analyzed in terms of oil removal efficiency (%), calculated according to Equation 1.

$$\text{Efficiency (\%)} = 100 - \frac{[(C_f) \times 100]}{C_0} \quad (1)$$

where, C_f is the final oil concentration and C₀ is the initial oil concentration.

The effect of the HL on oil removal by flotation was studied varying the feed liquid flow (1 – 3 m³ h⁻¹), with HL values in the range of 10 – 27.5 m h⁻¹.

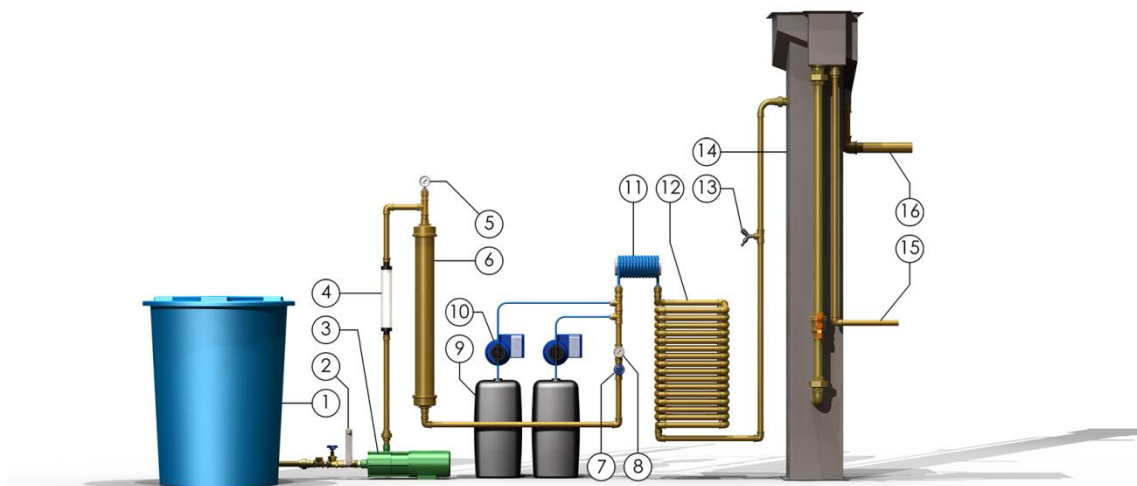


Figure 23. Oily emulsion treatment system by flocculation-column flotation. 1) Oily emulsion storage tank; 2) Air injection; 3) CMP; 4) Flow-meter; 5) Manometer; 6) Pressure vessel; 7) Needle valve; 8) Manometer; 9) Chemicals (flocculant polymer and

NaOH) tanks; 10) Dosing pumps; 11) Rapid mixing FGR®; 12) Slow mixing FGR®; 13) Sampling point; 14) Flotation column; 15) Treated water outlet; 16) Sludge outlet.

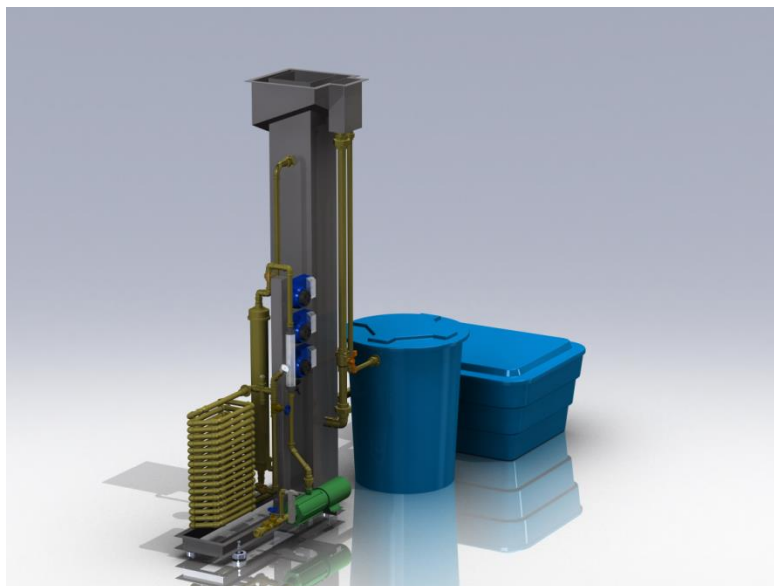


Figure 24. Flocculation-column flotation unit for oily water treatment (3D perspective).

5.3 RESULTS AND DISCUSSION

5.3.1 Effect of the flocculant concentration

Figure 25 shows the effect of the Dismulgan concentration on oil removal and turbidity reduction efficiencies, using a flotation column 1.5 m in height. Best results were obtained with a flocculant concentration of 20 mg L⁻¹, wherein the mean residual turbidity and oil concentration were 17 NTU and 20 mg L⁻¹, respectively.

These results are similar to those obtained by Santander et al. (2011), in our research group, who flocculated the crude oil emulsion (oil feed < 200 mg L⁻¹) with 10 mg L⁻¹ of Dismulgan and 3 mg L⁻¹ of a non-ionic polymer (Polyvinyl acetate - PVA) as flocculants. In that work, the flocs were then removed from water by a modified "jet" flotation process at a high HL (24.7 m h⁻¹), resulting in residual oil contents between 20 and 30 mg L⁻¹ in the treated water.

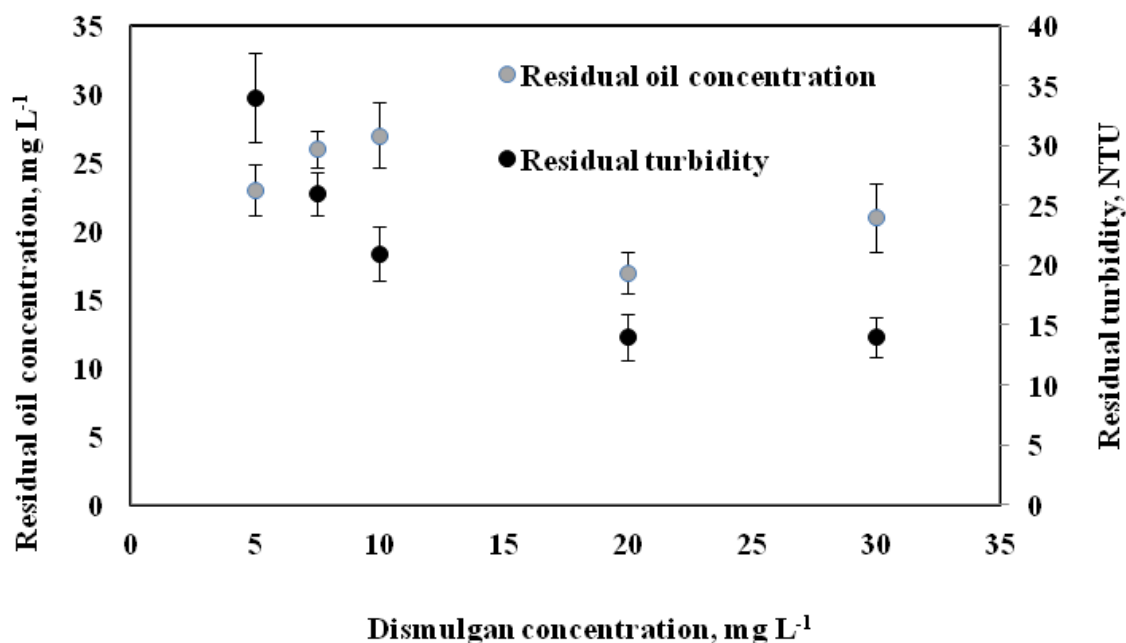


Figure 25. Emulsified oil separation by flocculation-column flotation. Effect of Dismulgan concentration on the residual oil and turbidity. Conditions: pH 7; liquid flow = $1 \text{ m}^3 \text{ h}^{-1}$; air/liquid ratio = 7.5% v/v; flotation column height = 1.5 m; HL = 10 m h^{-1} ; pump pressure = 4 bar; [oil feed] = $400 - 570 \text{ mg L}^{-1}$.

5.3.2 Effect of flotation column height

Figure 26 shows the results obtained with different flotation column heights. Increasing from 1.5 m to 2.5 m resulted in higher oil removal efficiency at the same process conditions. This effect proved to be more relevant in the treatment of oily emulsions with higher initial oil feed (above 200 mg L^{-1}), where the mean residual oil concentrations were reduced from 17 mg L^{-1} to 4 mg L^{-1} , comparing the two column heights at a HL of 10 m h^{-1} .

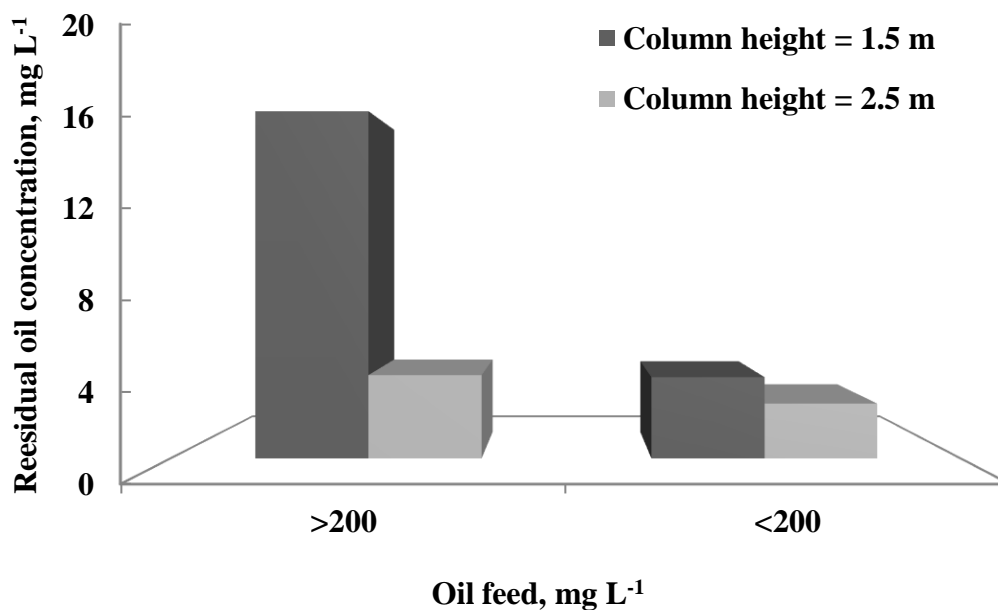


Figure 26. Emulsified oil separation by flocculation-column flotation. Effect of flotation column height. Conditions: pH 7; [Dismulgan] = 20 mg L⁻¹; air/liquid ratio = 7.5%; HL = 10 m h⁻¹; pump pressure = 4 bar.

Similar results were obtained by da Da Rosa (2002) for emulsified crude oil removal in flotation columns; higher oil separation efficiency was obtained with taller columns. The author explains the results in terms of less overflow of the oily flocs towards the treated water outlet, located in the bottom of the column 4.2 m height.

Filippov et al. (2000) showed that the limiting factor for metal-organic precipitate flotation in a column is the level of aggregate stability under the turbulence created by the rising bubbles. The hydrodynamic conditions in a 75 mm diameter pilot column were optimized by using different bubble spargers to control the air hold up, the gas flow rate and the feed flow rate in the column. This led to less turbulence and less entrainment of the floating particles. In a tall flotation column, this aggregate breakage under turbulence, would certainly be reduced compared to a short cell.

These results can also be related to studies on column flotation for ore beneficiation. Yianatos et al. (1988) observed an improvement in mineral recovery efficiency by increasing the column height/diameter (H/D), due to the longer fluid and particle residence time in the system that provides a higher probability of collision, adhesion and flotation of particle-bubble aggregates.

In this work, with respect to cell design, if the H/D relation increased from 4 to 6.7 for the taller column, better oil removal efficiencies were obtained.

Therefore, results obtained in this work appear to indicate that increasing the distance between the floated sludge collection zone and the outlet of treated water is responsible for the improvement in the efficiency of oil-water separation, due to reduced drag of flocs.

Table 8 presents the oil concentration and turbidity values of the emulsion and the treated effluent, obtained in each experiment assayed, with a 2.5 m column height and an HL of 10 m h⁻¹. Additional experiments with higher NaCl concentrations (100 g L⁻¹) were conducted. Excellent separation was obtained, attaining oil contents of 1 mg L⁻¹ in the treated water (>99% efficiency). Residual turbidity may be related to the salinity that ranged from 30 to 100 g L⁻¹.

Table 8. Emulsified oil separation by flocculation-column flotation with MBs and NBs. Oil removal and turbidity reduction results of 8 replicates. Conditions: pH 7; HL = 10 m h⁻¹; liquid flow = 1 m³ h⁻¹; air/liquid ratio = 7.5% v/v; column height = 2.5 m; [Dismulgan] = 20 mg L⁻¹, pump pressure = 4 bar, [NaCl] = 30 g L⁻¹ and 100 g L⁻¹.

	Oil concentration, mg L ⁻¹			Turbidity, NTU		
	Feed	Treated effluent	Removal (%)	Feed	Treated effluent	Reduction (%)
30 g L⁻¹ NaCl	320	1	99	171	9	95
	212	4	98	144	10	93
	209	6	97	139	9	93
	137	1	99	108	7	93
	73	2	97	77	7	91
	65	6	91	77	7	91
	65	3	96	98	11	89
	64	2	98	70	8	89
100 g L⁻¹ NaCl	303	2	99	160	7	95
	295	3	99	158	8	95
	171	1	99	129	7	94
	107	1	99	95	7	92

5.3.3 Effect of Hydraulic Loading

Figure 27 shows the results for the different HL studied. Discharge limits of these substances in produced water emanating from offshore petroleum plants are usually

regulated at a monthly average of 29-34 mg L⁻¹ with a daily maximum of 39-42 mg L⁻¹ (Rawlins, 2009). Oil and gas production plants in the northeast Atlantic are required to meet the 30 mg L⁻¹ oil and grease discharge standards set by Oslo Paris Convention (OSPAR) (Atarah, 2011). Herein, residual oil concentration values obtained were below the emission standards set by U.S. Environmental Protection Agency (U.S. EPA) for Oil and Gas Extraction (monthly average = 29 mg L⁻¹) (EPA, 1979) with all the HL lower than 27.5 m h⁻¹.

At HL lower than 18 m h⁻¹, the treated effluent reached a residual oil content less than 10 mg L⁻¹. Filippov et al. (2000) evaluated the influence of hydrodynamic conditions on the stability of colloidal precipitate flotation on the process of column flotation (diameter = 75 mm). It was found that with high HL, the breakage of the precipitates by shearing forces may occur. Yet, the author showed that decreasing the residence time by increasing the superficial velocity of the liquid, these flocs (broken) are more easily drawn, decreasing the efficiency of solid/liquid separation. These effects may be related to the flotation of oily flocs, explaining the decrease on separation efficiency at high HL. The good results obtained with high HL on oil removal appears to be due to the high flotation kinetics and the shear resistance of the aerated oily flocs formed in the flocculation step.

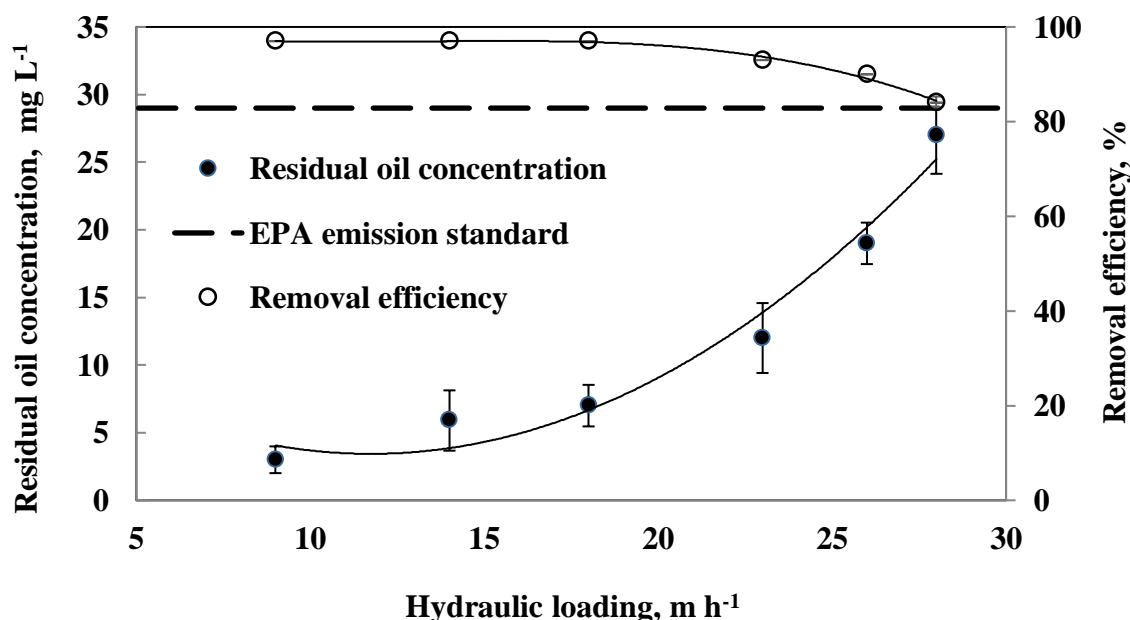


Figure 27. Separation of emulsified oil by flocculation-column flotation with MBs and NBs. Effect of HL on oil removal efficiency. Conditions: pH 7; [Dismulgan] = 20 mg L⁻¹

¹; air/liquid ratio = 7.5%; flotation column height = 2.5 m; pump pressure = 4 bar. [Oil feed] = 64 – 545 mg L⁻¹

The FGR[®] presented head-loss (Hf) values from 0.9 to 3.5 kgf cm⁻², measured from the pressure difference on gauges positioned upstream and downstream of the reactor. Da Rosa and Rubio (2005) evaluated different hydraulic flocculators in oily emulsion treatment by flocculation-flotation and found that the results obtained do not depend on the geometrics of the reactor, but on the Hf provided in the system, obtaining lower oil concentrations in the treated water (10-15 mg L⁻¹) when the Hf reached values between 0.5 and 1.0 kgf cm⁻². For higher values of Hf, the oil concentration has not decreased significantly.

5.4 FINAL REMARKS

The flotation process has been used for many years in the treatment of oily liquid effluents (removal of oil and water reuse). In these applications, the reported size and size distribution of bubbles have been 40-100 µm. Yet, the contribution of NBs has been ignored and unknown (until recently) to most engineers, researchers and flotation professionals, due to the absence and / or lack of knowledge of analytical techniques capable of characterizing and identifying NBs.

Thus, by taking advantage of the upcoming nanotechnology and the development of more advanced particle / bubble analysis techniques, our research group was able to evaluate the generation of NBs and understand some properties that improve flotation efficiency. Notably, the discovery that hydrodynamic cavitation using centrifugal multiphase pumps CMP generates a high concentration of these NBs (A. Azevedo et al., 2017; R. Etchepare, Oliveira, Nicknig, et al., 2017).

This flocculation-column flotation process, using RGF[®] for aerated floc formation and CMP for MBs and NBs generation, appears to present a great potential for oily wastewater treatment. Future applications for pollutant removal at high rates may be possible where small areas are required for equipment installation, namely, for industrial emulsified oils such as petroleum produced waters from offshore platforms.

The advantages of this proposed process are:

- iv. Efficient generation of bubbles with wide size distributions and a high concentration - MBs with a size distribution of 5-80 μm and air hold up in the range of 3 - 6 %; and NBs sizing between 50 -300 nm and a concentration of about 10^9 NBs mL^{-1} (R. Etchepare, Oliveira, Nicknig, et al., 2017; Ramiro Etchepare, 2016);
- v. Continuous generation of oil-bubble clusters (aerated flocs) in the FGR[®] –floc generator reactor;
- vi. A highly efficient separation process with high rates, obtaining low oil contents in the treated water;
- vii. Small foot-print area for equipment installation.

Regarding mechanisms involved, it is believed that NBs entrapped into flocs exert a strong bridging force, assisting oil droplet entrapment allowing the action of hydrophobic forces. These structures have a strong shear resistance and low density, avoiding the breakage and dragging the oil towards the treated water outlet.

5.5 CONCLUSIONS

Excellent results removing emulsified crude oil to levels below EPA Standard Emissions for offshore disposal (29 mg L^{-1}) were obtained at pilot scale, at high hydraulic loading (27.5 m h^{-1}) by flocculation-column flotation with micro and nanobubbles. The bubbles were generated by a novel hydrodynamic cavitation method using a centrifugal multiphase pump and flocculation was conducted in a FGR[®]. Two sizes of column flotation units were employed (1.5, 2.5 m tall). Best results (high oil removal and low residual oil content in the treated water) were attained at a hydraulic loading of 10 m h^{-1} with a flotation column 2.5 m in height, yielding treated water with an oil content $<5 \text{ mg L}^{-1}$. Results validated the role of the nanobubbles assisting the separation process and maximizing the plant treatment capacity. Further advantages are the low footprint required and the high efficiency of the pumps generating the nanobubbles ($4 \times 10^9 \text{ NB mL}^{-1}$; $D_{32} = 150\text{-}300 \text{ nm}$). The whole process appears to have great potential in the treatment of oily wastewaters.

5.6 ACKNOWLEDGEMENTS

The authors would like to thank Alberto Pasqualini refinery (REFAP/Petrobras) and Hidrocicle for partnership in this study, and all Brazilian research institutions: CNPq, Fapergs, UFRGS. Special thanks to all the students at our Lab, especially Alex Rodrigues, Luciana Kaori, Luisa Neves and to Marcelo Fermann and Rafael Zaneti (Hidrocicle) for their technical support.

PARTE III

6 OUTRAS PRODUÇÕES CIENTÍFICO-TECNOLÓGICAS

Além dos três artigos científicos publicados em periódicos internacionais e apresentados nessa dissertação, foi gerada outra publicação em periódico internacional, além de dois artigos (um publicado e outro submetido) em revistas tecnológicas nacionais, nas áreas mineral e ambiental.

- *Nanobubbles generation in a high-rate hydrodynamic cavitation tube.* **Oliveira, H., Azevedo, A., Rubio, J.** Minerals Engineering, 116, pp 32-34. 2018.

Nesse artigo foi apresentado um estudo de caracterização dos parâmetros de dispersão de ar (holdup de ar- ε_g , velocidade superficial de ar- J_g , e fluxo de área superficial de bolhas- S_b) e NBs geradas por um dispositivo cavitador comercial (Cavitation Tube, ERIEZ®), em regime de recirculação de água por bomba centrífuga multifásica, utilizando o aparato experimental (*skid*) de caracterização de bolhas projetado e utilizado no Artigo II desta dissertação. Os melhores resultados demonstraram que NBs (230–280 nm) foram geradas por cavitação hidrodinâmica em alta taxa, atingindo uma concentração de $6,4 \times 10^8$ NBs/mL após recirculação por 30 min, em uma solução de α -terpineol (100 mg L^{-1}) com tensão superficial de 49 mN/m , $\varepsilon_g = 16\%$, $J_g = 0,87 \text{ cm/s}$ e $S_b = 85/\text{s}$. Foram discutidos os efeitos das NBs na interação com sólidos e bolhas maiores, enfatizando as potencialidades na aplicação em processos de flotação de beneficiamento mineral e remoção de efluentes.

- *Remoção de petróleo emulsificado em água salina por floculação-lotação com micro e nanobolhas.* **Oliveira, H., Etchepare, R., Azevedo, A., Rubio, J.** Revista Saneamento Ambiental. 185, pp 26-30. 2017.

Este artigo foi publicado em periódico nacional com um enfoque mais processista e tecnológico, ressaltando as inovações proporcionadas pelo sistema de floculação em linha e flotação em coluna como alternativa para aumento da taxa de aplicação e capacidade de tratamento (m^3/hr) do processo estudado. A metodologia e os resultados apresentados são os mesmos do Artigo III

- *Nanobolhas: o panorama da pesquisa, propriedades e potencial nas áreas mineral e ambiental.* **Azevedo, A., Rosa, A. F., Oliveira, H., Rubio, J.** Submetido à Revista Brasil Mineral. 2018.

Este artigo descreve o panorama e evolução da pesquisa de geração e aplicações de nanobolhas. Um histórico resumido da pesquisa e desenvolvimento sobre nanobolhas é apresentado, assim como o resumo dos efeitos e aplicações nas áreas mineral e ambiental. Foram relatadas a pesquisa em nanotecnologia, as produções e descobertas científicas e produtos tecnológicos desenvolvidos no LTM (depósito de patente, equipamentos para geração e caracterização de dispersões de nanobolhas, sistema piloto para FAD com nanobolhas). Foi realizada uma análise sobre o panorama das necessidades da pesquisa sobre nanobolhas, visando à transferência da tecnologia para a indústria e mercado.

7 CONSIDERAÇÕES FINAIS

O processo de flotação vem sendo empregado há mais de 100 anos no tratamento de minérios (recuperação de espécies minerais de valor) e de efluentes líquidos (remoção de poluentes e reúso de água). A diferença nestas aplicações está no tamanho e distribuição de tamanho de bolhas gerada; macrobolhas (0,6-2 mm) na flotação de minérios e microbolhas (40-100 μm) na flotação (separação) de poluentes (partículas, coloides, gotículas). Entretanto, a contribuição das NBs ainda é desconhecida da maioria dos engenheiros, pesquisadores e profissionais da área de flotação. Este fato se deve principalmente pela ausência e/ou desconhecimento de técnicas analíticas capazes de caracterizar e identificar as NBs, até então.

Nas últimas décadas, houve um avanço significativo da nanotecnologia e o desenvolvimento de técnicas de análise de partículas/bolhas mais avançadas, permitiu uma melhor compreensão das propriedades destas bolhas. Nos últimos anos, os estudos envolvendo a aplicação das NBs no processo de flotação avançaram de forma crescente, especialmente no setor mineral e na área ambiental. Com as recentes pesquisas publicadas, os efeitos das interações de NBs com sistemas minerais e de nano e micro poluentes (orgânicos e inorgânicos) já são conhecidos e comprovados.

Neste sentido, o desenvolvimento de uma técnica de aplicação de NBs na separação de efluentes oleosos emulsificados em alta taxa de aplicação superficial foi uma das principais contribuições desta dissertação. Os resultados obtidos apresentaram uma maior eficiência do tratamento de óleo em relação aos equipamentos de flotação convencionalmente utilizados, e concluiu-se que é possível ampliar a capacidade de

tratamento de águas oleosas em plataformas marítimas utilizando uma ampla distribuição do tamanho de bolhas geradas por bomba centrífuga multifásica, reduzindo o tempo de residência do tratamento e o espaço ocupado pelo sistema de floculação em linha e flotação em coluna.

A flotação com NBs (em conjunto com as MBs ou não) foi bem-sucedida na remoção de óleo emulsificado, em escala de bancada e em nível piloto. Os resultados obtidos estimulam a utilização destas bolhas no desenvolvimento e aprimoramento de técnicas e tecnologias na remoção de dispersões/emulsões oleosas e outros tipos de poluentes; entre eles:

- i. Na mineração na remoção de reagentes “coletores” de flotação de minérios (xantatos e derivados, aminas, ácidos graxos e íons diversos);
- ii. Na petroquímica e na extração de petróleo no controle da emissão e reinjeção de águas produzidas;
- iii. No setor de industrial e de mitigação da poluição aquosa urbana, no tratamento de águas de lavagem de carros, caminhões, ônibus, aviões, maquinaria industrial pesada;
- iv. Tratamento e remoção de águas contendo micro-poluentes orgânicos (emergentes) como fármacos residuais, desreguladores endócrinos, vírus, bactérias, entre outros.
- v. Na remoção de nanopartículas residuais em águas e efluentes, pelo processo de agregação e flutuação por NBs, isoladas ou em conjunto com MBs
- vi. No clareamento e descontaminação de corpos hídricos (in situ), por meio da redução da turbidez, separação sólido/líquido e líquido/líquido, e remoção de matéria orgânica pelo aumento da atividade microbológica.
- vii. No aprimoramento de processos de transferência gasosa, como em processos oxidativos por ozonização e no desenvolvimento de culturas de algas (aumento da absorção de CO₂)
- viii. Na flotação (separação) em sistemas de cultivos de microalgas.

Assim, a pesquisa e inovação no processo de flotação continuam nos setores acadêmicos e produtivos, buscando processos de tratamento de águas e efluentes mais eficientes, tanto técnica como economicamente.

8 CONCLUSÕES

Os resultados obtidos permitem estabelecer as seguintes conclusões:

1. A floculação com 5 mg L⁻¹ de Dismulgan em pH 7, seguida por flotação (Psat = 5 bar) com MBs e NBs apresentou uma eficiência de remoção de óleo maior que 99%, com um teor de óleo residual de 1 mg L⁻¹. O uso de uma Psat = 3,5 bar resultou em uma água tratada com teor de óleo residual dentro da legislação para descarte offshore (29 mg L⁻¹).
2. A flotação de óleo emulsificado com MBs e NBs seguiu uma constante cinética com modelo de primeira ordem, com valores de 1,3 e 1,8 min⁻¹ para Psat = 3,5 e Psat = 5, respectivamente.
3. O condicionamento da emulsão oleosa com NBs após a etapa de floculação com 1 mg L⁻¹ de Dismulgan aumentou a eficiência da flotação de 73 para 84%.
4. “Flutuação” de flocos oleosos com NBs isoladas resultou numa remoção de 90%.
5. As NBs geradas por despressurização e cavitação hidrodinâmica em uma bomba centrífuga multifásica (BCM) atingiram uma concentração máxima (4,1 x 10⁹ NBs mL⁻¹) após aproximadamente 29 ciclos de geração (tempo de residência = 2,1 min)
6. As melhores condições de geração de NBs por BCM foram obtidas na pressão de operação de 4-5 bar, e uma baixa tensão superficial líquido/ar (49 mN m⁻¹)
7. A dispersão de NBs gerada por BCM demonstrou-se estável por mais de 60 dias, sem decréscimo na concentração ou alteração de tamanho, provando a estabilidade e longevidade dessas bolhas em dispersões aquosas.
8. As NBs foram resistentes às altas pressões e forças de cisalhamento exercidas no rotor da bomba durante os diversos ciclos de geração.
9. A remoção de óleo emulsificado pelo processo de floculação em linha e flotação em coluna com MBs e NBs geradas por bomba centrífuga multifásica demonstrou ser eficiente em uma grande faixa de taxa de aplicação superficial com a concentração de 20 mg L⁻¹ de Dismulgan
10. Os melhores resultados foram obtidos com uma coluna de flotação de 2,5 m e uma taxa de aplicação de 10 m hr⁻¹, resultando em uma água tratada com teor de óleo menor que 5 mg L⁻¹.

11. Em uma taxa de aplicação superficial bastante elevada ($27,5 \text{ m hr}^{-1}$), a água tratada apresentou teor de óleo compatível com a legislação de emissão offshore, sugerindo a aplicação deste processo como alternativa para tratamento de águas produzidas em plataformas marítimas.

9 SUGESTÕES DE TRABALHOS FUTUROS

A pesquisa de geração de NBs deve continuar a fim de se obter métodos cada vez mais eficientes e sustentáveis de geração de dispersões aquosas de NBs, em alta taxa (concentração numérica e volumétrica de NBs) e baixo gasto energético, explorando os mecanismos de despressurização de corrente líquida saturada em gás, cavitação hidrodinâmica e cisalhamento de massa líquida contendo gases dissolvidos. Além de se obter condições de geração de NBs modificadas (carregadas positiva ou negativamente), para possibilitar um aumento do campo de pesquisa nas aplicações de NBs.

Os recentes estudos desenvolvidos no LTM comprovam os efeitos das nanobolhas no aumento da eficiência de remoção de poluentes aquosos. Em nível piloto (contínuo), ainda não foram reportados estudos no meio científico de processos com a injeção de NBs isoladas para condicionamento e/ou “flutuação”. Estudos futuros podem avaliar a injeção de bolhas de tamanhos variados na flotação (sistema multibolhas) usando bombas multifásicas geradoras de bolhas, de forma que sejam testadas e validadas de maneira contínua e com diferentes tipos de águas de processo, visando à transferência de tecnologia do setor acadêmico ao mercado e indústria. A Figura 28 apresenta um exemplo deste futuro fluxograma proposto.

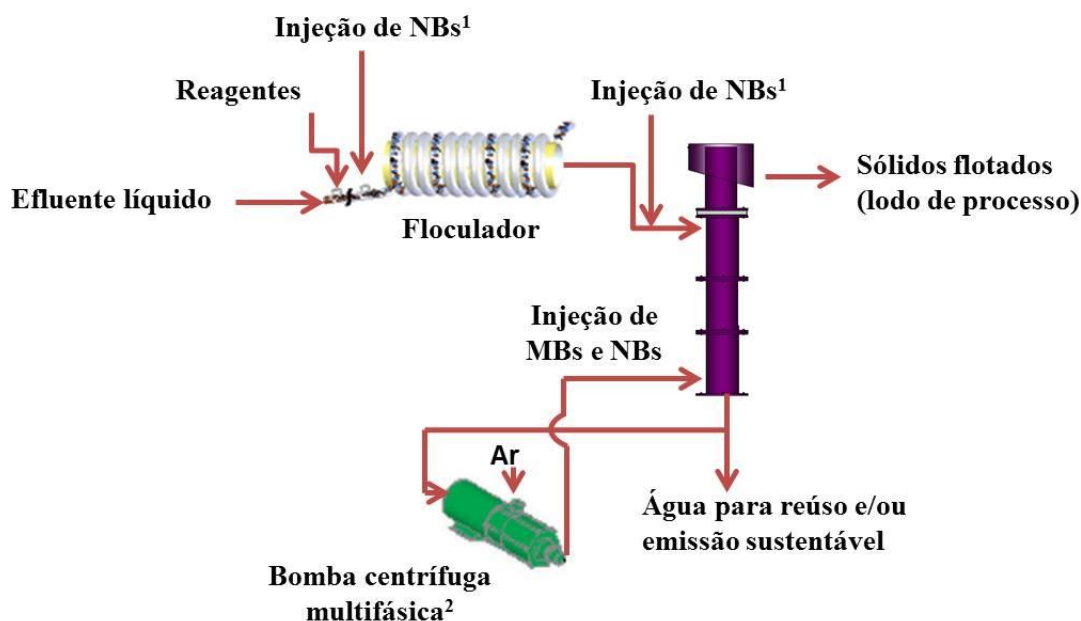


Figura 28. Fluxograma de processo de floculação-flotação para tratamento de efluentes líquidos com múltipla injeção de bolhas. ¹NBs geradas por vaso saturador ou bomba centrífuga multifásica – injeção de dispersão de NBs isoladas; ²Geração conjunta de MBs e NBs por bomba centrífuga multifásica.

Nas aplicações de NBs nas áreas mineral e ambiental, o potencial tecnológico das NBs traz uma vasta possibilidade de estudos futuros, dos quais alguns estão citados abaixo:

Aplicações de NBs na área mineral:

- Estudos de flotação em bancada (células mecânicas) com diferentes sistemas minerais, utilizando injeção de MBs e NBs no processo;
- Estudos em escala piloto (contínuo e/ou semi-contínuo) com aplicação de flotação multibolhas no tratamento de minérios, com injeção de NBs nas etapas de moagem e condicionamento da polpa e injeção de MBs e NBs, em conjunto com macrobolhas, na coluna de flotação;

Aplicações de NBs na área ambiental:

- Geração, caracterização e aplicação de NBs de ozônio para oxidação de poluentes diversos em águas residuárias (industriais e urbanas) e para desinfecção de águas de abastecimento;
- Estudos de validação em escala piloto (contínuo ou semi-contínuo) de flotação com NBs (assistida com NBs e/ou NBs isoladas) para remoção de poluentes

diversos (orgânicos e inorgânicos) em etapa de separação sólido-líquido no tratamento de efluentes;

- Uso de NBs de gases (ar ou ozônio) em processos mais limpos e sustentáveis de limpeza de superfícies sólidas;
- Uso de NBs de gases (ar ou ozônio) no *defouling* e/ou prevenção de *fouling* de membranas de tratamento de águas e efluentes ou da indústria química e alimentícia;
- Uso de NBs de ar ou gases ($O_2/CO_2/O_3$) no tratamento biológico de efluentes, na aeração de sistemas e no crescimento de micro-organismos específicos utilizados no tratamento de efluentes.

10 REFERÊNCIAS BIBLIOGRÁFICAS

- Agarwal, A., Ng, W. J., & Liu, Y. (2011). Principle and applications of microbubble and nanobubble technology for water treatment. *Chemosphere*, 84(9), 1175–80. <https://doi.org/10.1016/j.chemosphere.2011.05.054>
- Ahmadi, R., Khodadadi, D. A., Abdollahy, M., & Fan, M. (2014). Nano-microbubble flotation of fine and ultrafine chalcopyrite particles. *International Journal of Mining Science and Technology*, 24(4), 559–566. <https://doi.org/10.1016/j.ijmst.2014.05.021>
- Ahmed Sobhy, S. A. (2013). Cavitation nanobubble enhanced flotation process for more efficient coal recovery. University of Kentucky.
- Al-Shamrani, A. ., James, A., & Xiao, H. (2002a). Separation of oil from water by dissolved air flotation. *Colloids and Surfaces A: Physicochemical and Engineering Aspects*, 209(1), 15–26. [https://doi.org/10.1016/S0927-7757\(02\)00208-X](https://doi.org/10.1016/S0927-7757(02)00208-X)
- Al-Shamrani, A. A., James, A., & Xiao, H. (2002b). Destabilisation of oil–water emulsions and separation by dissolved air flotation. *Water Research*, 36(6), 1503–1512. [https://doi.org/10.1016/S0043-1354\(01\)00347-5](https://doi.org/10.1016/S0043-1354(01)00347-5)
- Amaral Filho, J., Azevedo, A., Etchepare, R., & Rubio, J. (2016). Removal of sulfate ions by dissolved air flotation (DAF) following precipitation and flocculation. *International Journal of Mineral Processing*, 149, 1–8. <https://doi.org/10.1016/j.minpro.2016.01.012>
- Atarah, J. J. A. (2011). The use of Flotation Technology in Produced Water Treatment in the Oil & Gas Industry. University of Stavanger, Norway.
- Attard, P. (2003). Nanobubbles and the hydrophobic attraction. *Advances in Colloid and Interface Science*, 104(1–3), 75–91. [https://doi.org/10.1016/S0001-8686\(03\)00037-X](https://doi.org/10.1016/S0001-8686(03)00037-X)
- Azevedo, A., Etchepare, R., Calgaroto, S., & Rubio, J. (2016). Aqueous dispersions of nanobubbles: Generation, properties and features. *Minerals Engineering*, 94, 29–37. <https://doi.org/10.1016/j.mineng.2016.05.001>

- Azevedo, A., Etchepare, R., & Rubio, J. (2017). Raw water clarification by flotation with micro and nanobubbles generated with a multiphase pump. *Water Science and Technology*, In Press.
- Azevedo, A., Etchepare, R., & Rubio, J. (2017). Raw water clarification by flotation with microbubbles and nanobubbles generated with a multiphase pump. *Water Science and Technology*, 75(10), 2342–2349. <https://doi.org/10.2166/wst.2017.113>
- Bensadok, K., Belkacem, M., & Nezzal, G. (2007). Treatment of cutting oil/water emulsion by coupling coagulation and dissolved air flotation. *Desalination*, 206(1–3), 440–448. <https://doi.org/10.1016/j.desal.2006.02.070>
- Brennen, C. E. (1994). *Hydrodynamics of pumps*. Concepts ETI, Inc and Oxford University Press.
- Brennen, C. E. (1995). *Cavitation and bubble dynamics*. Oxford University Press.
- Calgaroto, S., Azevedo, A., & Rubio, J. (2015). Flotation of quartz particles assisted by nanobubbles. *International Journal of Mineral Processing*, 137, 64–70. <https://doi.org/10.1016/j.minpro.2015.02.010>
- Calgaroto, S., Azevedo, A., & Rubio, J. (2016). Separation of amine-insoluble species by flotation with nano and microbubbles. *Minerals Engineering*, 89, 24–29. <https://doi.org/10.1016/j.mineng.2016.01.006>
- Calgaroto, S., Wilberg, K. Q., & Rubio, J. (2014). On the nanobubbles interfacial properties and future applications in flotation. *Minerals Engineering*, 60, 33–40. <https://doi.org/10.1016/j.mineng.2014.02.002>
- Carissimi, E., & Rubio, J. (2005). PI 0406106-3. <http://www.lume.ufrgs.br/handle/10183/62452>. Brazil.
- Carissimi, E., & Rubio, J. (2005). The flocs generator reactor-FGR: a new basis for flocculation and solid–liquid separation. *International Journal of Mineral Processing*, 75(3–4), 237–247. <https://doi.org/10.1016/J.MINPRO.2004.08.021>
- Cavalli, R., Argenziano, M., Vigna, E., Giustetto, P., Torres, E., Aime, S., & Terreno, E. (2015). Preparation and in vitro characterization of chitosan nanobubbles as

theranostic agents. *Colloids and Surfaces. B, Biointerfaces*, 129, 39–46. <https://doi.org/10.1016/j.colsurfb.2015.03.023>

Costa CA. Remoção de amônia de efluentes líquidos com o uso de microbolhas: fundamentos e aplicações. Tese de Doutorado PPGE3M/UFRGS; 2003.

Creux, P., Lachaise, J., Graciaa, A., & Beattie, J. K. (2007). Specific cation effects at the hydroxide-charged air/water interface. <https://doi.org/10.1021/JP070060S>

Da Rosa, J. J. (2002). Tratamento de efluentes oleosos por floculação pneumática em linha e separação por flotação : processo FF. Doctorate Thesis, UFRGS, Porto Alegre, Brazil.

Da Rosa, J. J., & Rubio, J. (2005). The FF (flocculation–flotation) process. *Minerals Engineering*, 18(7), 701–707. <https://doi.org/10.1016/j.mineng.2004.10.010>

Ebina, K., Shi, K., Hirao, M., Hashimoto, J., Kawato, Y., Kaneshiro, S., ... Yoshikawa, H. (2013). Oxygen and air nanobubble water solution promote the growth of plants, fishes, and mice. *PloS One*, 8(6), e65339. <https://doi.org/10.1371/journal.pone.0065339>

Edur. (2017). Edur Multiphase DAF pumps.

Edzwald, J., & Haarhoff, J. (2011). *Dissolved Air Flotation For Water Clarification* (1st ed.). McGraw Hill Professional.

El-Gohary, F., Tawfik, A., & Mahmoud, U. (2010). Comparative study between chemical coagulation/precipitation (C/P) versus coagulation/dissolved air flotation (C/DAF) for pre-treatment of personal care products (PCPs) wastewater. *Desalination*, 252(1), 106–112. <https://doi.org/10.1016/j.desal.2009.10.016>

EPA. EPA Effluent Guideline for Oil and Gas Extraction (CFR 40.435) (1979). United States.

Etchepare, R. (2016). Geração, caracterização e aplicação das nanobolhas na remoção de poluentes aquosos e reuso de água por flotação. UFRGS, Porto Alegre, Brazil.

- Etchepare, R., Azevedo, A., Calgaroto, S., & Rubio, J. (2017). Removal of ferric hydroxide by flotation with micro and nanobubbles. *Separation and Purification Technology*, 184, 347–353. <https://doi.org/10.1016/j.seppur.2017.05.014>
- Etchepare, R., Azevedo, A., & Rubio, J. (2016). Nanobubbles: their role in dissolved air flotation. In *The 7th International Conference on Flotation for Water and Wastewater Systems, Flotation 2016* (pp. 338–345). Toulouse, France: IWA Publishing.
- Etchepare, R., Oliveira, H., Azevedo, A., & Rubio, J. (2017). Separation of emulsified crude oil in saline water by dissolved air flotation with micro and nanobubbles. *Separation and Purification Technology*, 186, 326–332. <https://doi.org/10.1016/j.seppur.2017.06.007>
- Etchepare, R., Oliveira, H., Nicknig, M., Azevedo, A., & Rubio, J. (2017). Nanobubbles: generation using a multiphase pump, properties and features. *Minerals Engineering*, In Press, Proofs corrected.
- Fakhrul-Razi, A., Pendashteh, A., Abdullah, L. C., Biak, D. R. A., Madaeni, S. S., & Abidin, Z. Z. (2009). Review of technologies for oil and gas produced water treatment. *Journal of Hazardous Materials*, 170(2–3), 530–551. <https://doi.org/10.1016/j.jhazmat.2009.05.044>
- FAN, M., TAO, D., HONAKER, R., & LUO, Z. (2010a). Nanobubble generation and its application in froth flotation (part I): nanobubble generation and its effects on properties of microbubble and millimeter scale bubble solutions. *Mining Science and Technology*, 20(1), 1–19. [https://doi.org/10.1016/S1674-5264\(09\)60154-X](https://doi.org/10.1016/S1674-5264(09)60154-X)
- Fan, M., Tao, D., Honaker, R., & Luo, Z. (2010b). Nanobubble generation and its applications in froth flotation (part II): fundamental study and theoretical analysis. *Mining Science and Technology (China)*, 20(2), 159–177. [https://doi.org/10.1016/S1674-5264\(09\)60179-4](https://doi.org/10.1016/S1674-5264(09)60179-4)
- Fan, M., Tao, D., Honaker, R., & Luo, Z. (2010c). Nanobubble generation and its applications in froth flotation (part III): Specially designed laboratory scale column flotation of phosphate. *Mining Science and Technology*, 20(3), 317–338. [https://doi.org/10.1016/S1674-5264\(09\)60205-2](https://doi.org/10.1016/S1674-5264(09)60205-2)

- Fan, M., Tao, D., Honaker, R., & Luo, Z. (2010d). Nanobubble generation and its applications in froth flotation (part IV): Mechanical cells and specially designed column flotation of coal. *Mining Science and Technology*, 20(5), 641–671. [https://doi.org/10.1016/S1674-5264\(09\)60259-3](https://doi.org/10.1016/S1674-5264(09)60259-3)
- Fan, M., Tao, D., Zhao, Y., & Honaker, R. (2013). Effect of nanobubbles on the flotation of different sizes of coal particle. *Minerals & Metallurgical Processing Journal*, 30(3), 157–161.
- Fan, M., Zhao, Y., & Tao, D. (2012). Fundamental studies of nanobubble generation and applications in flotation. *Separation Technologies for Minerals, Coal and Earth Resources*.
- Filippov, L. O., Joussemet, R., & Houot, R. (2000). Bubble spargers in column flotation: Adaptation to precipitate flotation. *Minerals Engineering*, 13(1), 37–51. [https://doi.org/10.1016/S0892-6875\(99\)00148-X](https://doi.org/10.1016/S0892-6875(99)00148-X)
- Fraim, M., & Jakhete, S. (2015). 8945353. USA.
- Gabardo, I. T., Platte, E. B., Araujo, A. S., & Pulgatti, F. H. (2011). Evaluation of produced water from Brazilian offshore platforms. In K. Lee & J. Neff (Eds.), *Produced water: environmental risks and advances in mitigation technologies*. (pp. 89–113). New York: Springer.
- Ghadimkhani A, Zhang W, Marhaba T. Ceramic membrane defouling (cleaning) by air Nano Bubbles. *Chemosphere*. 2016;146:379–84.
- Gogate, P. R., & Pandit, A. B. (2000). Engineering design methods for cavitation reactors II: hydrodynamic cavitation. *AIChE Journal*, 46(8), 1641–1649. <https://doi.org/10.1002/aic.690460815>
- Gogate, P. R., & Pandit, A. B. (2001). Hydrodynamic cavitation reactors: a state of the art review. *Reviews in Chemical Engineering*, 17, 1–85. <https://doi.org/10.1515/REVCE.2001.17.1.1>
- Grainer-Allen, T. (1970). *Bubble generation in froth flotation machines*. London, UK: IMM.

- Hampton, M. A., & Nguyen, A. V. (2009). Accumulation of dissolved gases at hydrophobic surfaces in water and sodium chloride solutions: Implications for coal flotation. *Minerals Engineering*, 22(9–10), 786–792. <https://doi.org/10.1016/j.mineng.2009.02.006>
- Hellbender. (2017). Hellbender™ DAF Pumps HBP.
- Henry, C. L., Parkinson, L., Ralston, J. R., & Craig, V. S. J. (2008). A mobile gas–water interface in electrolyte solutions. *The Journal of Physical Chemistry C*, 112(39), 15094–15097. <https://doi.org/10.1021/jp8067969>
- Hu L, Xia Z. Application of ozone micro-nano-bubbles to groundwater remediation. *J Hazard Mater*. Elsevier; 2018;342:446–453.
- Hua, G., Falcone, G., Teodoriu, C., & Morrison, G. (2012). Comparison of multiphase pumping technologies for subsea and downhole applications. *Oil and Gas Facilities*, 1(1), 36–46. <https://doi.org/10.2118/146784-PA>
- Karhu, M., Kuokkanen, V., Kuokkanen, T., & Rämö, J. (2012). Bench scale electrocoagulation studies of bio oil-in-water and synthetic oil-in-water emulsions. *Separation and Purification Technology*, 96, 296–305. <https://doi.org/10.1016/j.seppur.2012.06.003>
- Khoshroo, M., Shirzadi Javid, A. A., & Katebi, A. (2018). Effects of micro-nano bubble water and binary mineral admixtures on the mechanical and durability properties of concrete. *Construction and Building Materials*, 164, 371–385. <https://doi.org/10.1016/j.conbuildmat.2017.12.225>
- Klaus Werner Stöckelhuber, *,†,‡, Boryan Radoev, †,§, Andreas Wenger, † and, & Schulze†, H. J. (2003). Rupture of Wetting Films Caused by Nanobubbles. <https://doi.org/10.1021/LA0354887>
- Lee, C. H., An, D. M., Kim, S. S., Ahn, K. H., & Cho, S. H. (2007). Full scale operation of dissolved air flotation process using microbubble generating pump. In *5th International Conference on Flotation in Water and Wastewater Systems*. Seoul: IWA - International Water Association.

- Liu G, Craig VSJ. Improved cleaning of hydrophilic protein-coated surfaces using the combination of Nanobubbles and SDS. *ACS Appl Mater Interfaces*. 2009;1:481–7.
- Liu, G., Wu, Z., & Craig, V. S. J. (2008). Cleaning of protein-coated surfaces using nanobubbles: An investigation using a Quartz Crystal Microbalance. *Journal of Physical Chemistry C*, 112(43), 16748–16753. <https://doi.org/10.1021/jp805143c>
- Liu, S., Enari, M., Kawagoe Yoshinori, Makino, Y., & Oshita, S. (2012). Properties of the water containing nanobubbles as a new technology of the acceleration of physiological activity. *Elsevier Chemical Engineering Science*, 93, 250–256.
- Liu, S., Kawagoe, Y., Makino, Y., & Oshita, S. (2013). Effects of nanobubbles on the physicochemical properties of water: The basis for peculiar properties of water containing nanobubbles. *Chemical Engineering Science*, 93, 250–256. <https://doi.org/10.1016/j.ces.2013.02.004>
- Lukianova-Hleb, E. Y., Campbell, K. M., Constantinou, P. E., Braam, J., Olson, J. S., Ware, R. E., ... Lapotko, D. O. (2014). Hemozoin-generated vapor nanobubbles for transdermal reagent- and needle-free detection of malaria. *Proceedings of the National Academy of Sciences of the United States of America*, 111(3), 900–5. <https://doi.org/10.1073/pnas.1316253111>
- Lukianova-Hleb, E. Y., Mutonga, M. B. G., & Lapotko, D. O. (2012). Cell-specific multifunctional processing of heterogeneous cell systems in a single laser pulse treatment. *ACS Nano*, 6(12), 10973–81. <https://doi.org/10.1021/nn3045243>
- Matiolo, E., Testa, F., Yianatos, J., & Rubio, J. (2011). On the gas dispersion measurements in the collection zone of flotation columns. *International Journal of Mineral Processing*, 99(1–4), 78–83. <https://doi.org/10.1016/j.minpro.2011.03.002>
- Mishchuk, N. (2005). The role of hydrophobicity and dissolved gases in non-equilibrium surface phenomena. *Colloids and Surfaces A: Physicochemical and Engineering Aspects*, 267(1), 139–152. <https://doi.org/10.1016/j.colsurfa.2005.06.052>

- Moosai, R., & Dawe, R. A. (2003). Gas attachment of oil droplets for gas flotation for oily wastewater cleanup. *Separation and Purification Technology*, 33(3), 303–314. [https://doi.org/10.1016/S1383-5866\(03\)00091-1](https://doi.org/10.1016/S1383-5866(03)00091-1)
- Nikuni. (2017). Nikuni KTM DAF pumps.
- NSC. (2002). The Prevention of Pollution from Offshore Installations. In *Fifth International Conference on the Protection of the North Sea* (pp. 29–31). Bergen, Norway.
- Oh, S. H., Han, J. G., & Kim, J.-M. (2015). Long-term stability of hydrogen nanobubble fuel. *Fuel*, 158, 399–404. <https://doi.org/10.1016/j.fuel.2015.05.072>
- Ohgaki, K., Khanh, N. Q., Joden, Y., Tsuji, A., & Nakagawa, T. (2010). Physicochemical approach to nanobubble solutions. *Chemical Engineering Science*, 65(3), 1296–1300. <https://doi.org/10.1016/j.ces.2009.10.003>
- Oliveira, C., & Rubio, J. (2012). A short overview of the formation of aerated flocs and their applications in solid/liquid separation by flotation. *Minerals Engineering*, 39, 124–132. <https://doi.org/10.1016/j.mineng.2012.05.024>
- Oshita, S., & Liu, S. (2013). Nanobubble Characteristics and Its Application to Agriculture and Foods. *International Symposium on Agri-Foods for Health and Wealth*, (2011), 23–32.
- Pioltine, A., & Reali, M. A. P. (2011). Emprego de bomba multifásica como unidade geradora de microbolhas de ar em sistema de flotação aplicado ao pré-tratamento de efluente têxtil. *Engenharia Sanitaria E Ambiental*, 16(2), 167–174. <https://doi.org/10.1590/S1413-41522011000200010>
- Polman, A. (2013). Solar steam nanobubbles. *ACS Nano*, 7(1), 15–18. <https://doi.org/10.1021/nm305869y>
- Rawlins, C. H. (2009). Flotation of fine oil droplets in petroleum production circuits. In D. Malhotra, P. Taylor, E. Spiller, & M. Lavier (Eds.), *Recent advances in mineral processing plant design* (pp. 232–246). Society for Mining, Metallurgy, & Exploration.

- Rodrigues, R. T., & Rubio, J. (2003). New basis for measuring the size distribution of bubbles. *Minerals Engineering*, 16(8), 757–765. [https://doi.org/10.1016/S0892-6875\(03\)00181-X](https://doi.org/10.1016/S0892-6875(03)00181-X)
- Rodrigues, R. T., & Rubio, J. (2007). DAF-dissolved air flotation: Potential applications in the mining and mineral processing industry. *International Journal of Mineral Processing*, 82(1), 1–13. <https://doi.org/10.1016/j.minpro.2006.07.019>
- Ross, C. C., Smith, B. M., & Valentine, G. E. (2000). Rethinking dissolved air flotation (DAF) design for industrial pretreatment. *Proceedings of the Water Environment Federation*, 5, 43–56. <https://doi.org/10.2175/193864700785155795>
- Rubio, J., Carissimi, E., & Rosa, J. J. (2007). Flotation in water and wastewater treatment and reuse: recent trends in Brazil. *International Journal of Environment and Pollution*, 30(2), 197–212.
- Rubio, J., Souza, M. ., & Smith, R. . (2002). Overview of flotation as a wastewater treatment technique. *Minerals Engineering*, 15(3), 139–155. [https://doi.org/10.1016/S0892-6875\(01\)00216-3](https://doi.org/10.1016/S0892-6875(01)00216-3)
- Rubio, J., & Zaneti, R. N. (2009). Treatment of washrack wastewater with water recycling by advanced flocculation–column flotation. *Desalination and Water Treatment*, 8(1–3), 146–153. <https://doi.org/10.5004/dwt.2009.679>
- Santander, M., Rodrigues, R. T., & Rubio, J. (2011). Modified jet flotation in oil (petroleum) emulsion/water separations. *Colloids and Surfaces A: Physicochemical and Engineering Aspects*, 375(1), 237–244. <https://doi.org/10.1016/j.colsurfa.2010.12.027>
- Santo, C. E., Vilar, V. J. P., Botelho, C. M. S., Bhatnagar, A., Kumar, E., & Boaventura, R. A. R. (2012). Optimization of coagulation–flocculation and flotation parameters for the treatment of a petroleum refinery effluent from a Portuguese plant. *Chemical Engineering Journal*, 183, 117–123. <https://doi.org/10.1016/j.cej.2011.12.041>
- Saththasivam, J., Loganathan, K., & Sarp, S. (2016). An overview of oil–water separation using gas flotation systems. *Chemosphere*, 144, 671–680. <https://doi.org/10.1016/j.chemosphere.2015.08.087>

- Schubert, H. (2005). Nanobubbles, hydrophobic effect, heterocoagulation and hydrodynamics in flotation. *International Journal of Mineral Processing*, 78(1), 11–21. <https://doi.org/10.1016/j.minpro.2005.07.002>
- Seddon, J. R. T., Lohse, D., Ducker, W. A., & Craig, V. S. J. (2012). A deliberation on nanobubbles at surfaces and in bulk. *ChemPhysChem*, 13(8), 2179–2187. <https://doi.org/10.1002/cphc.201100900>
- Sobhy, A., & Tao, D. (2013). Nanobubble column flotation of fine coal particles and associated fundamentals. *International Journal of Mineral Processing*, 124, 109–116. <https://doi.org/10.1016/j.minpro.2013.04.016>
- Sobhy, S. A. (2013). Cavitation nanobubble enhanced flotation process for more efficient coal recovery. Thesis and Dissertations--Mining Engineering. Kentucky State University.
- Sobhy, & Tao, D. (2013). Nanobubble column flotation of fine coal particles and associated fundamentals. *International Journal of Mineral Processing*, 124, 109–116. <https://doi.org/10.1016/j.minpro.2013.04.016>
- Takahashi, M., & Chiba, K. M. (2007, December). US20070286795.
- Takahashi, T., Miyahara, T., & Mochizuki, H. (1979). Fundamental Study of Bubble Formation in Dissolved Air Pressure Flotation. *Journal of Chemical Engineering of Japan*, 12(4), 275–280. <https://doi.org/10.1252/jcej.12.275>
- Tansel, B., & Pascual, B. (2011). Removal of emulsified fuel oils from brackish and pond water by dissolved air flotation with and without polyelectrolyte use: Pilot-scale investigation for estuarine and near shore applications. *Chemosphere* (Vol. 85). <https://doi.org/10.1016/j.chemosphere.2011.07.006>
- Tchobanoglous, G., Burton, F. L. (Franklin L., Stensel, H. D., & Metcalf & Eddy. (2003). *Wastewater engineering : treatment and reuse*. McGraw-Hill.
- Temesgen T, Bui TT, Han M, Kim T il, Park H. Micro and nanobubble technologies as a new horizon for water-treatment techniques: A review. *Adv. Colloid Interface Sci.* 2017.

- Ushikubo, F. Y., Furukawa, T., Nakagawa, R., Enari, M., Makino, Y., Kawagoe, Y., ... Oshita, S. (2010). Evidence of the existence and the stability of nano-bubbles in water. *Colloids and Surfaces A: Physicochemical and Engineering Aspects*, 361(1–3), 31–37. <https://doi.org/10.1016/j.colsurfa.2010.03.005>
- Veil, J. A., Puder, M. G., Elcock, D., & Redweik, R. J. J. (2004). A White Paper Describing Produced Water from Production of Crude Oil, Natural Gas, and Coal Bed Methane. Prepared by: Argonne National Laboratory. Prepared for: U.S. Department of Energy National Energy Technology Laboratory Under Contract W-31-109-Eng-38.
- Weijjs, J. H., Seddon, J. R. T., & Lohse, D. (2012). Diffusive shielding stabilizes bulk nanobubble clusters. *ChemPhysChem*, 13(8), 2197–2204. <https://doi.org/10.1002/cphc.201100807>
- Wu Z, Chen H, Dong Y, Mao H, Sun J, Chen S, Craig VSJ, Hu J. Cleaning using nanobubbles: defouling by electrochemical generation of bubbles. *J Colloid Interface Sci*. 2008;328:10–4.
- Yianatos, J. B., Finch, J. A., Espinosa-Gomez, R., & Dobby, G. S. (1988). Effect of Column Height on Flotation Column Performance. *Minerals and Metallurgical Processing*, 5(1), 11–14.
- Zaneti, R., Etchepare, R., & Rubio, J. (2011). Car wash wastewater reclamation. Full-scale application and upcoming features. *Resources, Conservation and Recycling*, 55(11), 953–959. <https://doi.org/10.1016/j.resconrec.2011.05.002>
- Zaneti, R., Etchepare, R., & Rubio, J. (2012). More environmentally friendly vehicle washes: water reclamation. *Journal of Cleaner Production*, 37, 115–124. <https://doi.org/10.1016/j.jclepro.2012.06.017>
- Zaneti, R. N., Etchepare, R., & Rubio, J. (2013). Car wash wastewater treatment and water reuse - a case study. *Water Science and Technology: A Journal of the International Association on Water Pollution Research*, 67(1), 82–8. <https://doi.org/10.2166/wst.2012.492>

- Zhang, M., & Seddon, J. R. T. (2016). Nanobubble-Nanoparticle Interactions in Bulk Solutions. *Langmuir*, 32(43), 11280–11286. <https://doi.org/10.1021/acs.langmuir.6b02419>
- Zheng, J., Chen, B., Thanyamanta, W., Hawboldt, K., Zhang, B., & Liu, B. (2016). Offshore produced water management: A review of current practice and challenges in harsh/Arctic environments. *Marine Pollution Bulletin*, 104(1), 7–19. <https://doi.org/10.1016/j.marpolbul.2016.01.004>
- Zhou, Z. A. (1996). Gas nucleation and cavitation in flotation. McGill University.
- Zhou, Z. A., Xu, Z., Finch, J. A., Hu, H., & Rao, S. R. (1997). Role of hydrodynamic cavitation in fine particle flotation. *International Journal of Mineral Processing*, 51(1), 139–149. [https://doi.org/10.1016/S0301-7516\(97\)00026-4](https://doi.org/10.1016/S0301-7516(97)00026-4)
- Zhou, Z. A., Xu, Z., Finch, J. A., Masliyah, J. H., & Chow, R. S. (2009). On the role of cavitation in particle collection in flotation - A critical review. II. *Minerals Engineering*, 22(5), 419–433. <https://doi.org/10.1016/j.mineng.2008.12.010>
- Zhu J, An H, Alheshibri M, Liu L, Terpstra PMJ, Liu G, Craig VSJ. Cleaning with Bulk Nanobubbles. *Langmuir*. American Chemical Society; 2016;32:11203–11211.
- Zouboulis, A. I., & Avranas, A. (2000). Treatment of oil-in-water emulsions by coagulation and dissolved-air flotation. *Colloids and Surfaces A: Physicochemical and Engineering Aspects*, 172(1–3), 153–161. [https://doi.org/10.1016/S0927-7757\(00\)00561-6](https://doi.org/10.1016/S0927-7757(00)00561-6)
- Zuñiga, G. (1935). The efficiency obtained by flotation is an exponential function of time. *Boletín Minero*, 47, 83–86.